Gravitational Collapses in Five-dimensional Space-time

Hisa-aki Shinkai　真貝 寿明 （大阪工業大学）

(Osaka Institute of Technology, Japan)

work with Yuta Yamada 山田 祐太*(OIT)*

Initial Data (Spheroid, Ring)

Yamada & HS, CQG 27 (2010) 045012

Evolution

Yamada & HS, arXiv:1102.2090 (PRD in print)

Yamada & HS, in preparation.

http://www.is.oit.ac.jp/~shinkai/

2011 Shanghai Asia-Pacific School and Workshop on Gravitation, Feb 2011

1. Motivation and Goal

Higher-Dim Black Holes have Rich Structures

Brane-World models give new viewpoints to gravity and cosmology

LHC experiments will (or will not) reveal Higher-Dim BHs in near future

4-dim BH : horizon is S^2,

stable solutions

Schwarzschild --- Birkoff theorem (M)

Kerr --- uniqueness theorem (M, J)

1. Motivation and Goal

Higher-Dim Black Holes have Rich Structures

	4-dim BHs	Higher-dim BHs :
"Black Objects"	Schwarzschild ⟶	Tangherlini --- unique & stable
	Kerr ⟶	Myers-Perry --- maybe unstable in higher J
		black ring (Emparan-Reall) black Saturn di-rings, orthogonal di-rings, ...

1. Motivation and Goal

Higher-Dim Black Holes have Rich Structures

4-dim BHs — Higher-dim BHs :

Schwarzschild ⟶ Tangherlini

--- unique & stable

Kerr ⟶ Myers-Perry

--- maybe unstable in higher J

"Black Objects"

black ring (Emparan-Reall)
black Saturn
di-rings, orthogonal di-rings, ...

1. Motivation and Goal

Higher-Dim Black Holes have Rich Structures

"Black Objects"

black hole
black string
black ring
black Saturn
di-rings, orthogonal di-rings ...

Uniqueness (only in spherical sym.)
Stability?
Formation Process?
Dynamical Features? ...

1. Motivation and Goal

Higher-Dim Black Holes have Rich Structures

"Black Objects"

black hole
black string
black ring
black Saturn
di-rings, orthogonal di-rings ...

Uniqueness (only in spherical sym.)

Stability?
Formation Process?
Dynamical Features? ...

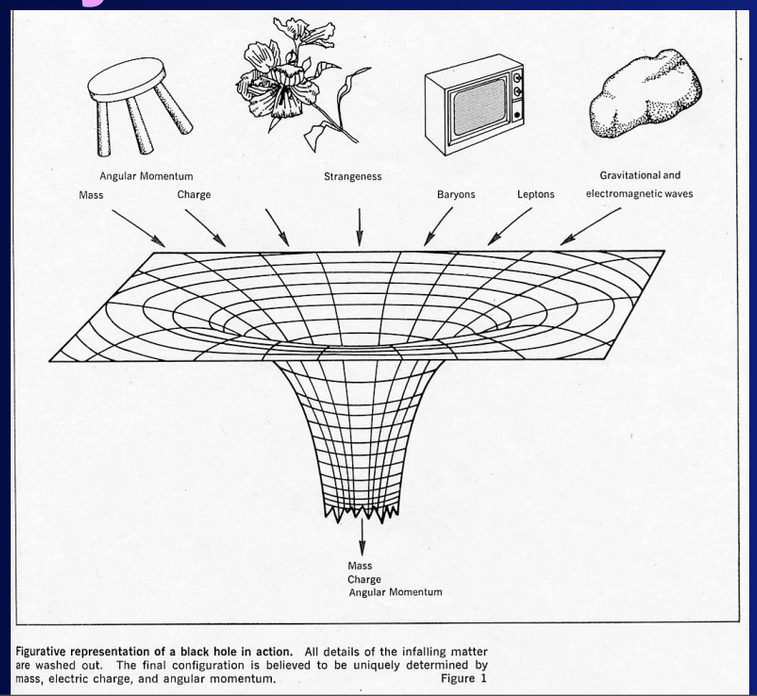

Figurative representation of a black hole in action. All details of the infalling matter are washed out. The final configuration is believed to be uniquely determined by mass, electric charge, and angular momentum. Figure 1

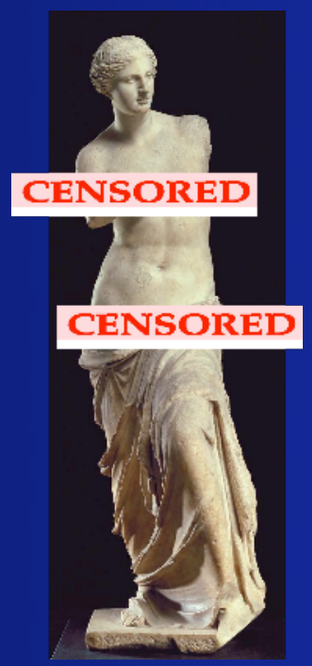

No Hair Conjecture?
Cosmic Censorship?
Hoop Conjecture?

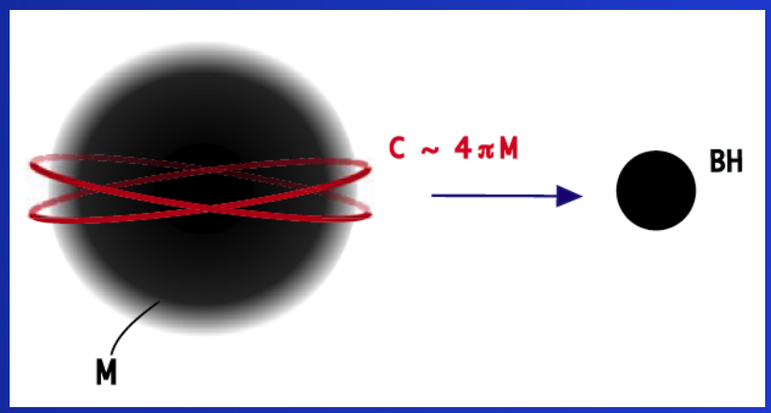

Plan of the talk

2. Spheroidal matter collapse
Initial data analysis
Evolutions

S^3 horizon

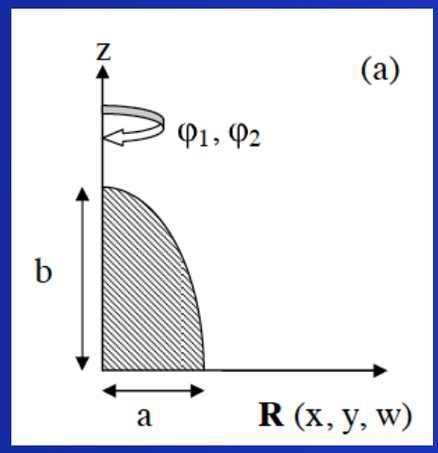

$SO(3)$

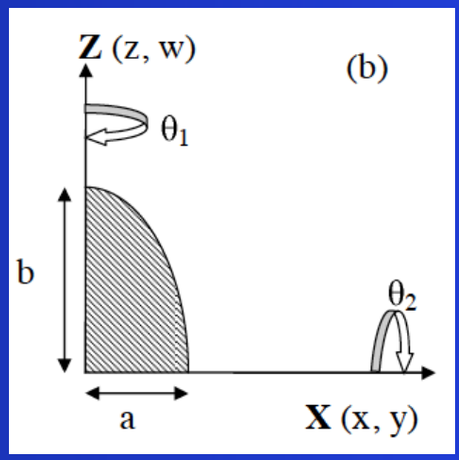

$U(1) \times U(1)$

3. Ring matter collapse
Initial data analysis
Evolutions

$S^2 \times S^1$ horizon

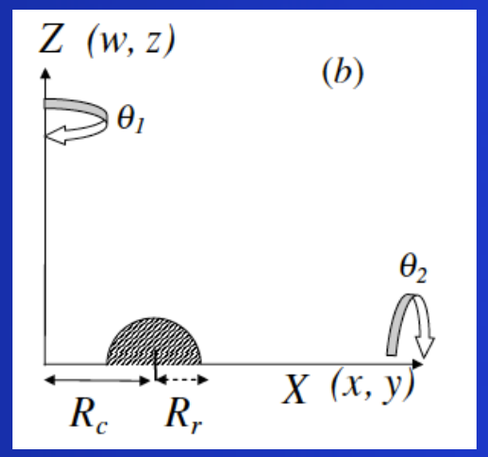

4. Hoop Conjecture?

2. Spheroidal matter collapse
A. Initial data construction

- time symmetric, asymptotically flat
- conformal flat
- non-rotating homogeneous dust

- solve the Hamiltonian constraint eq. 512^2 grids
- Apparent Horizon Search
- Define Hoop and check the Hoop Conjecture

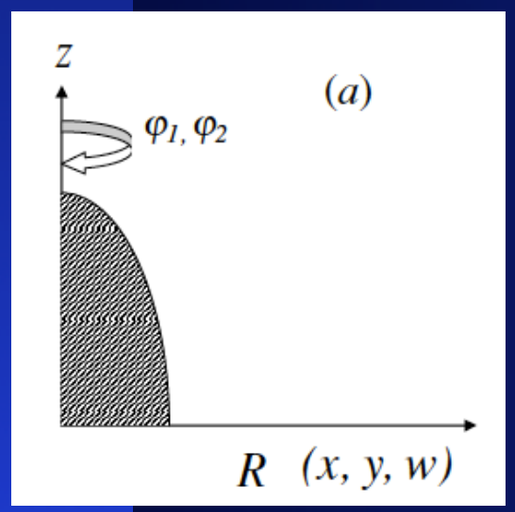

$$ds^2 = \psi(R,z)^2 \left[dR^2 + R^2(d\varphi_1^2 + \sin^2\varphi_1 d\varphi_2^2) + dz^2\right]$$

$$R = \sqrt{x^2+y^2+z^2},\quad \varphi_1 = \tan^{-1}\left(\frac{w}{\sqrt{x^2+y^2}}\right),\quad \varphi_2 = \tan^{-1}\left(\frac{y}{x}\right).$$

$$\frac{\partial^2\psi}{\partial R^2} + \frac{2}{R}\frac{\partial\psi}{\partial R} + \frac{\partial^2\psi}{\partial z^2} = -4\pi^2 G_5 \rho$$

2. Spheroidal matter collapse
B. Initial data sequence

cf. (3-dim.) Nakamura-Shapiro-Teukolsky (1988)

4+1
initial data

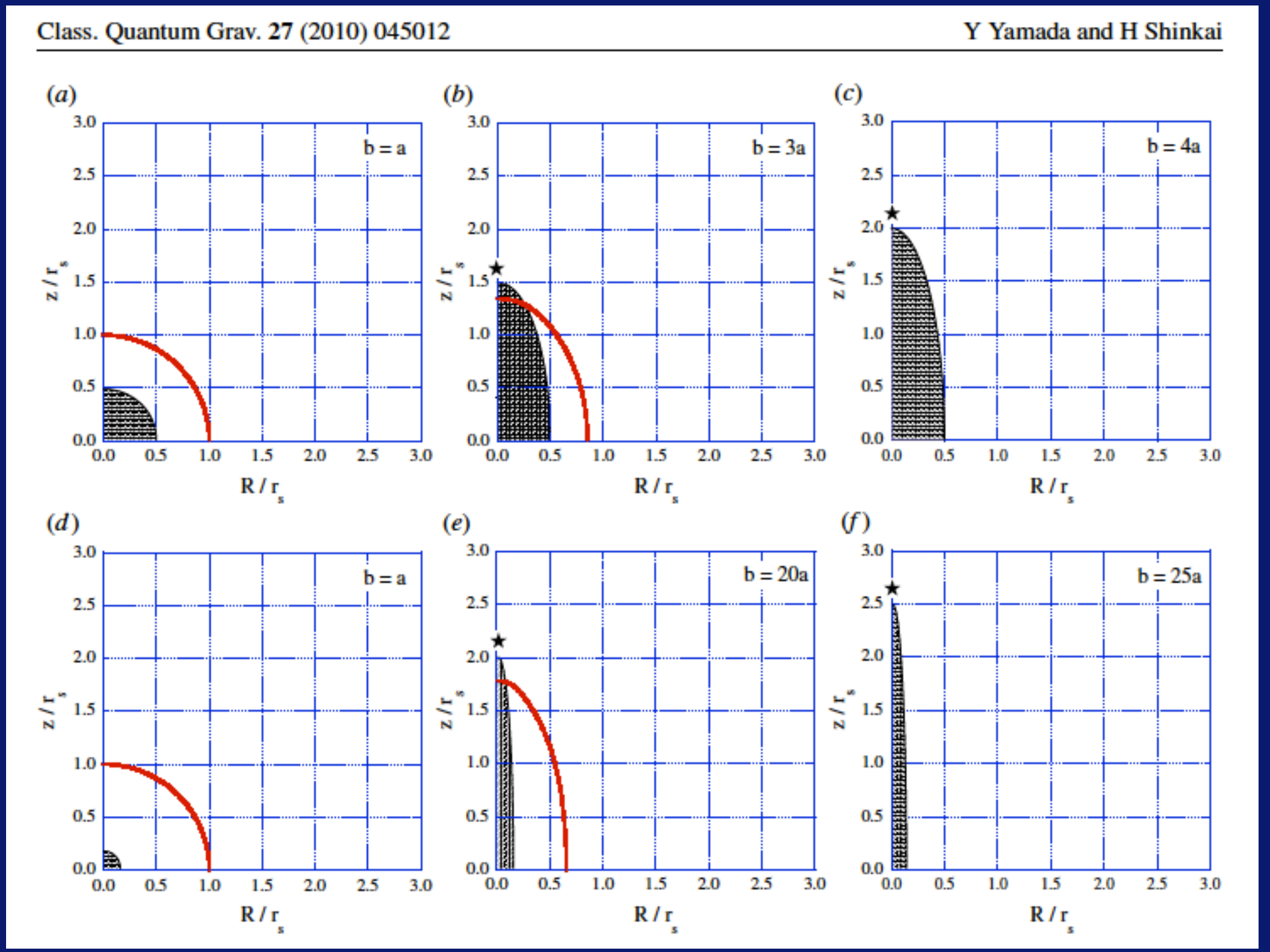

2. Spheroidal matter collapse
B. Initial data sequence

cf. (3-dim.) Nakamura-Shapiro-Teukolsky (1988)

4+1
initial data

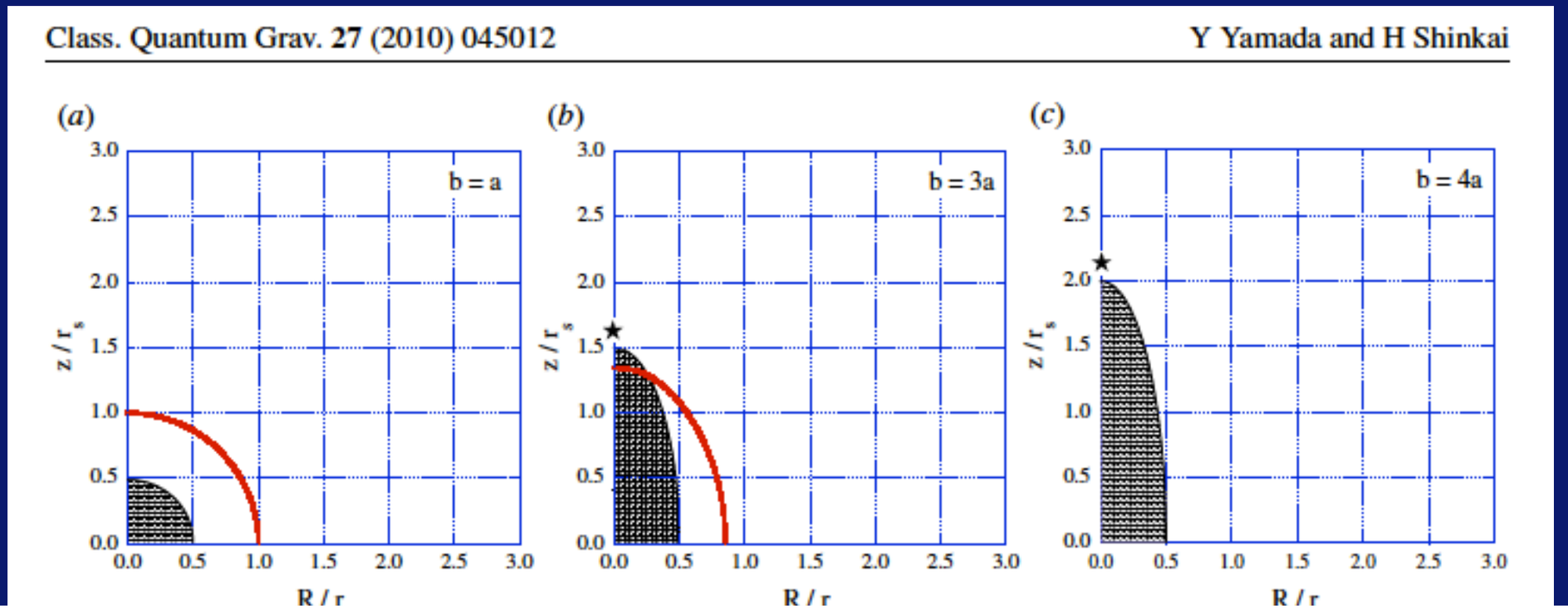

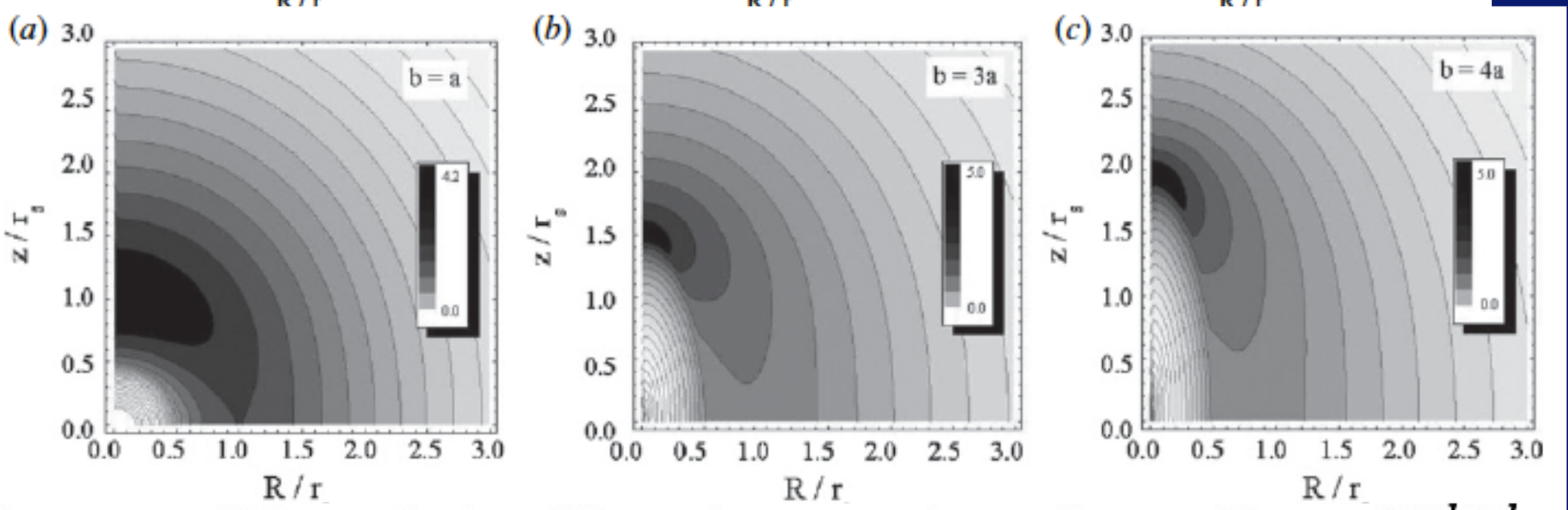

Contour Plot of the Kretchmann invariant, $R_{abcd}R^{abcd}$

2. Spheroidal matter collapse
C. Evolution method

- ADM 2+1 Double Axisym Cartoon
- 130^2 x 2^2 grids

- lapse function: Maximal slicing condition
- shift vectors: Minimum distortion condition
- asymptotically flat

- Collisionless Particles (5000)
- the same total mass
- no rotation

- Apparent Horizon Search

2. Spheroidal matter collapse
C. Evolution examples (4D, ST1991)

VOLUME 66, NUMBER 8 PHYSICAL REVIEW LETTERS 25 FEBRUARY 1991

Formation of Naked Singularities: The Violation of Cosmic Censorship

Stuart L. Shapiro and Saul A. Teukolsky
Center for Radiophysics and Space Research and Departments of Astronomy and Physics, Cornell University, Ithaca, New York 14853
(Received 7 September 1990)

We use a new numerical code to evolve collisionless gas spheroids in full general relativity. In all cases the spheroids collapse to singularities. When the spheroids are sufficiently compact, the singularities are hidden inside black holes. However, when the spheroids are sufficiently large, there are no apparent horizons. These results lend support to the hoop conjecture and appear to demonstrate that naked singularities can form in asymptotically flat spacetimes.

2. Spheroidal matter collapse
C. Evolution examples (4D, ST1991)

VOLUME 66, NUMBER 8 PHYSICAL REVIEW LETTERS 25 FEBRUARY 1991

Formation of Naked Singularities: The Violation of Cosmic Censorship

Stuart L. Shapiro and Saul A. Teukolsky

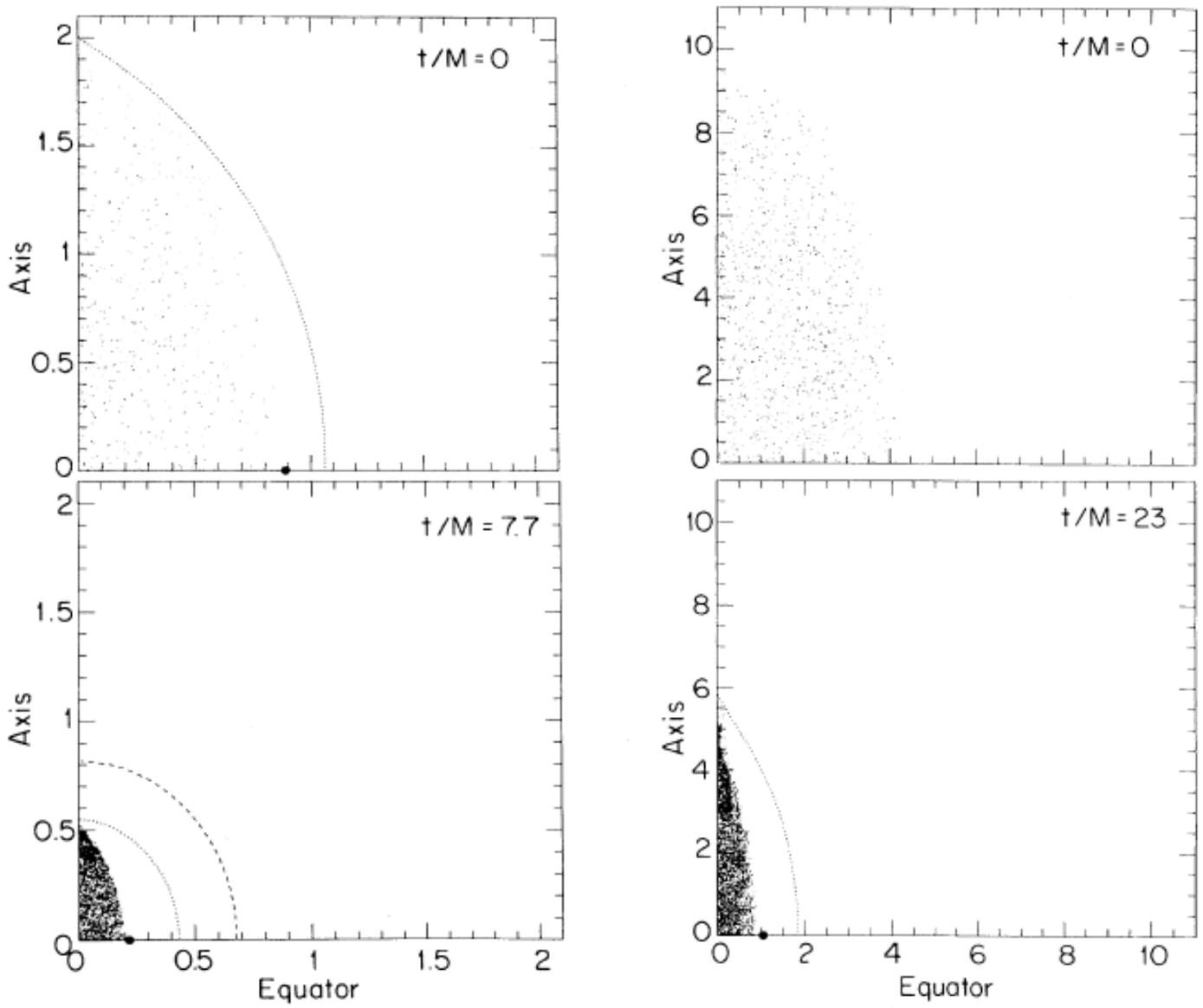

FIG. 1. Snapshots of the particle positions at initial and late times for prolate collapse. The positions (in units of M) are projected onto a meridional plane. Initially the semimajor axis of the spheroid is $2M$ and the eccentricity is 0.9. The collapse proceeds nonhomologously and terminates with the formation of a spindle singularity on the axis. However, an apparent horizon (dashed line) forms to cover the singularity. At $t/M=7.7$ its area is $\mathcal{A}/16\pi M^2=0.98$, close to the asymptotic theoretical limit of 1. Its polar and equatorial circumferences at that time are $\mathcal{C}^{\rm AH}_{\rm pole}/4\pi M=1.03$ and $\mathcal{C}^{\rm AH}_{\rm eq}/4\pi M=0.91$. At later times these circumferences become equal and approach the expected theoretical value 1. The minimum exterior polar circumference is shown by a dotted line when it does not coincide with the matter surface. Likewise, the minimum equatorial circumference, which is a circle, is indicated by a solid dot. Here $\mathcal{C}^{\rm min}_{\rm eq}/4\pi M=0.59$ and $\mathcal{C}^{\rm min}_{\rm pole}/4\pi M=0.99$. The formation of a black hole is thus consistent with the hoop conjecture.

FIG. 2. Snapshots of the particle positions at initial and final times for prolate collapse with the same initial eccentricity as Fig. 1 but with initial semimajor axis equal to $10M$. The collapse proceeds as in Fig. 1, and terminates with the formation of a spindle singularity on the axis at $t/M=23$. The minimum polar circumference is $\mathcal{C}^{\rm min}_{\rm pole}/4\pi M=2.8$. There is no apparent horizon, in agreement with the hoop conjecture. This is a good candidate for a naked singularity, which would violate the cosmic censorship hypothesis.

2. Spheroidal matter collapse
C. Evolution examples (4D, ST1991)

VOLUME 66, NUMBER 8 PHYSICAL REVIEW LETTERS 25 FEBRUARY 1991

Formation of Naked Singularities: The Violation of Cosmic Censorship

Stuart L. Shapiro and Saul A. Teukolsky

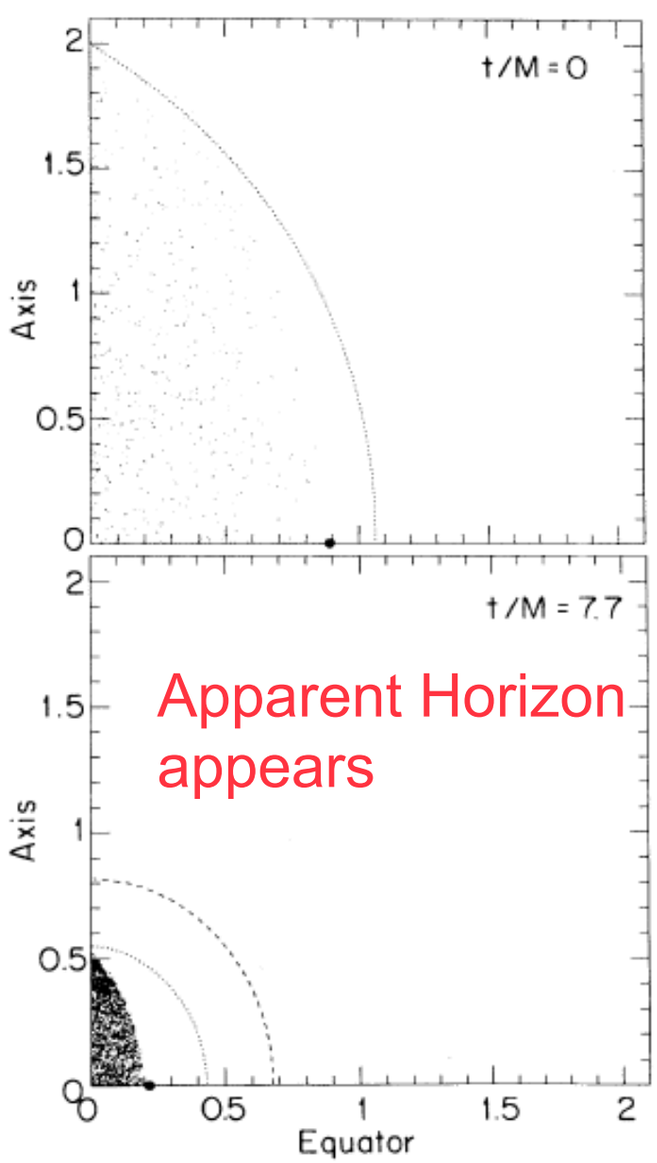

Apparent Horizon appears

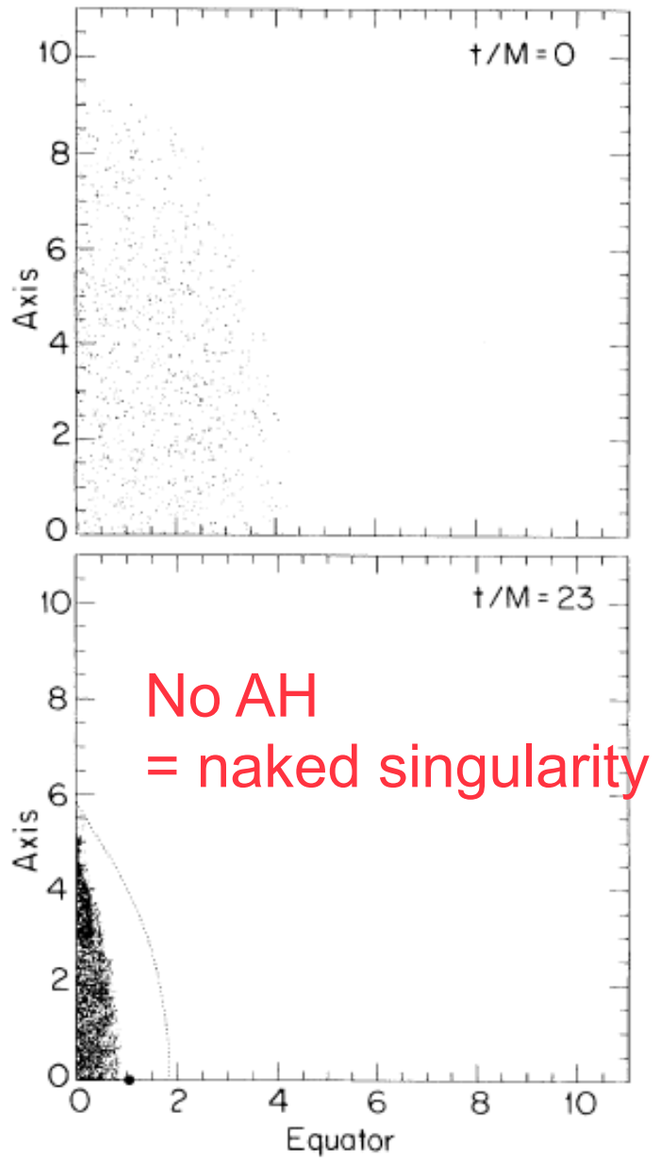

No AH
= naked singularity

FIG. 1. Snapshots of the particle positions at initial and late times for prolate collapse. The positions (in units of M) are projected onto a meridional plane. Initially the semimajor axis of the spheroid is $2M$ and the eccentricity is 0.9. The collapse proceeds nonhomologously and terminates with the formation of a spindle singularity on the axis. However, an apparent horizon (dashed line) forms to cover the singularity. At $t/M=7.7$ its area is $\mathcal{A}/16\pi M^2=0.98$, close to the asymptotic theoretical limit of 1. Its polar and equatorial circumferences at that time are $\mathcal{C}^{\rm AH}_{\rm pole}/4\pi M=1.03$ and $\mathcal{C}^{\rm AH}_{\rm eq}/4\pi M=0.91$. At later times these circumferences become equal and approach the expected theoretical value 1. The minimum exterior polar circumference is shown by a dotted line when it does not coincide with the matter surface. Likewise, the minimum equatorial circumference, which is a circle, is indicated by a solid dot. Here $\mathcal{C}^{\rm min}_{\rm eq}/4\pi M=0.59$ and $\mathcal{C}^{\rm min}_{\rm pole}/4\pi M=0.99$. The formation of a black hole is thus consistent with the hoop conjecture.

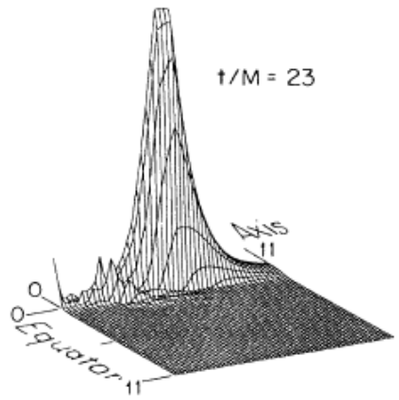

FIG. 4. Profile of I in a meridional plane for the collapse shown in Fig. 2. For the case of 32 angular zones shown here, the peak value of I is $24/M^4$ and occurs on the axis just outside the matter.

2. Spheroidal matter collapse
C. Evolution examples (5D, ours)

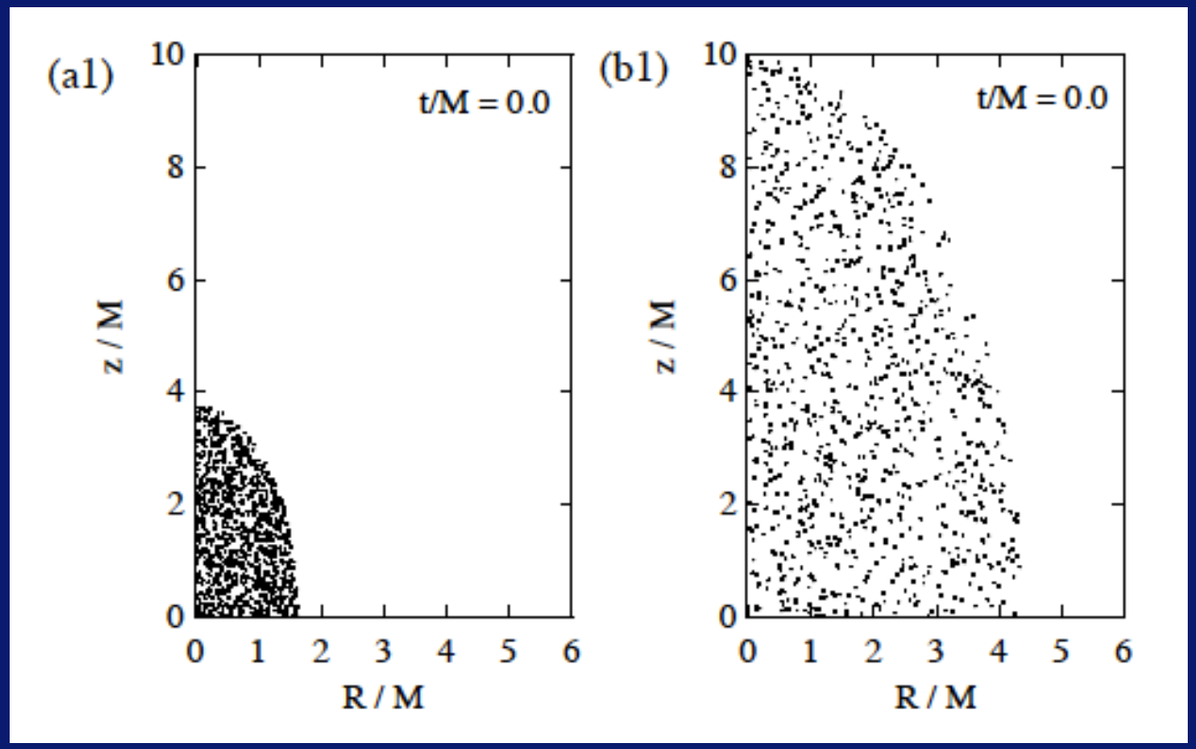

FIG. 2: Snapshots of 5D axisymmetric evolution with the initial matter distribution of $b/M = 4$ [Fig.(a1) and (a2); model 5DSβ in Table I] and 10 [Fig.(b1) and (b2); model 5DSδ]. We see the apparent horizon (AH) is formed at the coordinate time $t/M = 3.3$ for the former model and the area of AH increases, while AH is not observed for the latter model up to the time $t/M = 15.4$ when our code stops due to the large curvature. The big circle indicates the location of the maximum Kretschmann invariant $\mathcal{I}_{\max}$ at the final time at each evolution. Number of particles are reduced to 1/10 for figures.

2. Spheroidal matter collapse
C. Evolution examples (5D, ours)

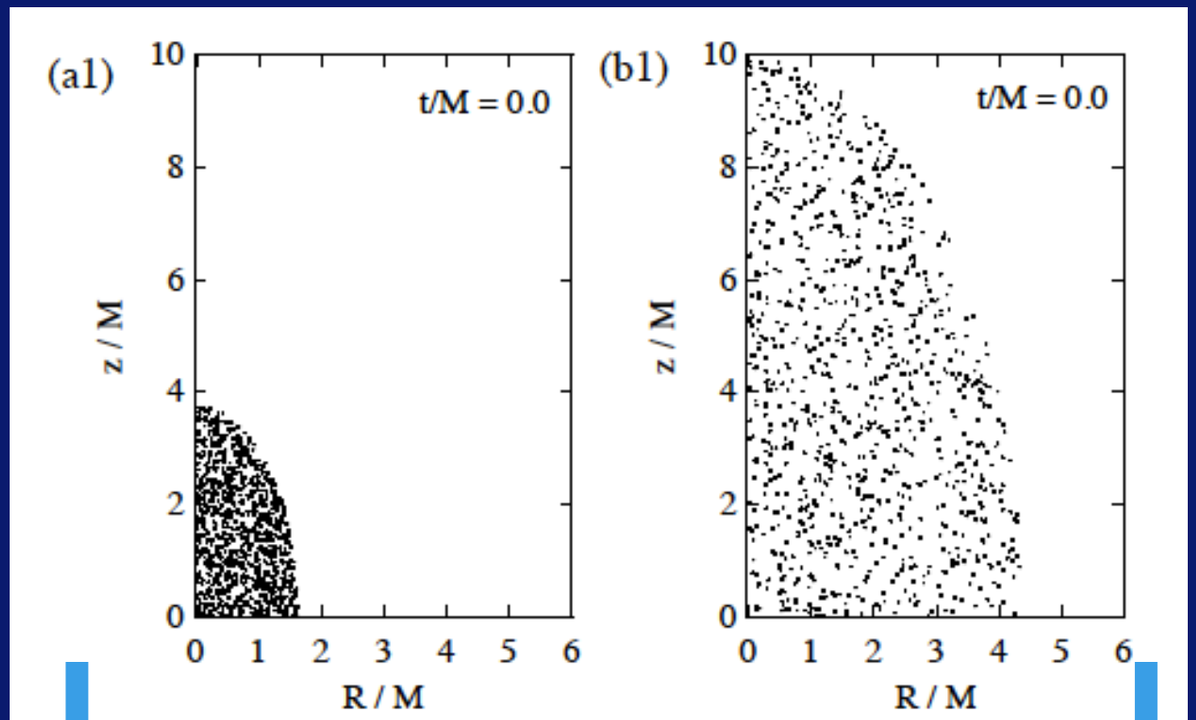

FIG. 2: Snapshots of 5D axisymmetric evolution with the initial matter distribution of $b/M = 4$ [Fig.(a1) and (a2); model 5DSβ in Table I] and 10 [Fig.(b1) and (b2); model 5DSδ]. We see the apparent horizon (AH) is formed at the coordinate time $t/M = 3.3$ for the former model and the area of AH increases, while AH is not observed for the latter model up to the time $t/M = 15.4$ when our code stops due to the large curvature. The big circle indicates the location of the maximum Kretschmann invariant $\mathcal{I}_{\max}$ at the final time at each evolution. Number of particles are reduced to 1/10 for figures.

2. Spheroidal matter collapse
C. Evolution examples (5D, ours)

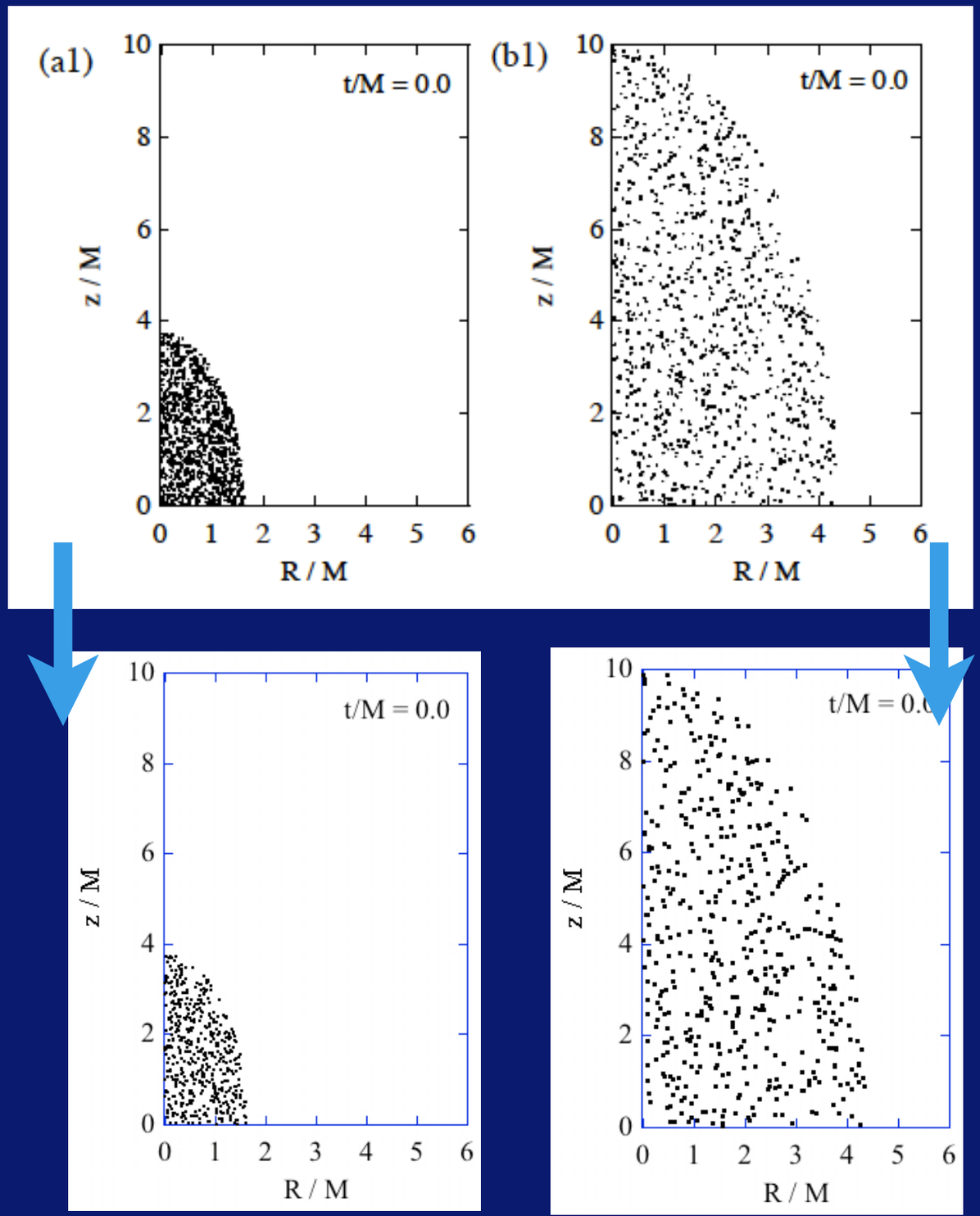

FIG. 2: Snapshots of 5D axisymmetric evolution with the initial matter distribution of $b/M = 4$ [Fig.(a1) and (a2); model 5DSβ in Table I] and 10 [Fig.(b1) and (b2); model 5DSδ]. We see the apparent horizon (AH) is formed at the coordinate time $t/M = 3.3$ for the former model and the area of AH increases, while AH is not observed for the latter model up to the time $t/M = 15.4$ when our code stops due to the large curvature. The big circle indicates the location of the maximum Kretschmann invariant $\mathcal{I}_{\rm max}$ at the final time at each evolution. Number of particles are reduced to 1/10 for figures.

2. Spheroidal matter collapse
C. Evolution examples (5D, ours)

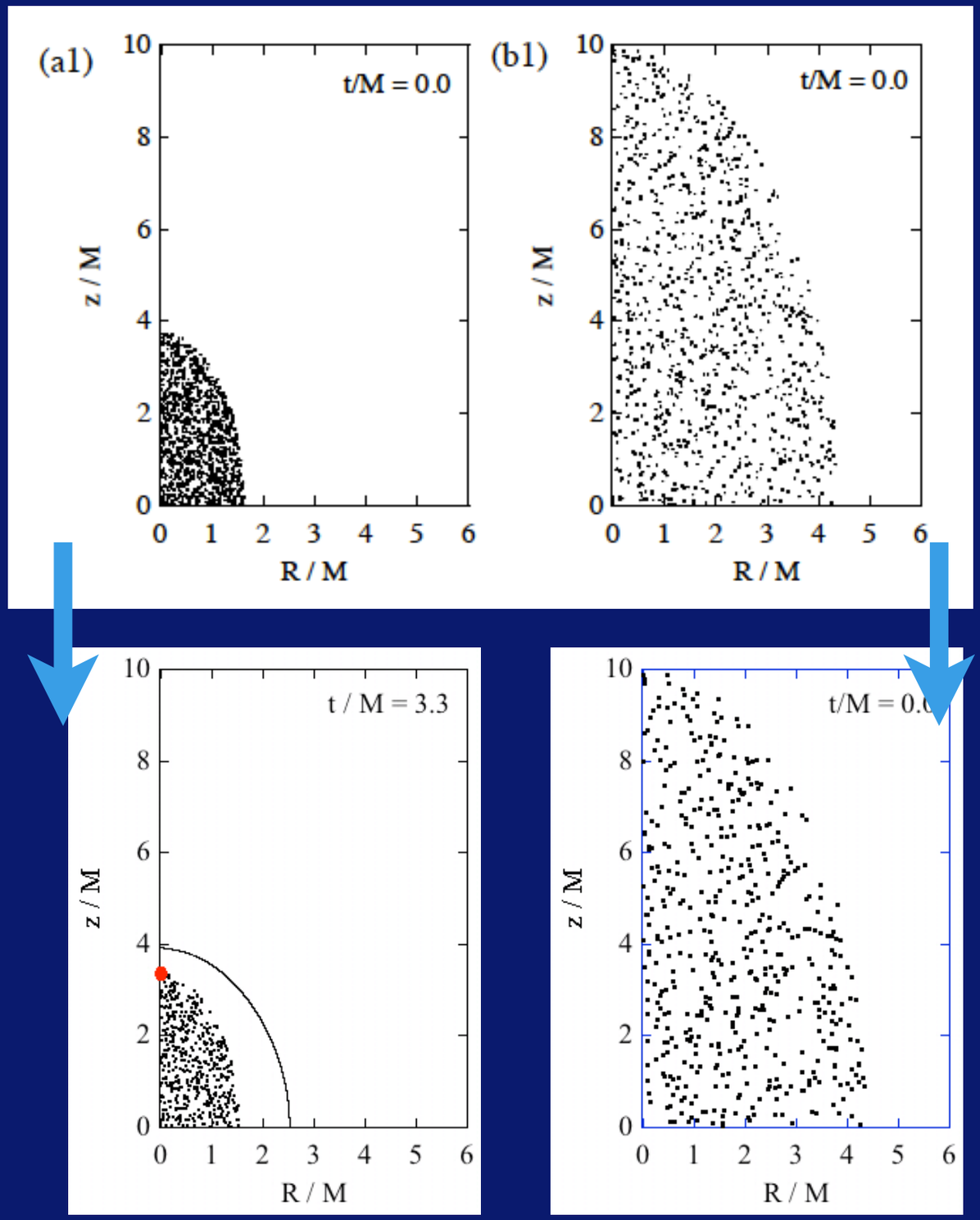

FIG. 2: Snapshots of 5D axisymmetric evolution with the initial matter distribution of $b/M = 4$ [Fig.(a1) and (a2); model 5DSβ in Table I] and 10 [Fig.(b1) and (b2); model 5DSδ]. We see the apparent horizon (AH) is formed at the coordinate time $t/M = 3.3$ for the former model and the area of AH increases, while AH is not observed for the latter model up to the time $t/M = 15.4$ when our code stops due to the large curvature. The big circle indicates the location of the maximum Kretschmann invariant $\mathcal{I}_{\rm max}$ at the final time at each evolution. Number of particles are reduced to 1/10 for figures.

2. Spheroidal matter collapse
C. Evolution examples (5D, ours)

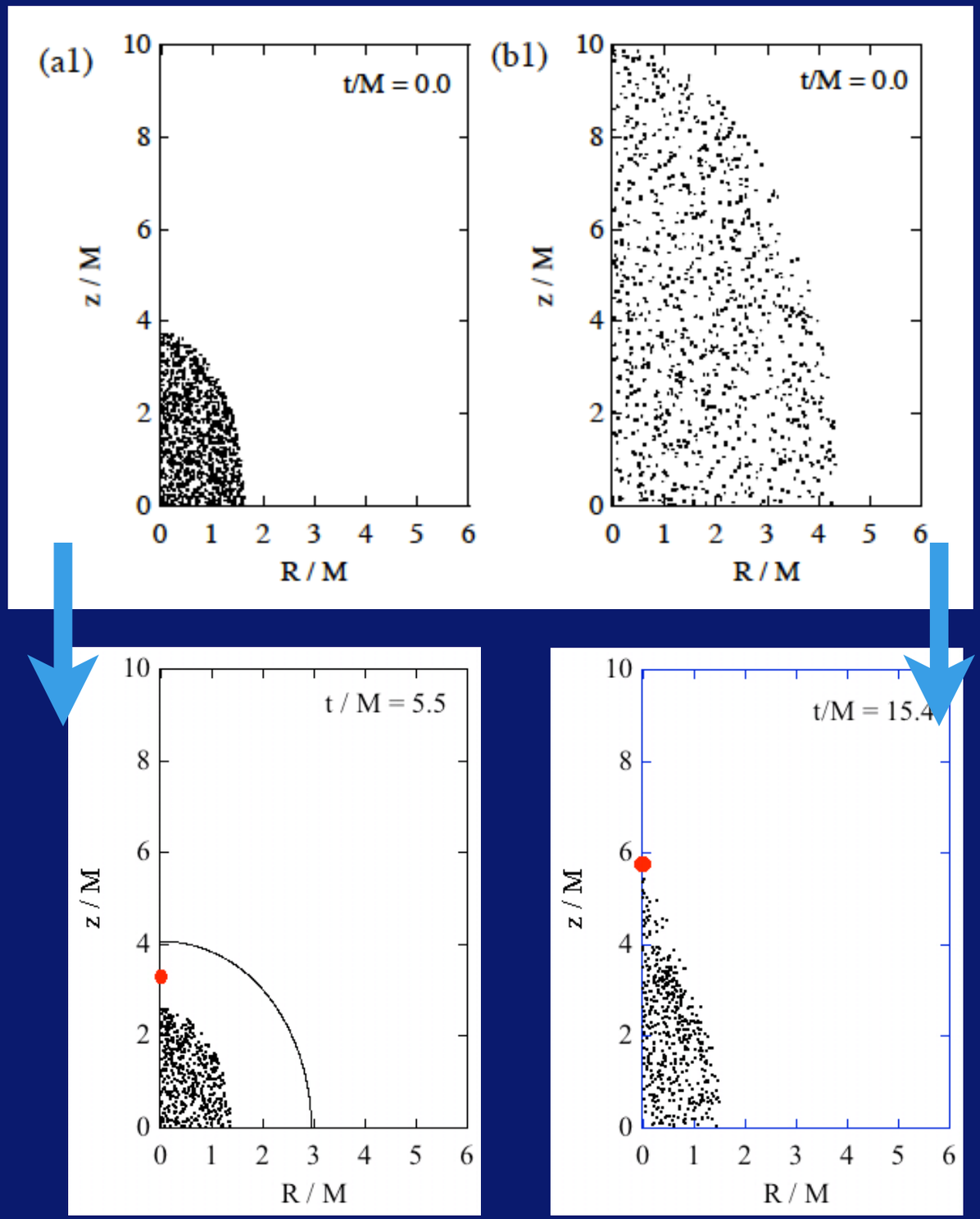

FIG. 2: Snapshots of 5D axisymmetric evolution with the initial matter distribution of $b/M = 4$ [Fig.(a1) and (a2); model 5DSβ in Table I] and 10 [Fig.(b1) and (b2); model 5DSδ]. We see the apparent horizon (AH) is formed at the coordinate time $t/M = 3.3$ for the former model and the area of AH increases, while AH is not observed for the latter model up to the time $t/M = 15.4$ when our code stops due to the large curvature. The big circle indicates the location of the maximum Kretschmann invariant $\mathcal{I}_{\max}$ at the final time at each evolution. Number of particles are reduced to 1/10 for figures.

2. Spheroidal matter collapse
C. Evolution examples (5D, ours)

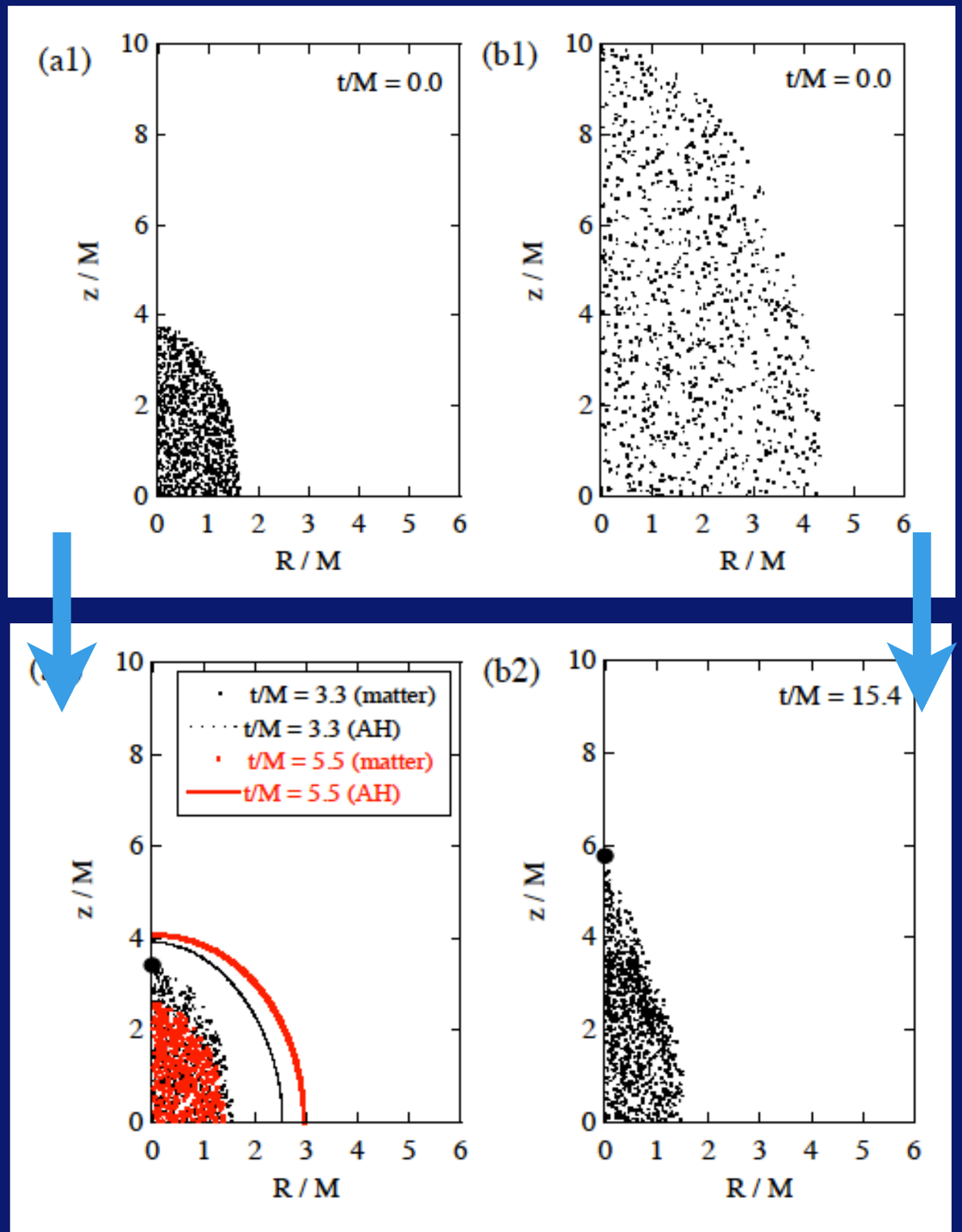

FIG. 2: Snapshots of 5D axisymmetric evolution with the initial matter distribution of $b/M = 4$ [Fig.(a1) and (a2); model 5DSβ in Table I] and 10 [Fig.(b1) and (b2); model 5DSδ]. We see the apparent horizon (AH) is formed at the coordinate time $t/M = 3.3$ for the former model and the area of AH increases, while AH is not observed for the latter model up to the time $t/M = 15.4$ when our code stops due to the large curvature. The big circle indicates the location of the maximum Kretschmann invariant $\mathcal{I}_{\rm max}$ at the final time at each evolution. Number of particles are reduced to 1/10 for figures.

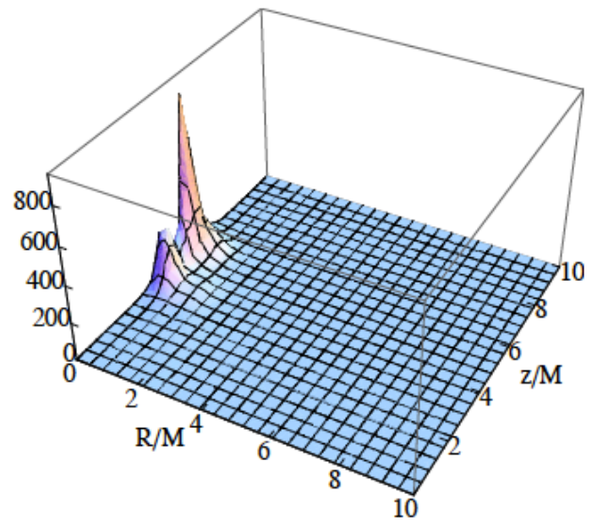

FIG. 3: Kretschmann invariant $\mathcal{I}$ for model 5DSδ at $t/M = 15.4$. The maximum is $O(1000)$, and its location is on z-axis, just outside of the matter.

2. Spheroidal matter collapse
C. Evolution examples (5D, ours)

$SO(3)$

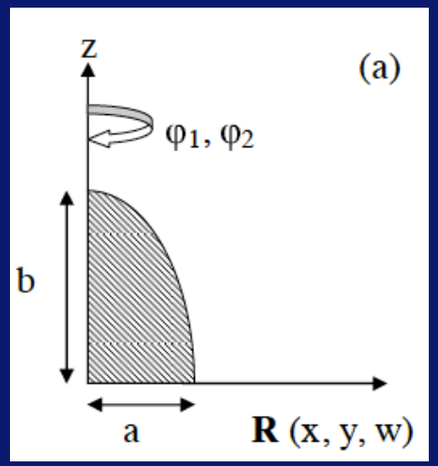

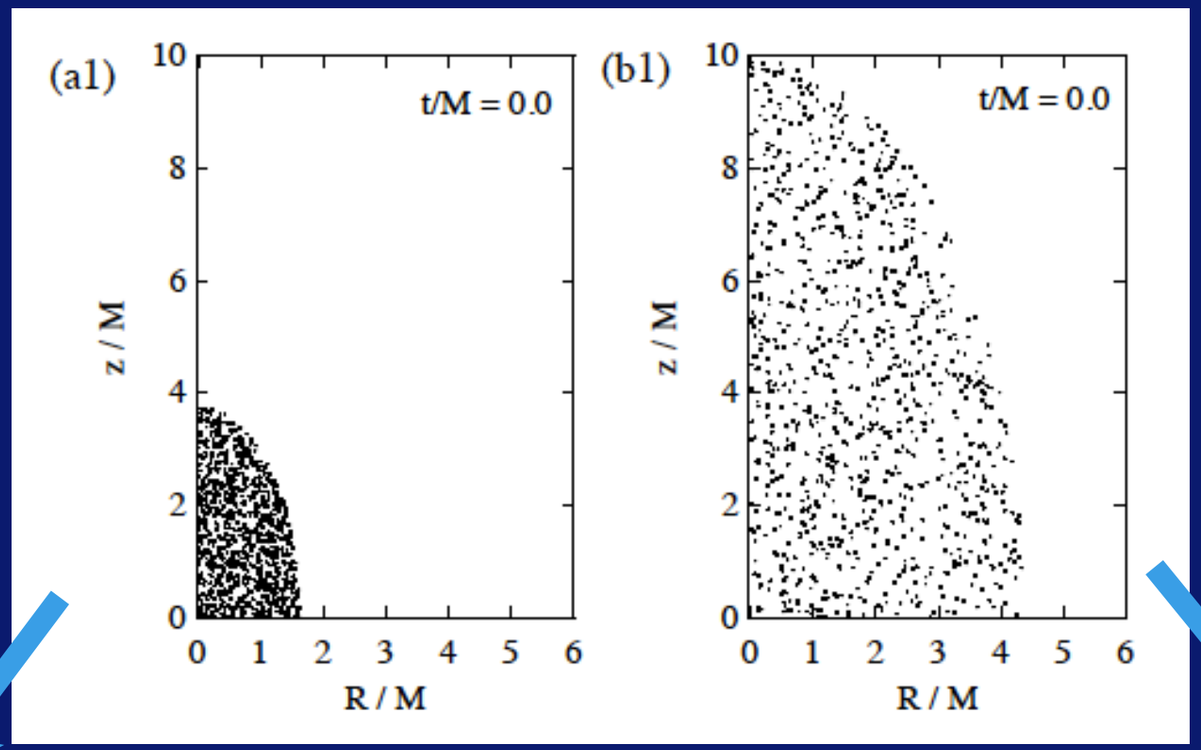

$U(1) \times U(1)$

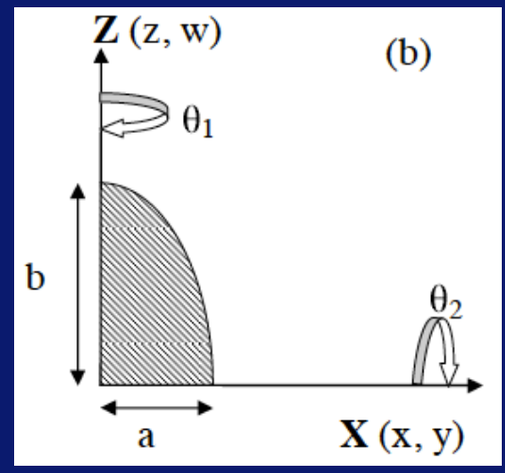

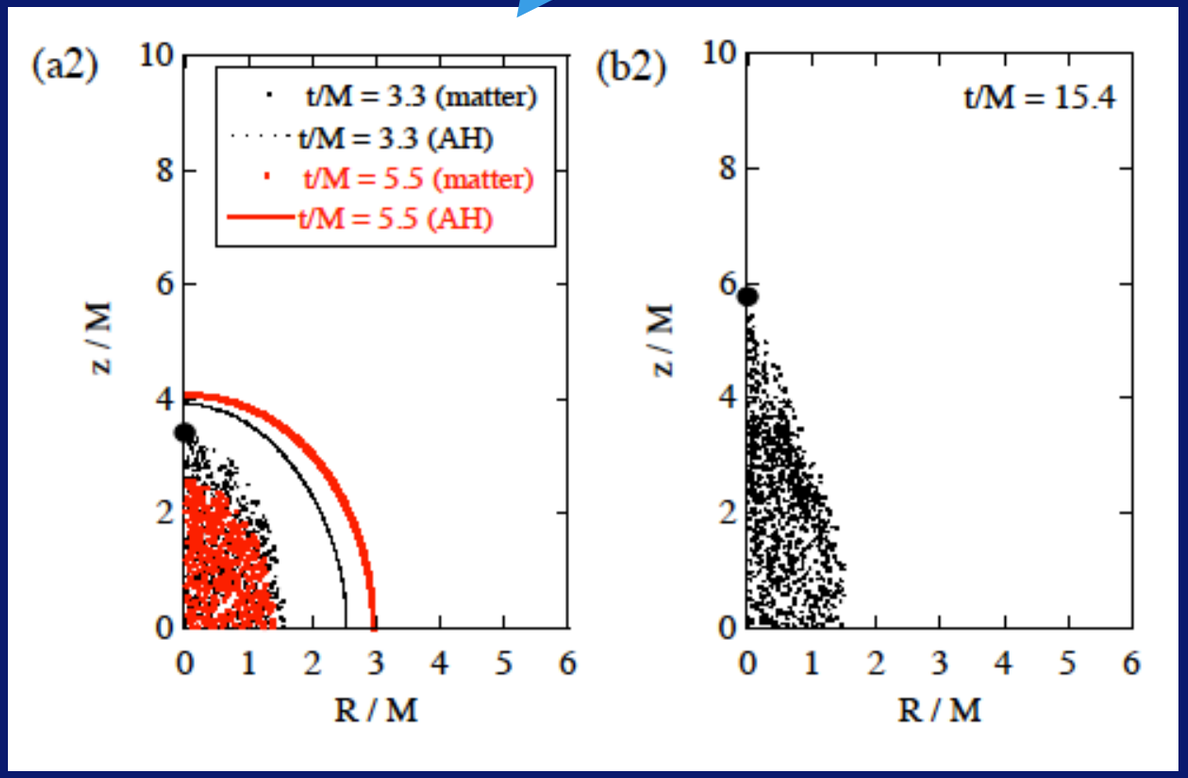

2. Spheroidal matter collapse
C. Evolution examples (5D, ours)

$SO(3)$

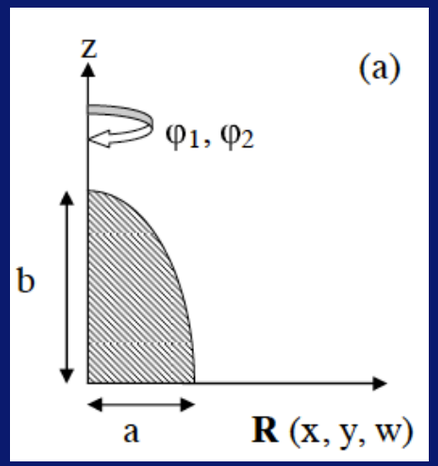

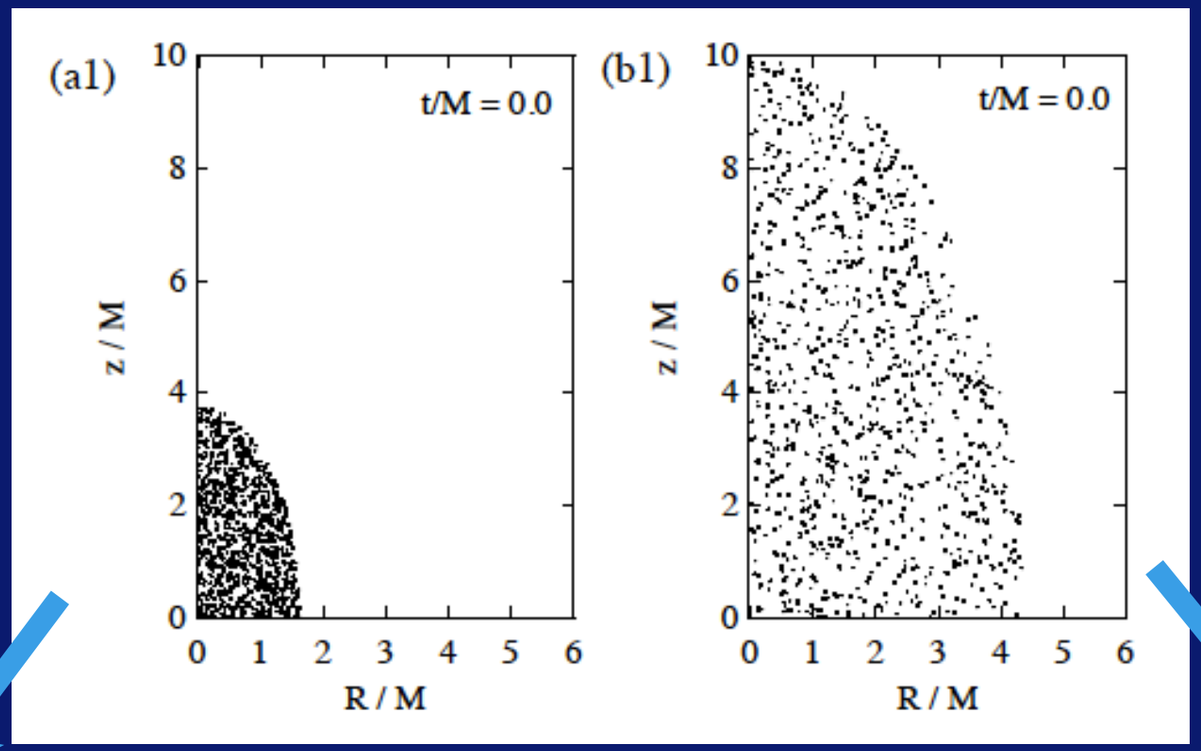

$U(1) \times U(1)$

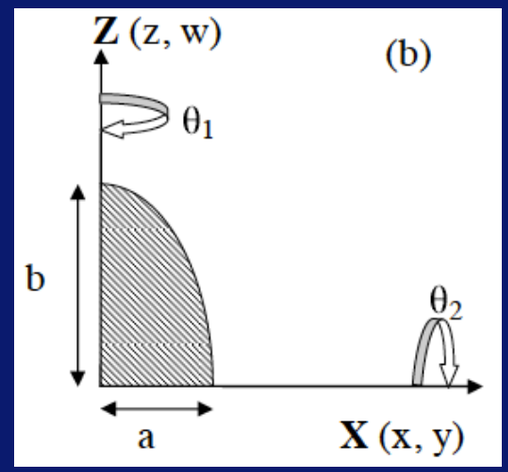

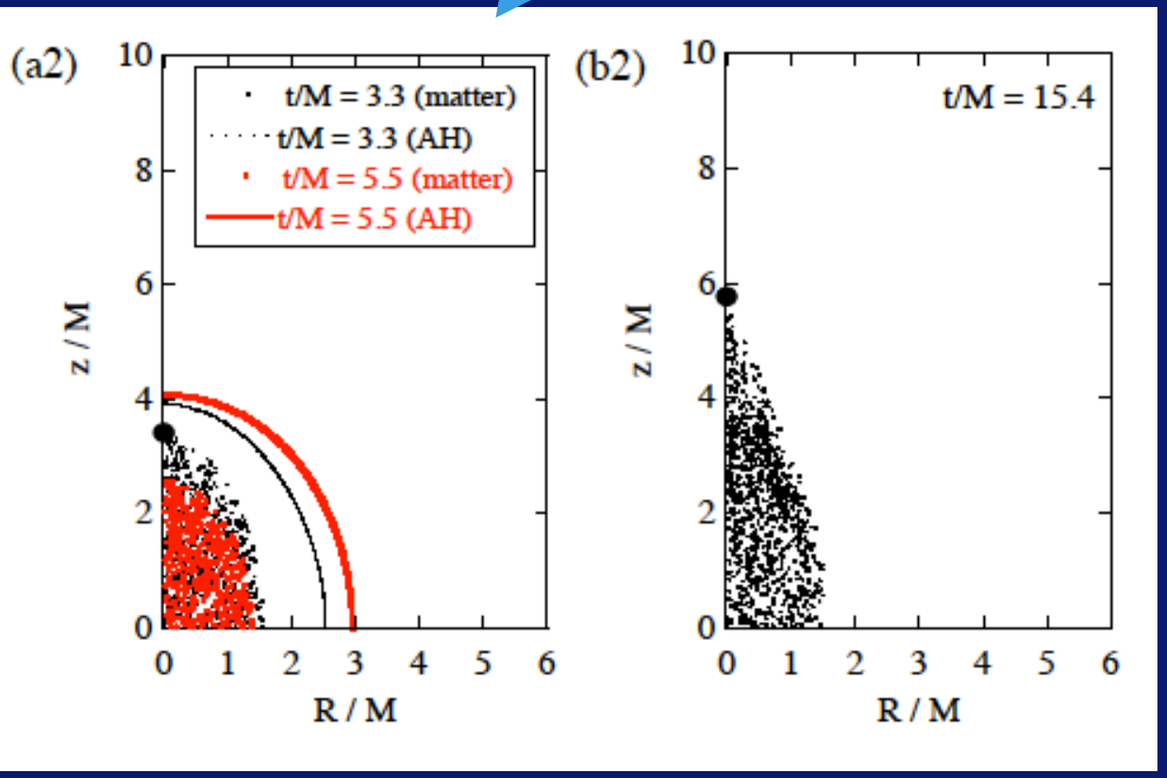

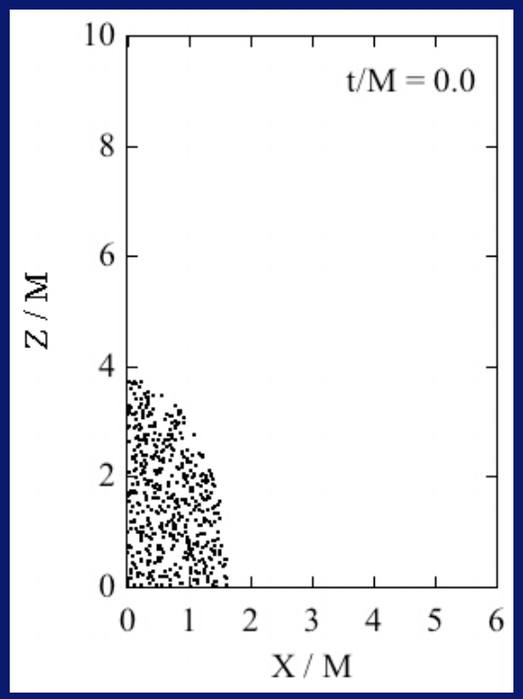

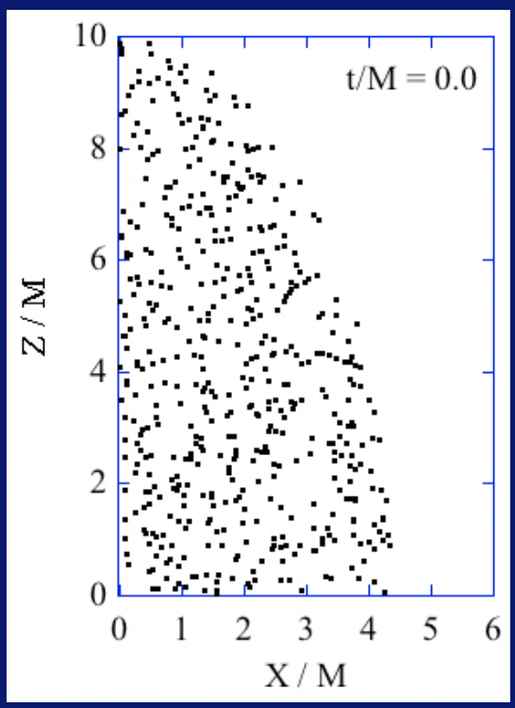

2. Spheroidal matter collapse
C. Evolution examples (5D, ours)

$SO(3)$

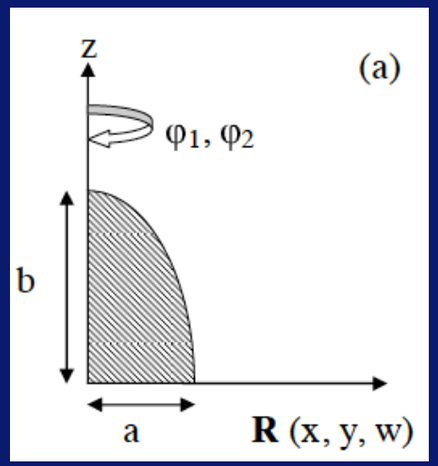

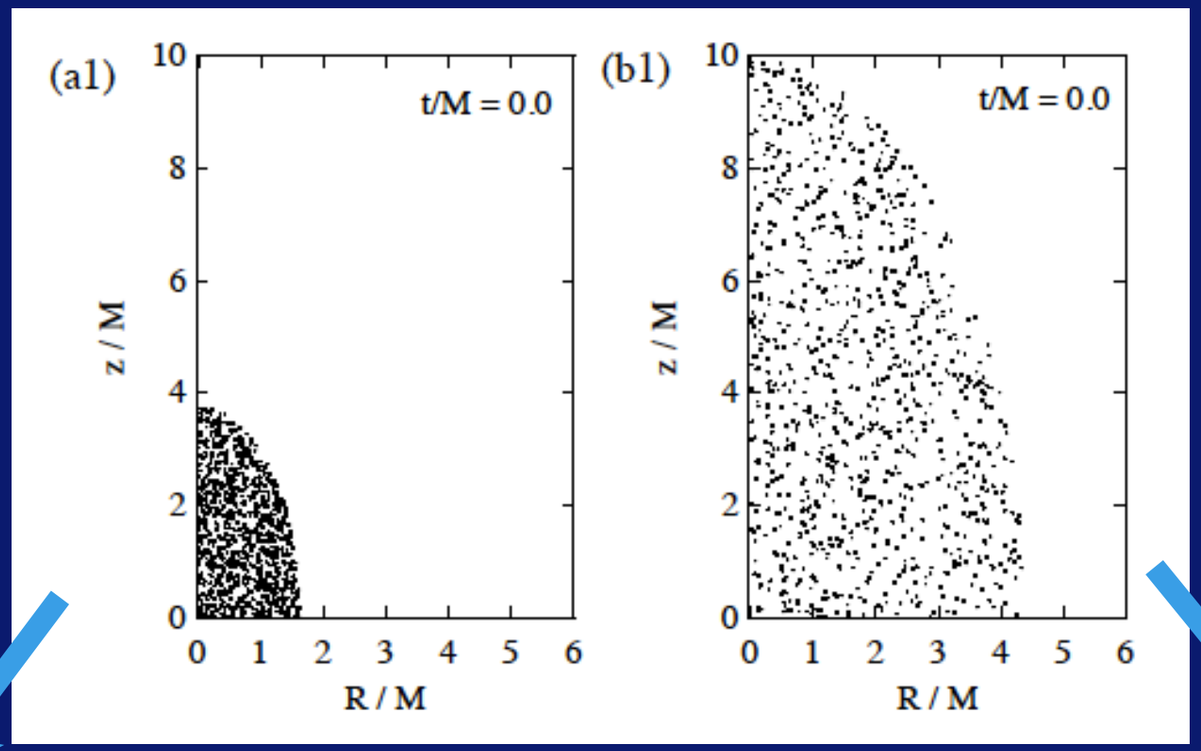

$U(1) \times U(1)$

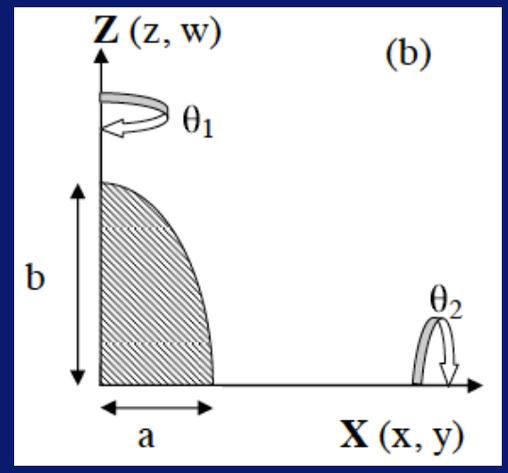

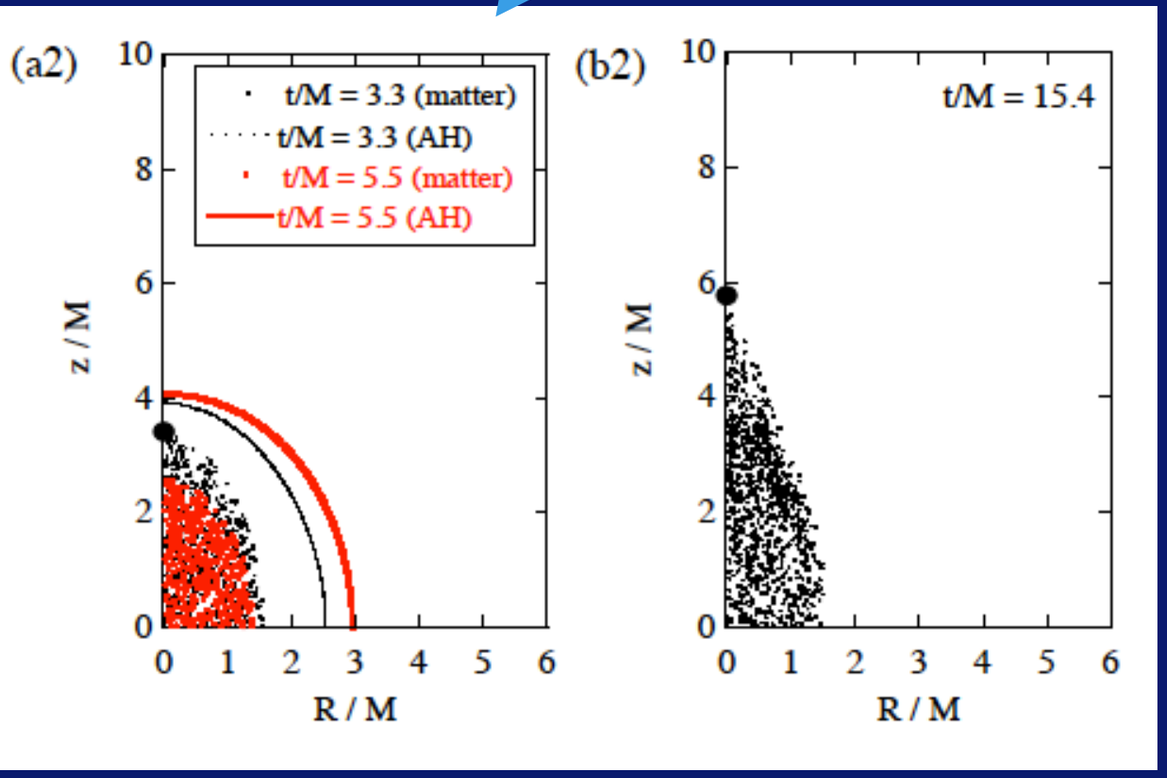

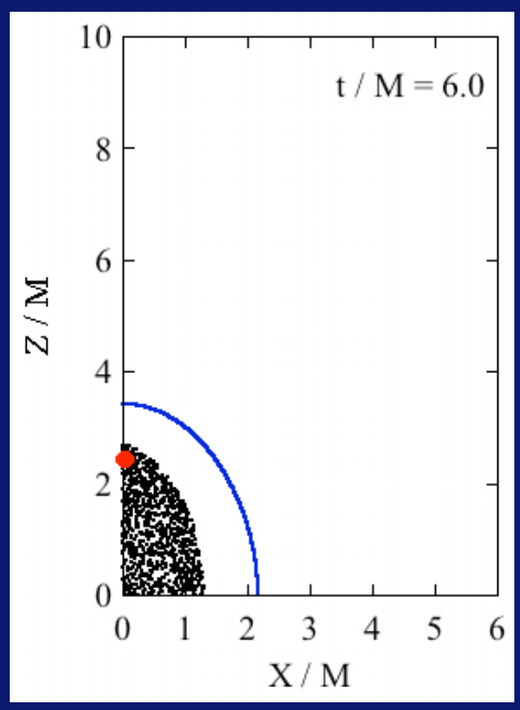

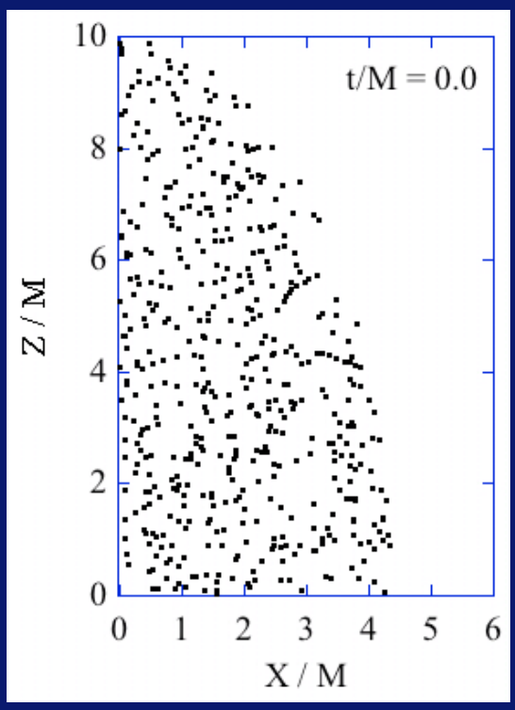

2. Spheroidal matter collapse
C. Evolution examples (5D, ours)

$SO(3)$

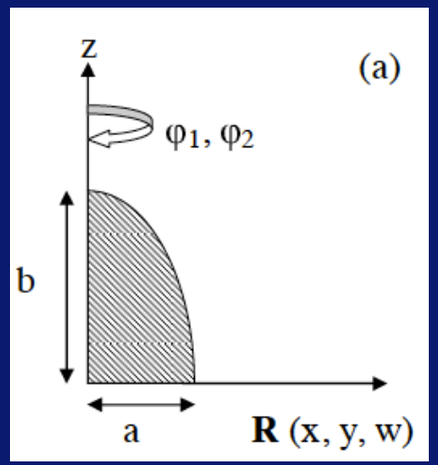

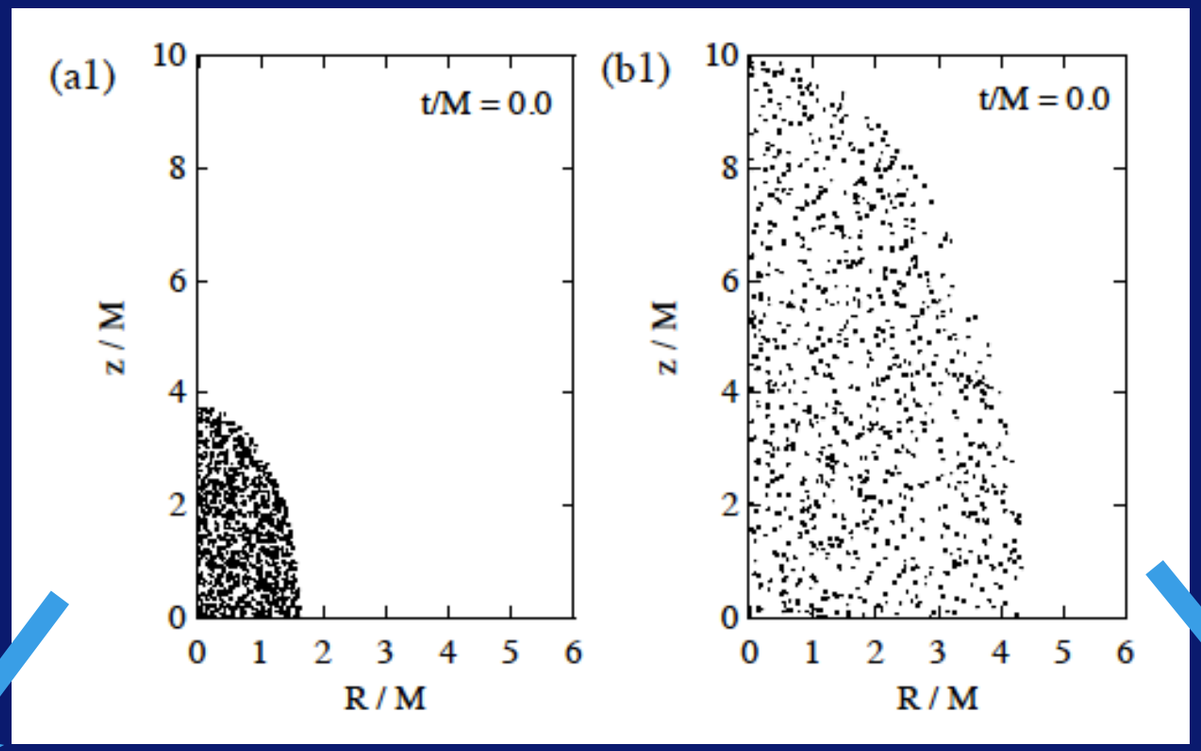

$U(1) \times U(1)$

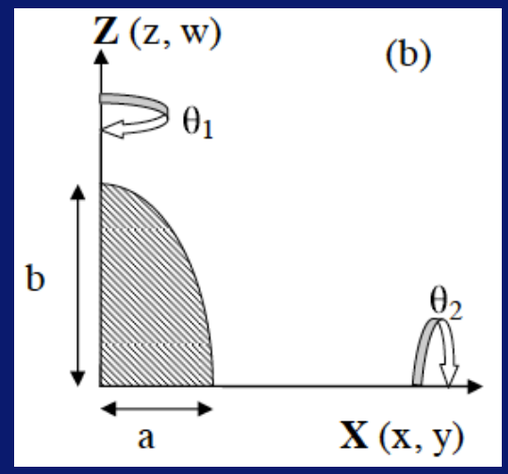

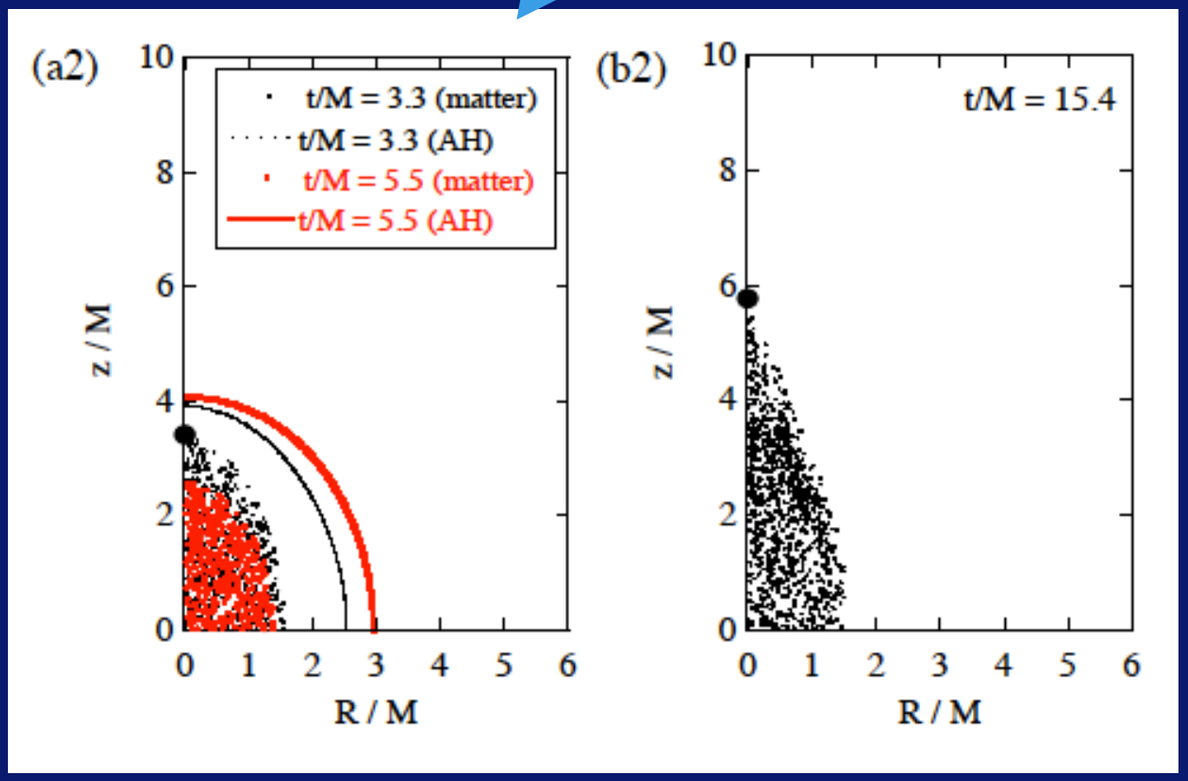

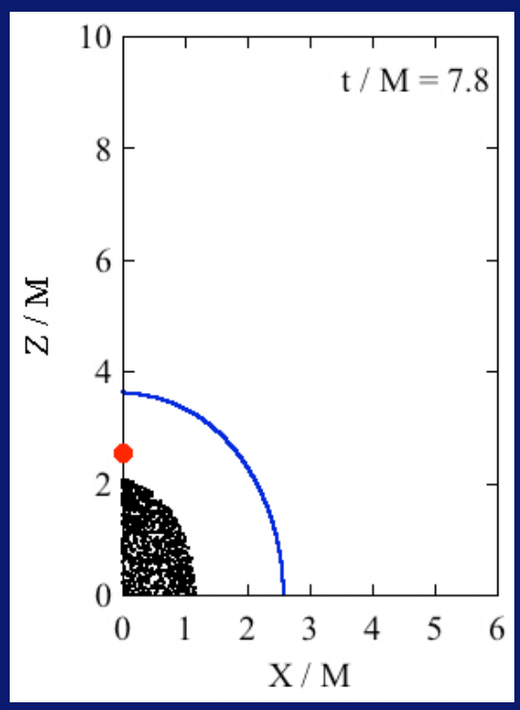

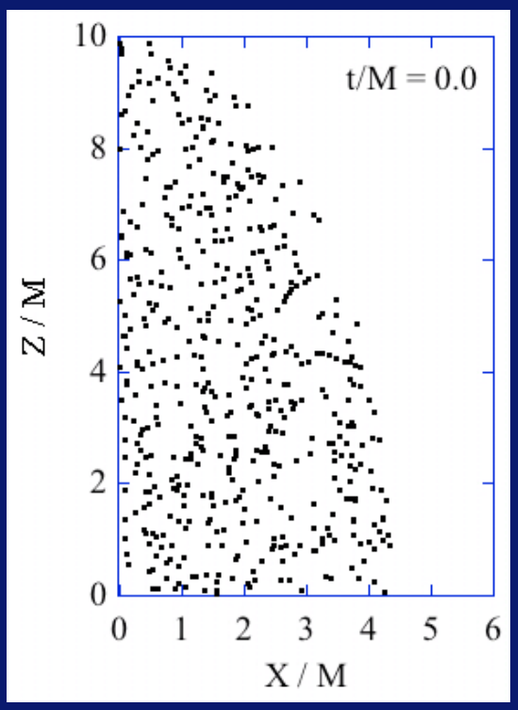

2. Spheroidal matter collapse
C. Evolution examples (5D, ours)

$SO(3)$

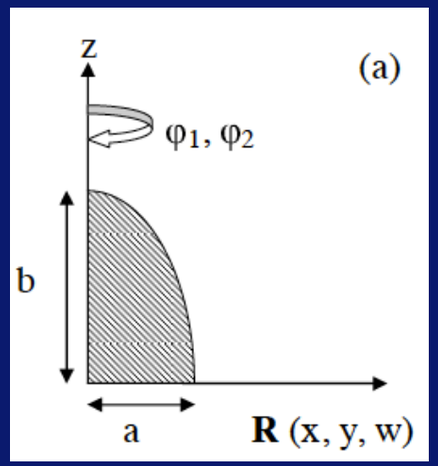

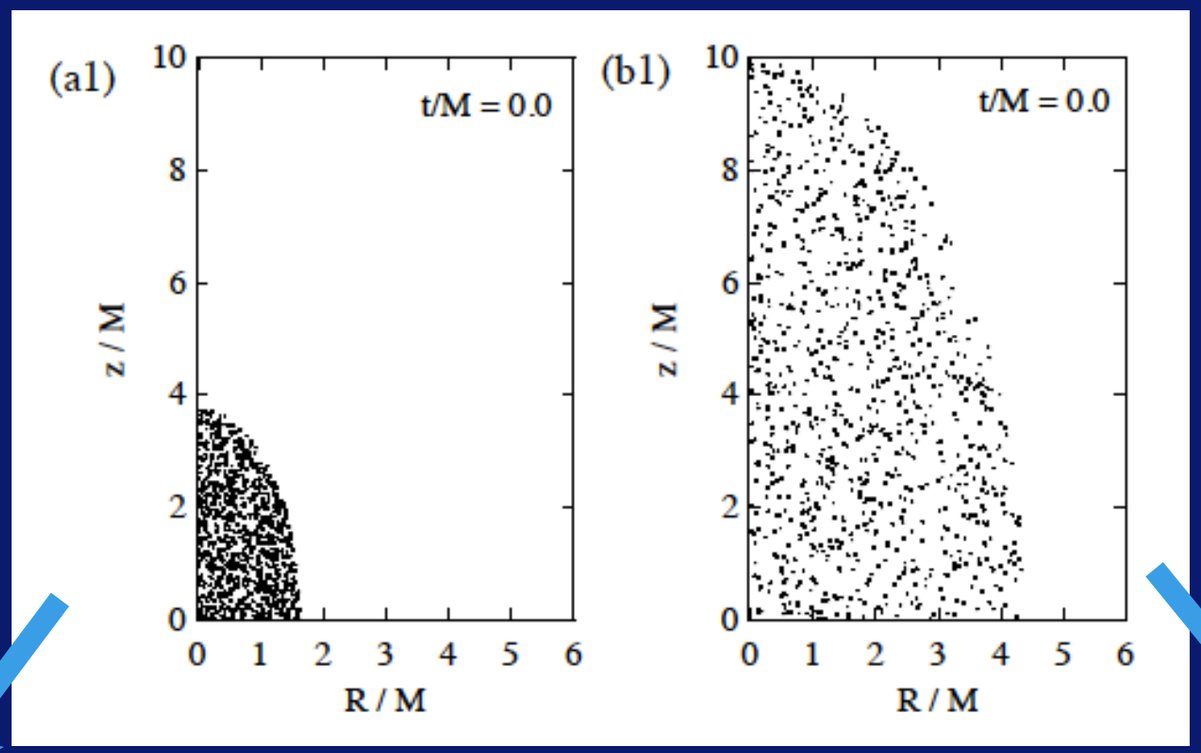

$U(1) \times U(1)$

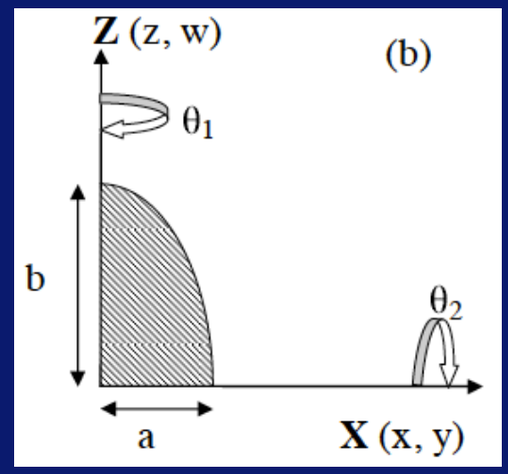

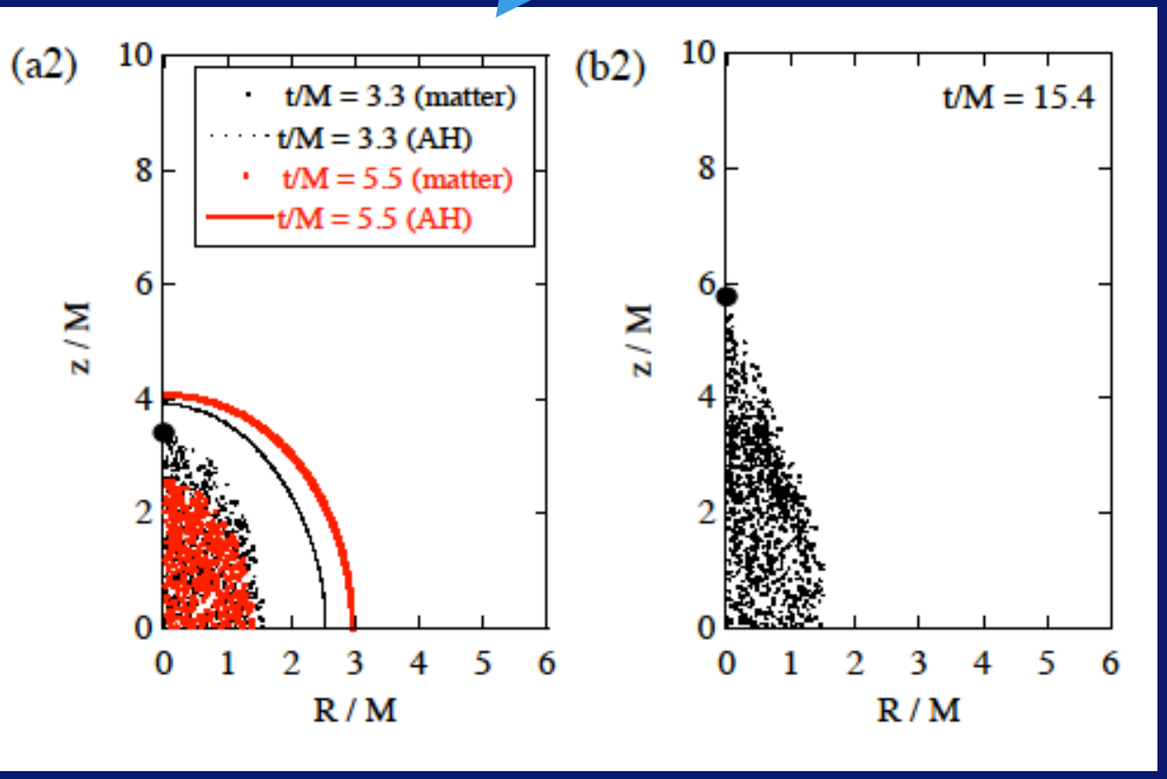

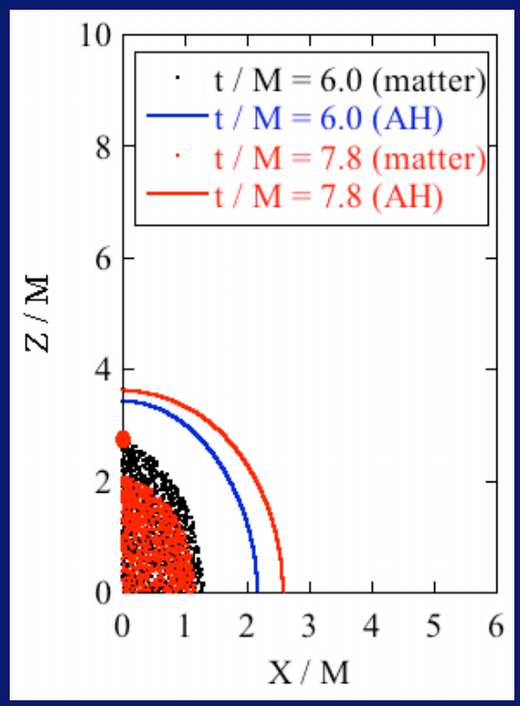

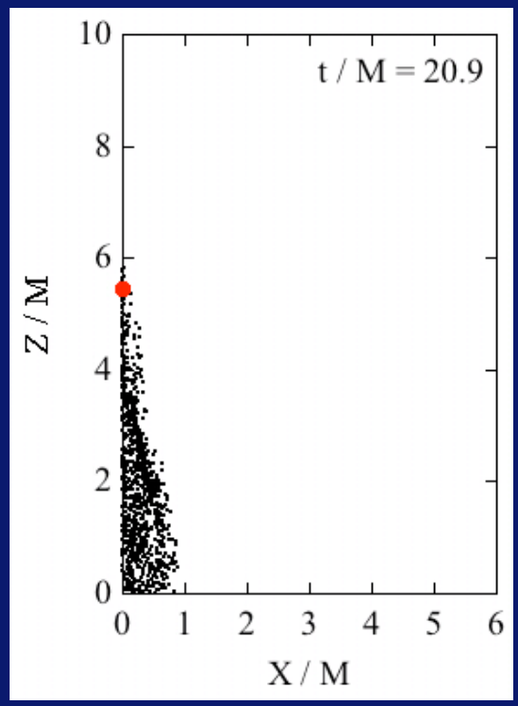

2. Spheroidal matter collapse
D. Comparisons 4D vs. 5D

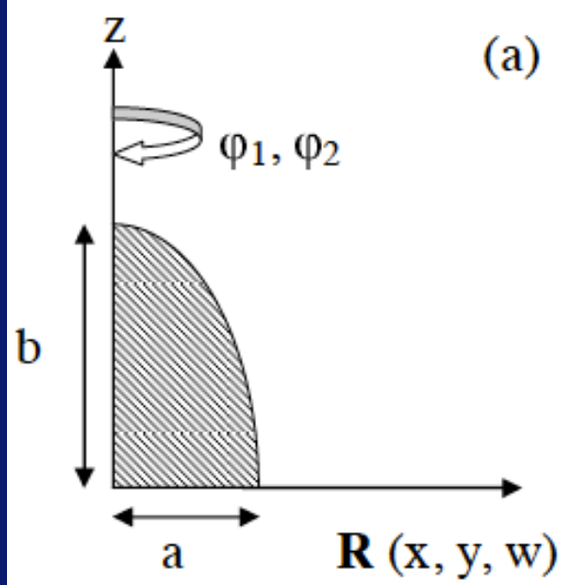

b/M $(t=0)$	2.50	4.00	6.25	10.00
4D axisym.	4Dα	4Dβ	4Dγ	4Dδ
	AH-formed	no	no	no
	$e_{\rm AH}=0.90$			
	$e_{\rm f}=0.92$	$e_{\rm f}=0.89$	$e_{\rm f}=0.92$	$e_{\rm f}=0.96$
5D axisym. SO(3)	5DSα	5DSβ	5DSγ	5DSδ
	AH-formed	AH-formed	no	no
	$e_{\rm AH}=0.88$	$e_{\rm AH}=0.88$		
	$e_{\rm f}=0.82$	$e_{\rm f}=0.84$	$e_{\rm f}=0.88$	$e_{\rm f}=0.96$

TABLE I: Model-names and the results of their evolutions whether we observed AH or not. The eccentricity e of the collapsed matter configurations is also shown; $e_{\rm AH}$ and $e_{\rm f}$ are at the time of AH formation (if formed), and on the numerically obtained final hypersurface, respectively.

2. Spheroidal matter collapse
D. Comparisons 4D vs. 5D

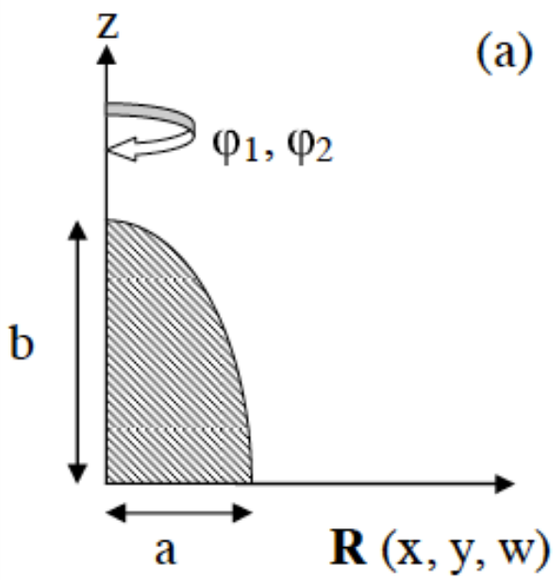

b/M $(t=0)$	2.50	4.00	6.25	10.00
4D axisym.	4Dα	4Dβ	4Dγ	4Dδ
	AH-formed	no	no	no
	$e_{\rm AH}=0.90$			
	$e_{\rm f}=0.92$	$e_{\rm f}=0.89$	$e_{\rm f}=0.92$	$e_{\rm f}=0.96$
5D axisym. SO(3)	5DSα	5DSβ	5DSγ	5DSδ
	AH-formed	AH-formed	no	no
	$e_{\rm AH}=0.88$	$e_{\rm AH}=0.88$		
	$e_{\rm f}=0.82$	$e_{\rm f}=0.84$	$e_{\rm f}=0.88$	$e_{\rm f}=0.96$

TABLE I: Model-names and the results of their evolutions whether we observed AH or not. The eccentricity e of the collapsed matter configurations is also shown; $e_{\rm AH}$ and $e_{\rm f}$ are at the time of AH formation (if formed), and on the numerically obtained final hypersurface, respectively.

2. Spheroidal matter collapse
D. Comparisons 4D vs. 5D

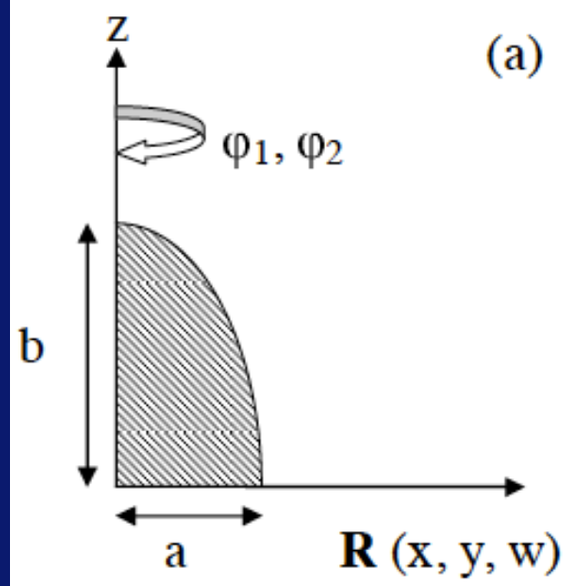

b/M $(t=0)$	2.50	4.00	6.25	10.00
4D axisym.	4Dα	4Dβ	4Dγ	4Dδ
	AH-formed	no	no	no
	$e_{\rm AH}=0.90$			
	$e_{\rm f}=0.92$	$e_{\rm f}=0.89$	$e_{\rm f}=0.92$	$e_{\rm f}=0.96$
5D axisym. SO(3)	5DSα	5DSβ	5DSγ	5DSδ
	AH-formed	AH-formed	no	no
	$e_{\rm AH}=0.88$	$e_{\rm AH}=0.88$		
	$e_{\rm f}=0.82$	$e_{\rm f}=0.84$	$e_{\rm f}=0.88$	$e_{\rm f}=0.96$

towards spindle

towards spherical

TABLE I: Model-names and the results of their evolutions whether we observed AH or not. The eccentricity e of the collapsed matter configurations is also shown; $e_{\rm AH}$ and $e_{\rm f}$ are at the time of AH formation (if formed), and on the numerically obtained final hypersurface, respectively.

2. Spheroidal matter collapse
D. Comparisons 4D vs. 5D

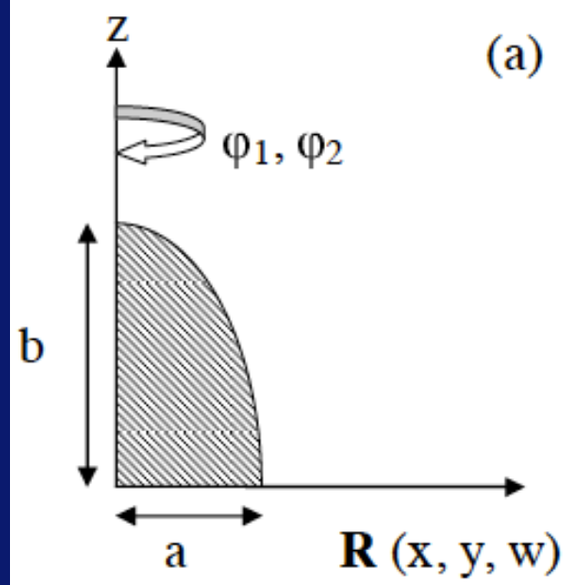

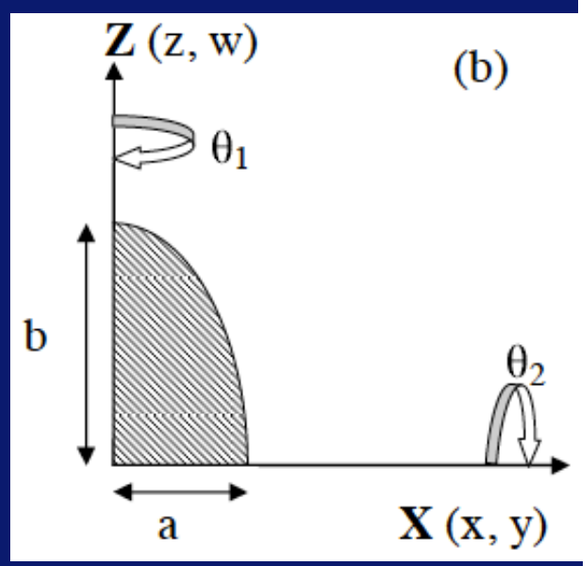

b/M $(t=0)$	2.50	4.00	6.25	10.00
4D axisym.	4Dα	4Dβ	4Dγ	4Dδ
	AH-formed	no	no	no
	$e_{\rm AH}=0.90$			
	$e_{\rm f}=0.92$	$e_{\rm f}=0.89$	$e_{\rm f}=0.92$	$e_{\rm f}=0.96$
5D axisym. SO(3)	5DSα	5DSβ	5DSγ	5DSδ
	AH-formed	AH-formed	no	no
	$e_{\rm AH}=0.88$	$e_{\rm AH}=0.88$		
	$e_{\rm f}=0.82$	$e_{\rm f}=0.84$	$e_{\rm f}=0.88$	$e_{\rm f}=0.96$
5D double axisym. U(1)×U(1)	5DUα	5DUβ	5DUγ	5DUδ
	AH-formed	AH-formed	AH-formed	no
	$e_{\rm AH}=0.86$	$e_{\rm AH}=0.87$	$e_{\rm AH}=0.92$	
	$e_{\rm f}=0.79$	$e_{\rm f}=0.81$	$e_{\rm f}=0.90$	$e_{\rm f}=0.98$

towards spindle

towards spherical

2. Spheroidal matter collapse
D. Comparisons 4D vs. 5D

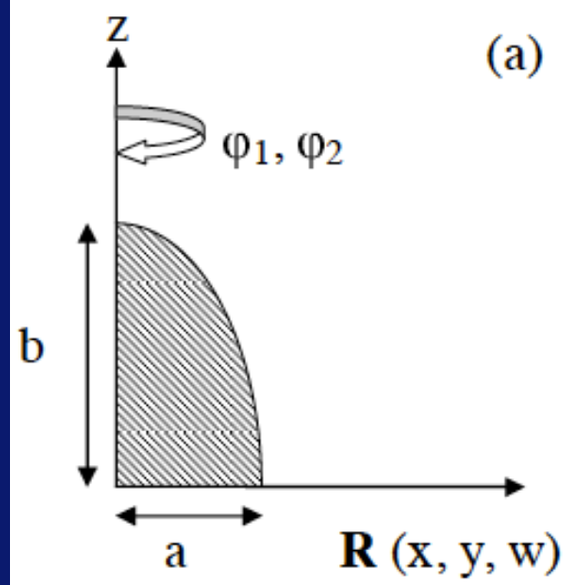

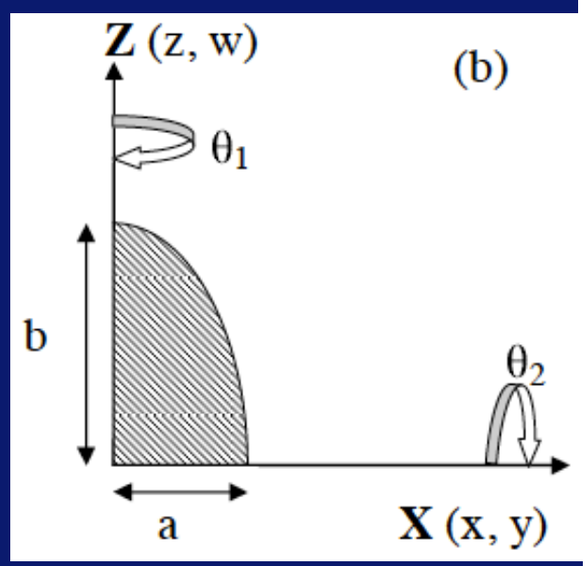

b/M $(t=0)$	2.50	4.00	6.25	10.00
4D axisym.	4Dα	4Dβ	4Dγ	4Dδ
	AH-formed	no	no	no
	$e_{\rm AH}=0.90$			
	$e_{\rm f}=0.92$	$e_{\rm f}=0.89$	$e_{\rm f}=0.92$	$e_{\rm f}=0.96$
5D axisym. SO(3)	5DSα	5DSβ	5DSγ	5DSδ
	AH-formed	AH-formed	no	no
	$e_{\rm AH}=0.88$	$e_{\rm AH}=0.88$		
	$e_{\rm f}=0.82$	$e_{\rm f}=0.84$	$e_{\rm f}=0.88$	$e_{\rm f}=0.96$
5D double axisym. U(1)×U(1)	5DUα	5DUβ	5DUγ	5DUδ
	AH-formed	AH-formed	AH-formed	no
	$e_{\rm AH}=0.86$	$e_{\rm AH}=0.87$	$e_{\rm AH}=0.92$	
	$e_{\rm f}=0.79$	$e_{\rm f}=0.81$	$e_{\rm f}=0.90$	$e_{\rm f}=0.98$

towards spindle

towards spherical

towards spherical towards spindle

2. Spheroidal matter collapse
D. Comparisons 4D vs. 5D

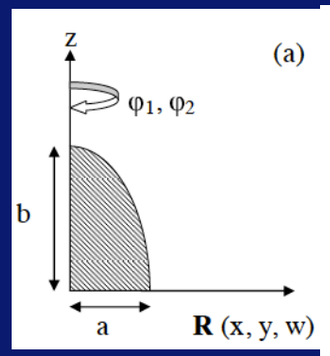

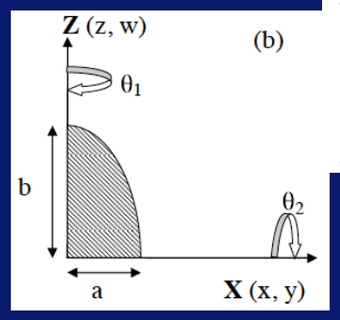

b/M $(t=0)$	2.50	4.00	6.25	10.00
4D axisym.	4Dα	4Dβ	4Dγ	4Dδ
	AH-formed	no	no	no
	$e_{\rm AH}=0.90$			
	$e_{\rm f}=0.92$	$e_{\rm f}=0.89$	$e_{\rm f}=0.92$	$e_{\rm f}=0.96$
5D axisym. SO(3)	5DSα	5DSβ	5DSγ	5DSδ
	AH-formed	AH-formed	no	no
	$e_{\rm AH}=0.88$	$e_{\rm AH}=0.88$		
	$e_{\rm f}=0.82$	$e_{\rm f}=0.84$	$e_{\rm f}=0.88$	$e_{\rm f}=0.96$
5D double axisym. U(1)×U(1)	5DUα	5DUβ	5DUγ	5DUδ
	AH-formed	AH-formed	AH-formed	no
	$e_{\rm AH}=0.86$	$e_{\rm AH}=0.87$	$e_{\rm AH}=0.92$	
	$e_{\rm f}=0.79$	$e_{\rm f}=0.81$	$e_{\rm f}=0.90$	$e_{\rm f}=0.98$

$$I = R_{abcd}R^{abcd}$$
$$\text{at } I(t_{\rm end})$$

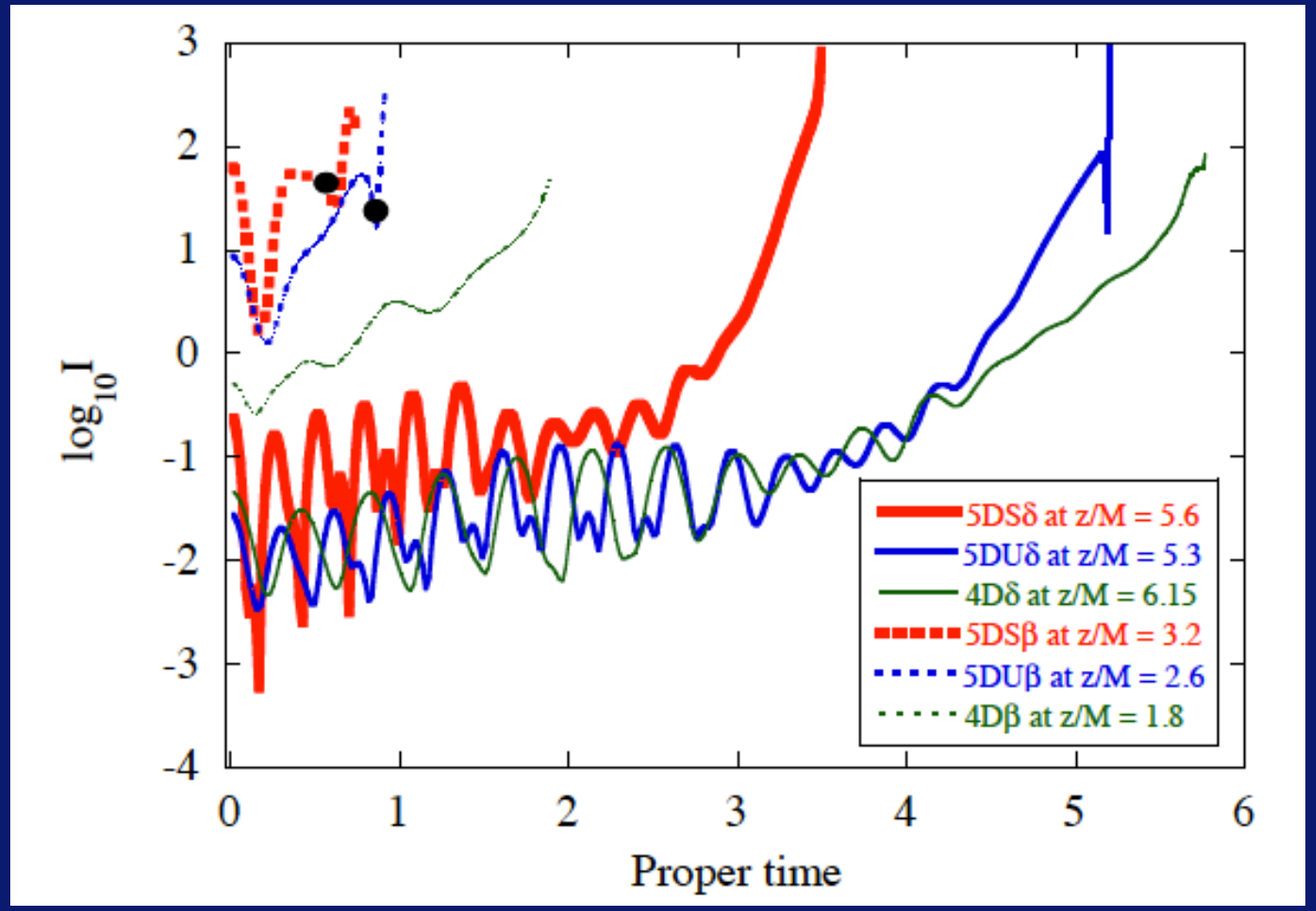

2. Spheroidal matter collapse
D. Comparisons 4D vs. 5D

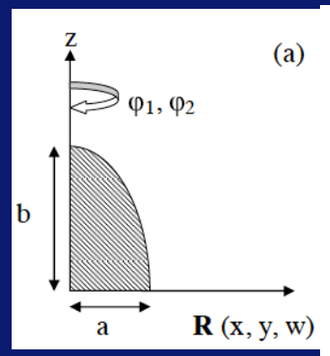

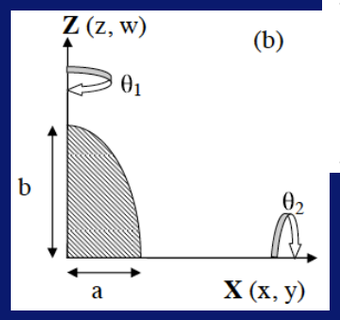

b/M $(t=0)$	2.50	4.00	6.25	10.00
4D axisym.	4Dα AH-formed $e_{AH}=0.90$ $e_f=0.92$	4Dβ no $e_f=0.89$	4Dγ no $e_f=0.92$	4Dδ no $e_f=0.96$
5D axisym. SO(3)	5DSα AH-formed $e_{AH}=0.88$ $e_f=0.82$	5DSβ AH-formed $e_{AH}=0.88$ $e_f=0.84$	5DSγ no $e_f=0.88$	5DSδ no $e_f=0.96$
5D double axisym. U(1)×U(1)	5DUα AH-formed $e_{AH}=0.86$ $e_f=0.79$	5DUβ AH-formed $e_{AH}=0.87$ $e_f=0.81$	5DUγ AH-formed $e_{AH}=0.9$ $e_f=0.90$	5DUδ no $e_f=0.98$

$$I = R_{abcd}R^{abcd}$$
at $I(t_{\rm end})$

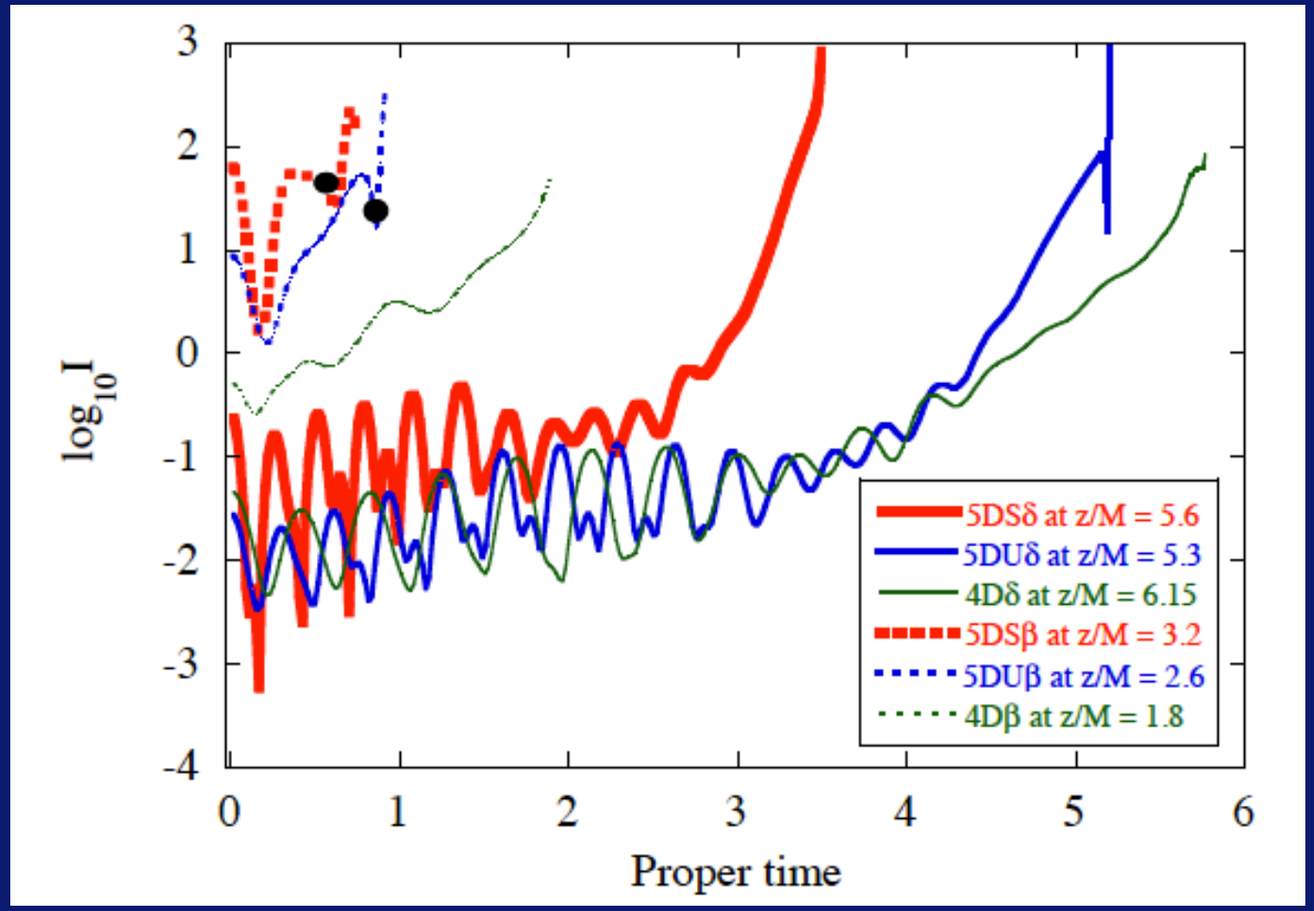

2. Spheroidal matter collapse
D. Comparisons 4D vs. 5D

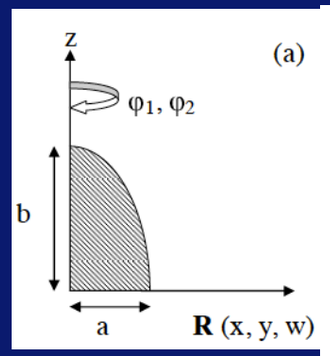

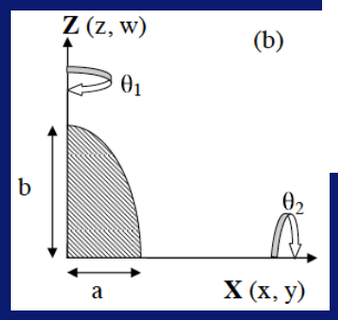

b/M $(t=0)$	2.50	4.00	6.25	10.00
4D axisym.	4Dα AH-formed $e_{\rm AH}=0.90$ $e_{\rm f}=0.92$	4Dβ no $e_{\rm f}=0.89$	4Dγ no $e_{\rm f}=0.92$	4Dδ no $e_{\rm f}=0.96$
5D axisym. SO(3)	5DSα AH-formed $e_{\rm AH}=0.88$ $e_{\rm f}=0.82$	5DSβ AH-formed $e_{\rm AH}=0.88$ $e_{\rm f}=0.84$	5DSγ no $e_{\rm f}=0.88$	5DSδ no $e_{\rm f}=0.96$
5D double axisym. U(1)×U(1)	5DUα AH-formed $e_{\rm AH}=0.86$ $e_{\rm f}=0.79$	5DUβ AH-formed $e_{\rm AH}=0.87$ $e_{\rm f}=0.81$	5DUγ AH-formed $e_{\rm AH}=0.9$ $e_{\rm f}=0.90$	5DUδ no $e_{\rm f}=0.98$

5D collapses
-- proceed rapidly.
-- towards spherically.
-- AH forms in wider ranges.

$$I = R_{abcd}R^{abcd}$$
at $I(t_{\rm end})$

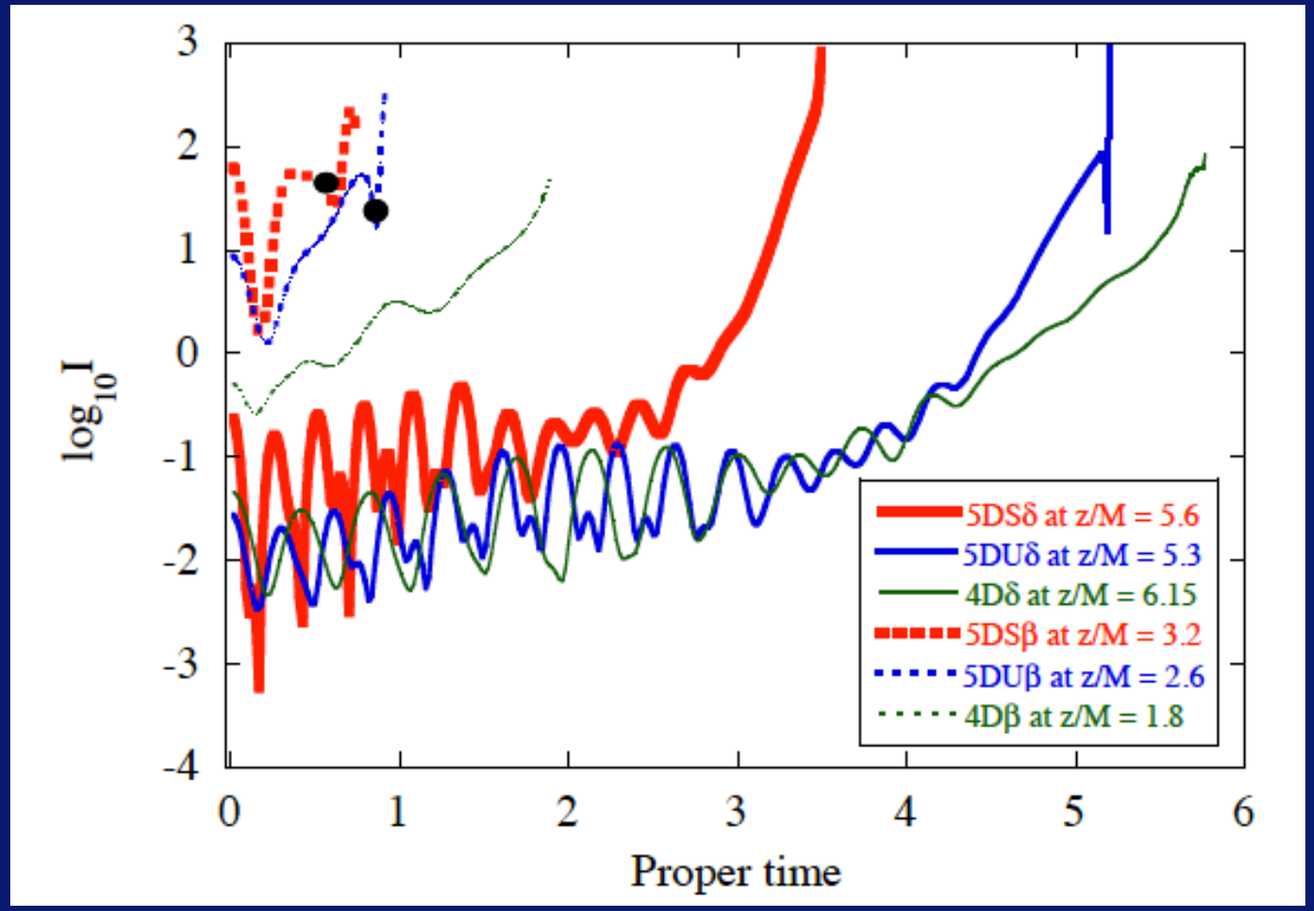

3. Ring matter collapse
A. Initial data construction

- time symmetric, asymptotically flat
- conformal flat
- non-rotating homogeneous dust

- solve the Hamiltonian constraint eq. 512^2 grids
- Apparent Horizon Search
  both for Ring Horizon and Common Horizon
- Define Hoop and check the Hoop Conjecture

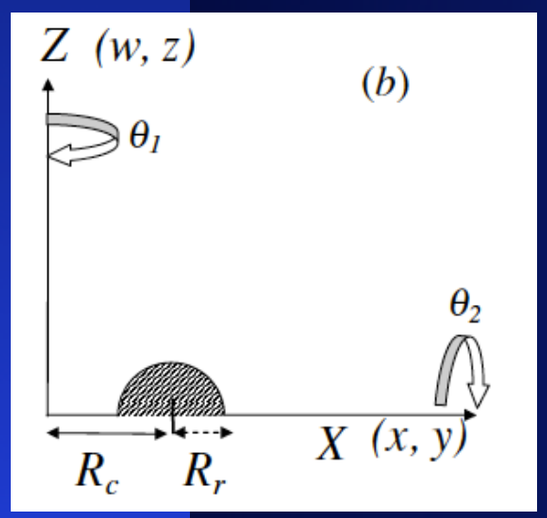

$$ds^2 = \psi(X,Z)^2(dX^2 + dZ^2 + X^2 d\vartheta_1 + Z^2 d\vartheta_2)$$

$$X = \sqrt{x^2+y^2},\quad Z = \sqrt{z^2+w^2},\quad \vartheta_1 = \tan^{-1}\left(\frac{y}{x}\right),\ \vartheta_2 = \tan^{-1}\left(\frac{z}{w}\right)$$

$$\frac{1}{X}\frac{\partial}{\partial X}\left(X\frac{\partial \psi}{\partial X}\right) + \frac{1}{Z}\frac{\partial}{\partial Z}\left(Z\frac{\partial \psi}{\partial Z}\right) = -4\pi^2 G_5 \rho$$

3. Ring matter collapse

A. Apparent Horizon Search, and its Area

Common Horizon

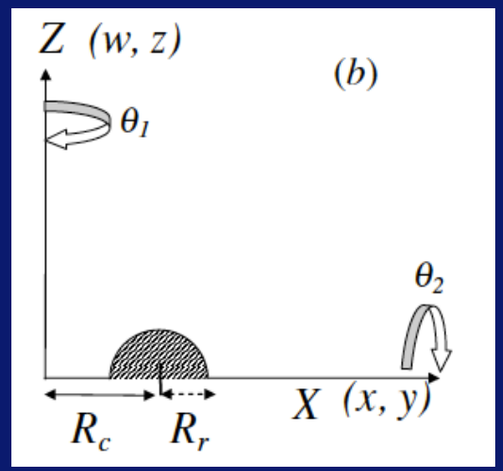

$$\ddot{r_m} - 4\frac{\dot{r_m}^2}{r_m} - 3r_m - \frac{r_m^2 + \dot{r_m}^2}{r_m}\left[2\frac{\dot{r_m}}{r_m}\cot(2\phi) - \frac{3}{\psi}(\dot{r_m}\sin\phi + r\cos\phi)\frac{\partial\psi}{\partial X} + \frac{3}{\psi}(\dot{r_m}\cos\phi - r_m\sin\phi)\frac{\partial\psi}{\partial Z}\right] = 0$$

$$A_3^{(T1)} = 4\pi^2\int_0^{\pi/2}\psi^3 r_m^2\cos\phi\sin\phi\sqrt{\dot{r_m}^2 + r_m^2}\,d\phi$$

Ring Horizon

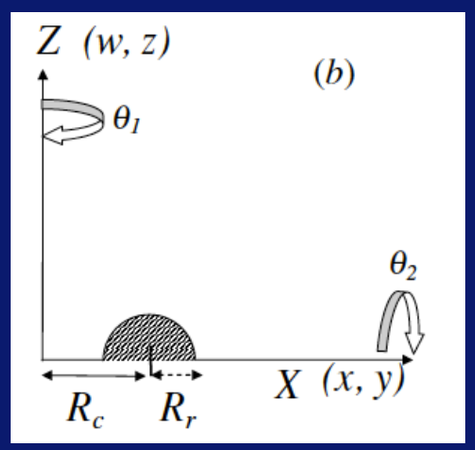

$$\ddot{r_m} - \frac{3\dot{r_m}^2}{r_m} - 2r_m - \frac{r_m^2 + \dot{r_m}^2}{r_m} \times \left[\frac{\dot{r_m}\sin\xi + r_m\cos\xi}{r_m\cos\xi + R_c} - \frac{\dot{r_m}}{r_m}\cot\xi + \frac{3}{\psi}(\dot{r_m}\sin\xi + r\cos\xi)\frac{\partial\psi}{\partial x} - \frac{3}{\psi}(\dot{r_m}\cos\xi - r\sin\xi)\frac{\partial\psi}{\partial z}\right] = 0$$

$$A_3^{(T2)} = 4\pi^2\int_0^{\pi}\psi^3(R_c + r_m\cos\xi)r_m\sin\xi\sqrt{\dot{r_m}^2 + r_m^2}\,d\xi$$

3. Ring matter collapse

A. Apparent Horizon Search, and its Area

Common Horizon

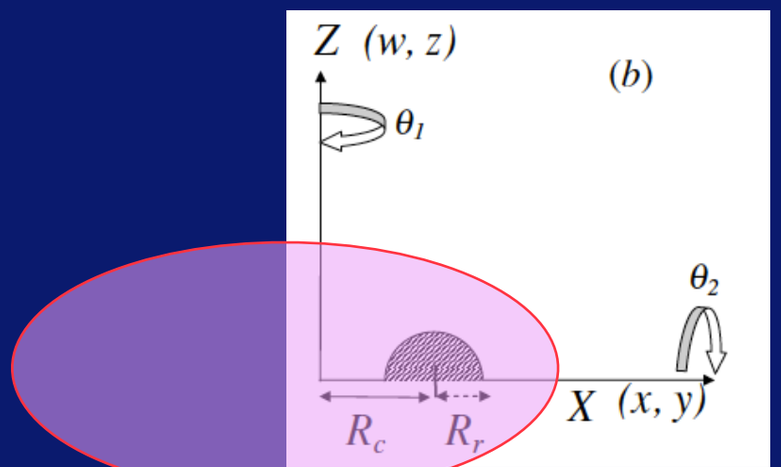

$$\ddot{r_m} - 4\frac{\dot{r_m}^2}{r_m} - 3r_m - \frac{r_m^2 + \dot{r_m}^2}{r_m}\left[2\frac{\dot{r_m}}{r_m}\cot(2\phi) - \frac{3}{\psi}(\dot{r_m}\sin\phi + r\cos\phi)\frac{\partial\psi}{\partial X} + \frac{3}{\psi}(\dot{r_m}\cos\phi - r_m\sin\phi)\frac{\partial\psi}{\partial Z}\right] = 0$$

$$A_3^{(T1)} = 4\pi^2\int_0^{\pi/2}\psi^3 r_m^2\cos\phi\sin\phi\sqrt{\dot{r_m}^2 + r_m^2}\,d\phi$$

Ring Horizon

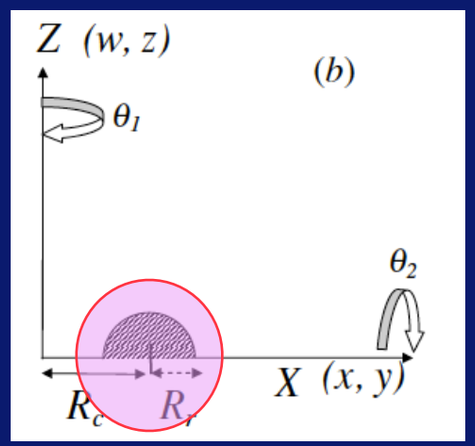

$$\ddot{r_m} - \frac{3\dot{r_m}^2}{r_m} - 2r_m - \frac{r_m^2 + \dot{r_m}^2}{r_m} \times \left[\frac{\dot{r_m}\sin\xi + r_m\cos\xi}{r_m\cos\xi + R_c} - \frac{\dot{r_m}}{r_m}\cot\xi + \frac{3}{\psi}(\dot{r_m}\sin\xi + r\cos\xi)\frac{\partial\psi}{\partial x} - \frac{3}{\psi}(\dot{r_m}\cos\xi - r\sin\xi)\frac{\partial\psi}{\partial z}\right] = 0$$

$$A_3^{(T2)} = 4\pi^2\int_0^{\pi}\psi^3(R_c + r_m\cos\xi)r_m\sin\xi\sqrt{\dot{r_m}^2 + r_m^2}\,d\xi$$

3. Ring matter collapse
B. Initial data sequence

Apparent Horizons Search

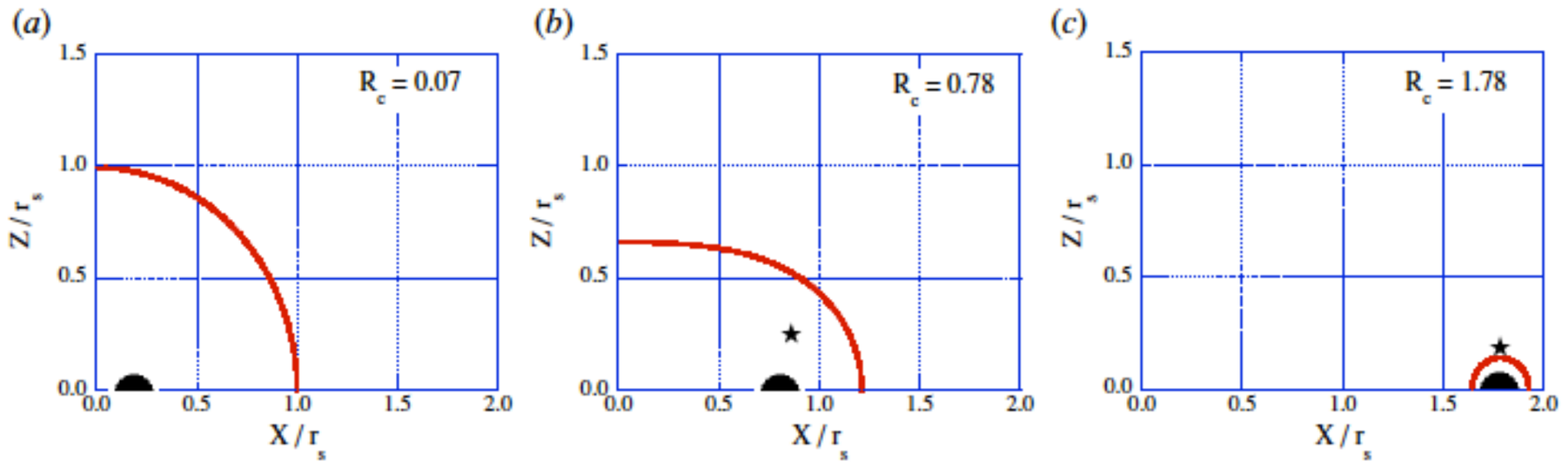

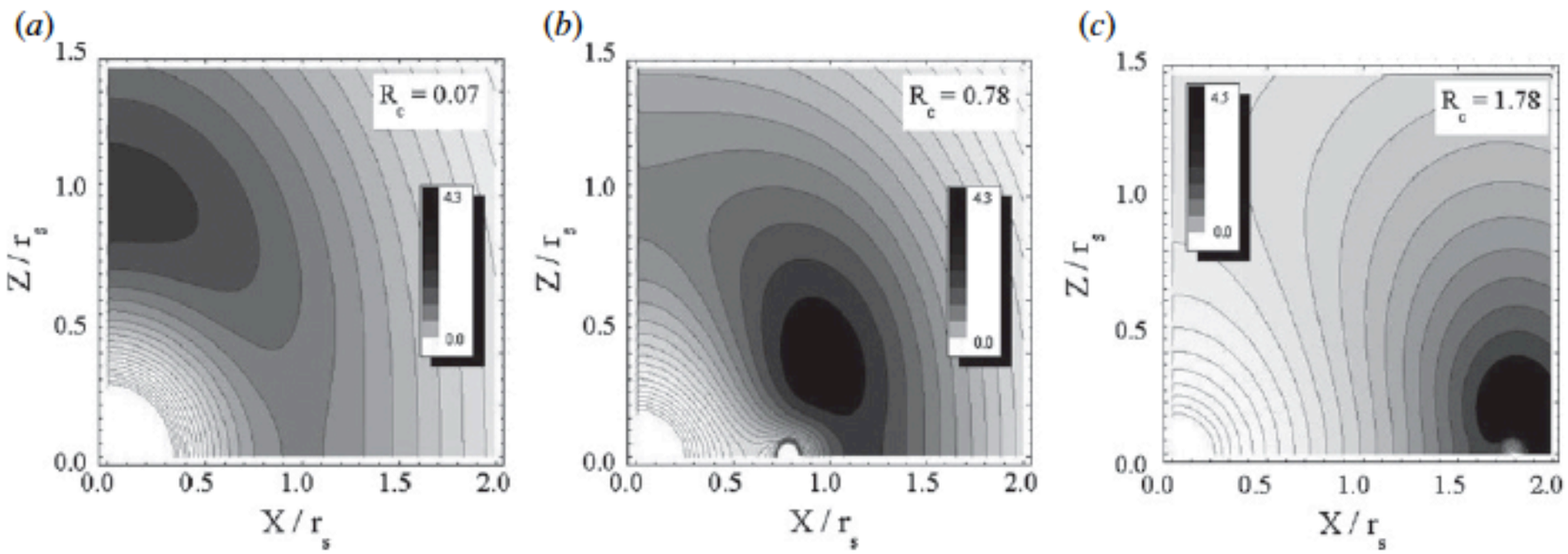

Figure 8. Contours of Kretchmann invariant, $\log_{10} \mathcal{I}^{(4)}$, corresponding to figure 7.

3. Ring matter collapse
B. Initial data sequence

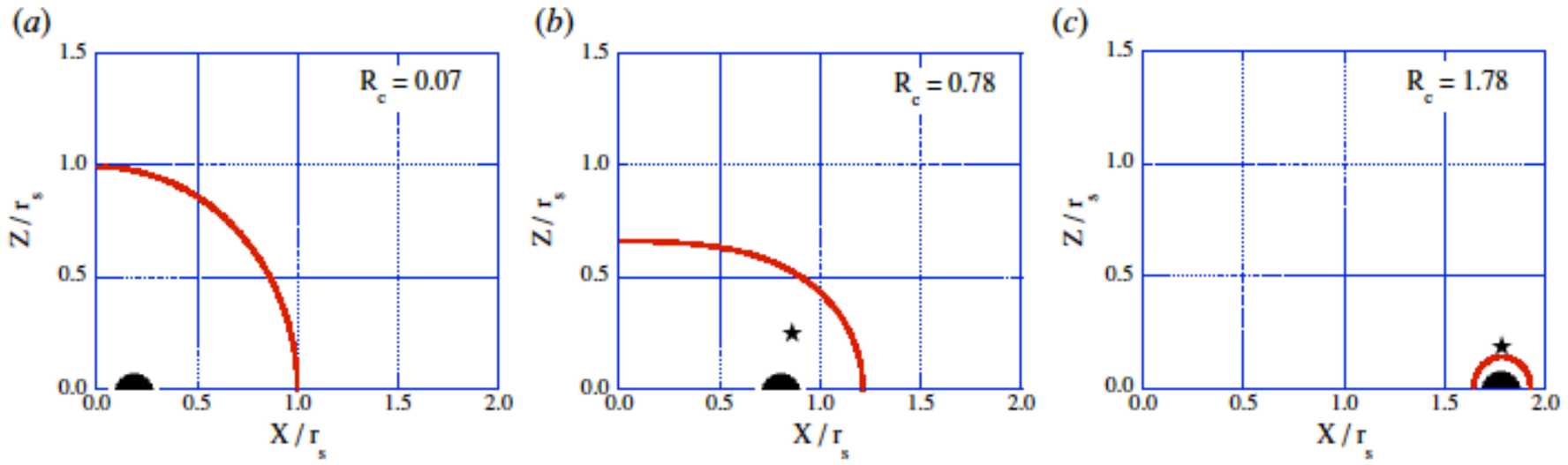

Area of Apparent Horizon

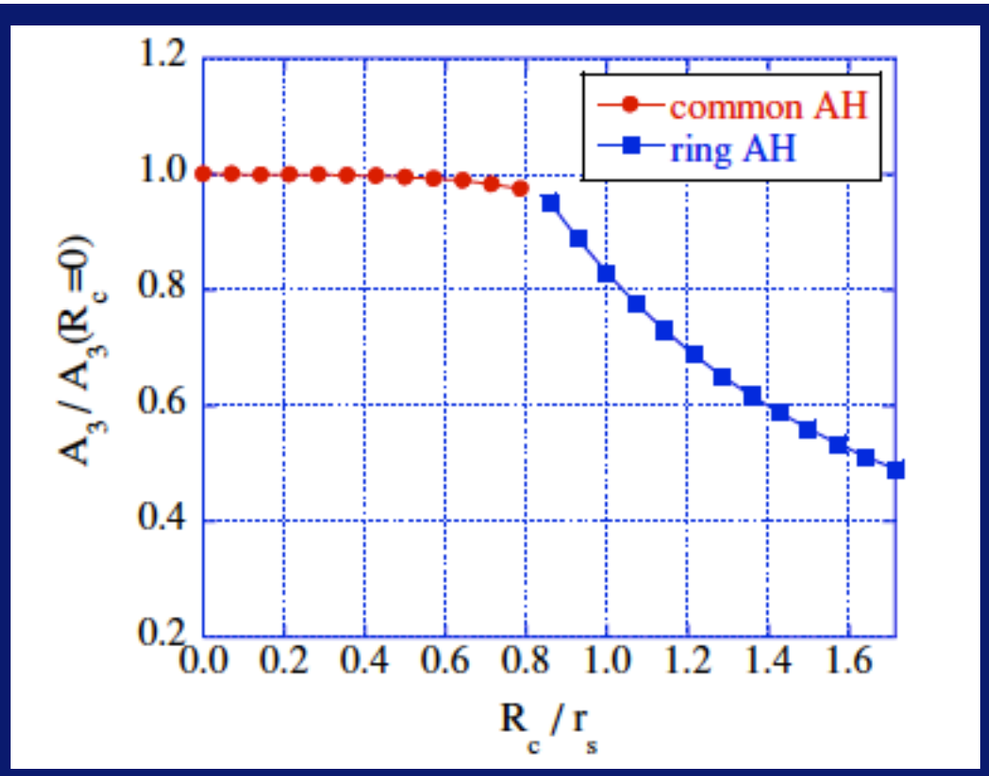

3. Ring matter collapse
C. Evolution method

- ADM full 4+1, ADM 2+1 Double Axisym Cartoon
- 33^4 grids, 130^2 x 2^2 grids

- lapse function: Maximal slicing condition
- shift vectors: zero
- asymptotically flat

- Collisionless Particles (5000)
- the same total mass
- no rotation

- Apparent Horizon Search
  both for Ring Horizon and Common Horizon

3. Ring matter collapse
D. Evolution examples

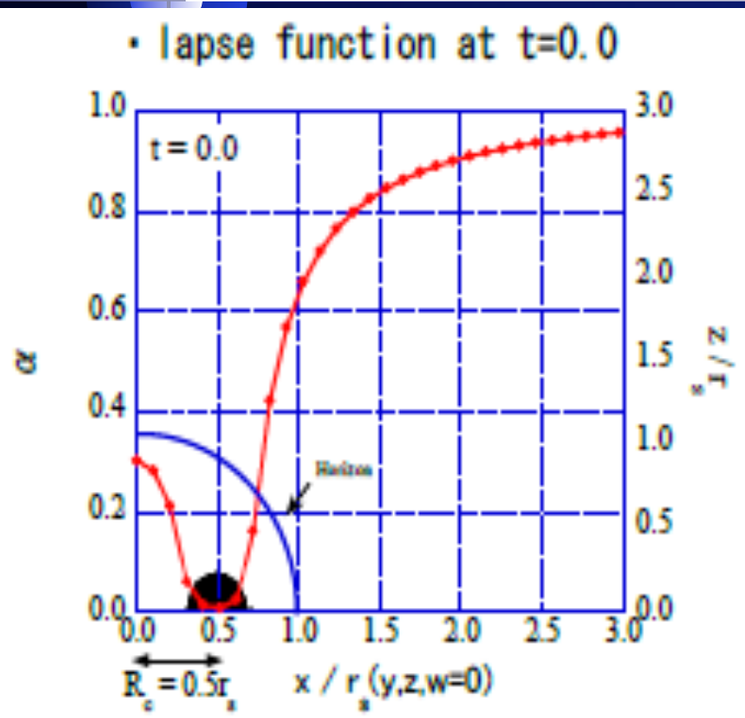

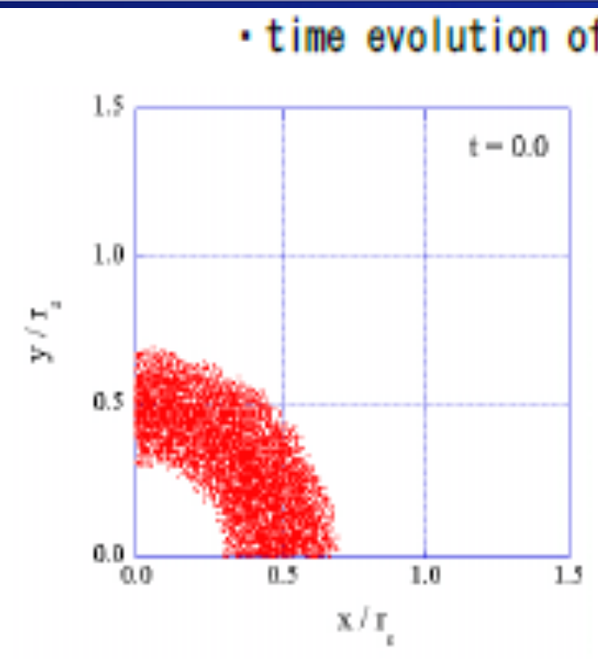

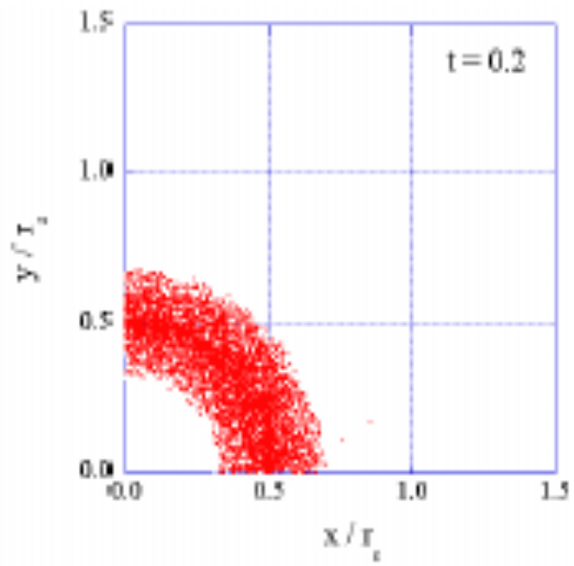

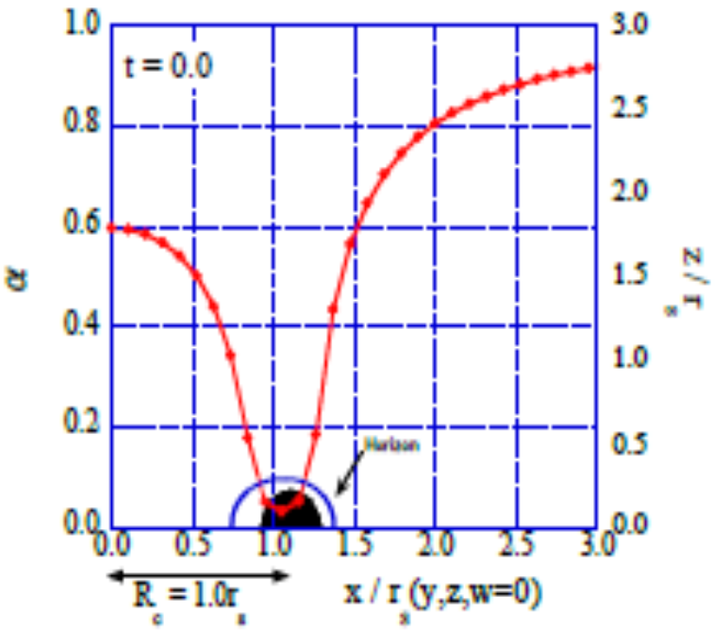

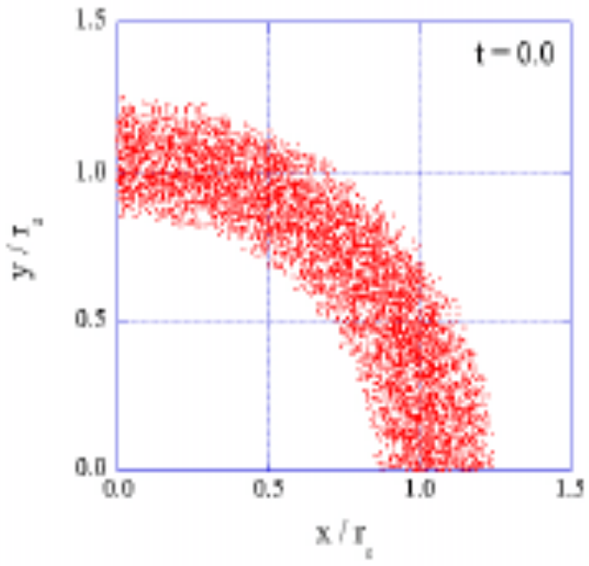

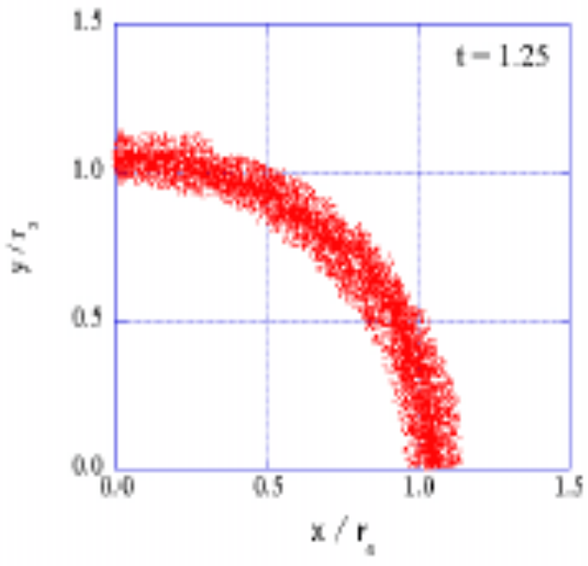

3. Ring matter collapse
D. Evolution examples

t=0 No Horizon

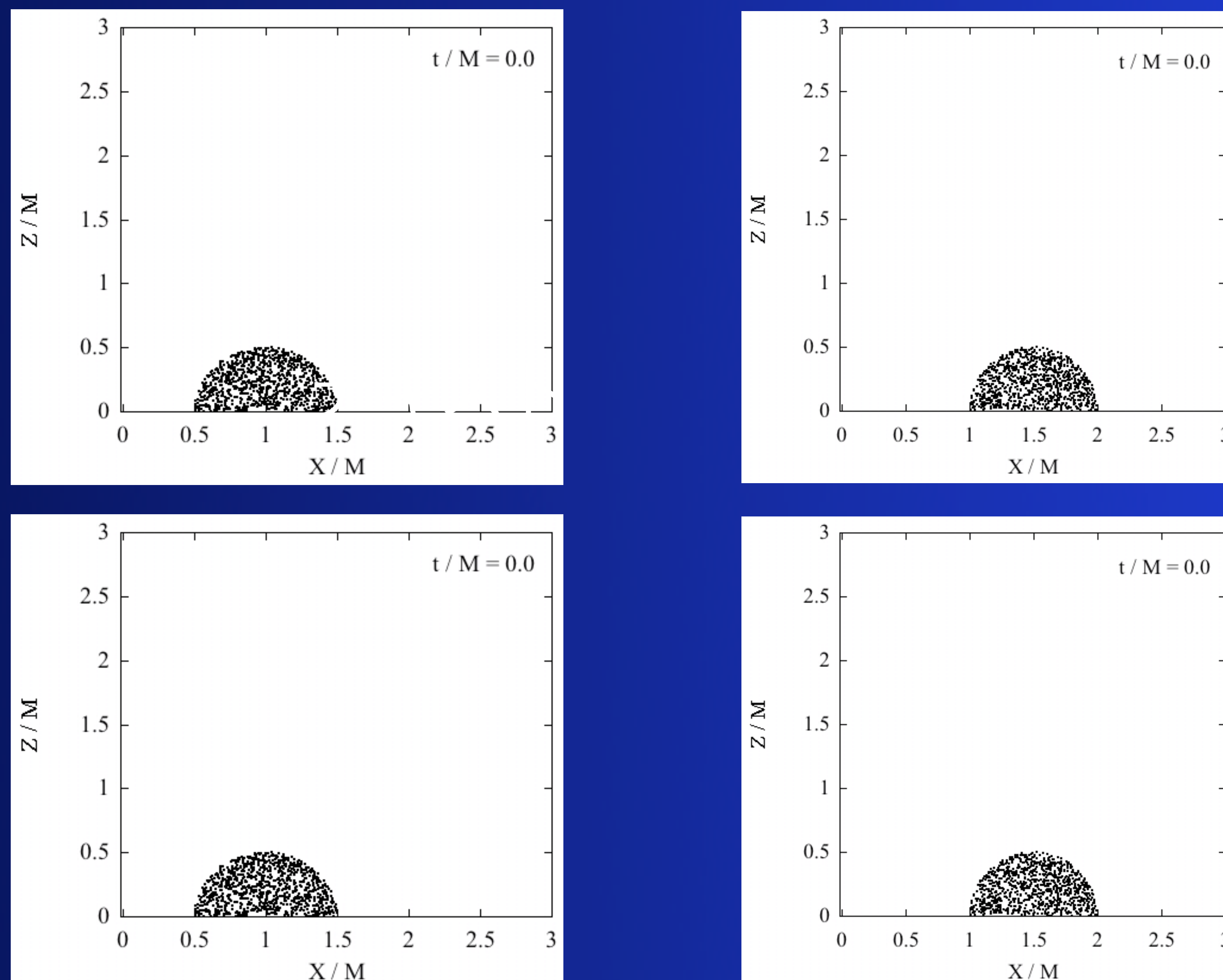

3. Ring matter collapse
D. Evolution examples

t=0 No Horizon

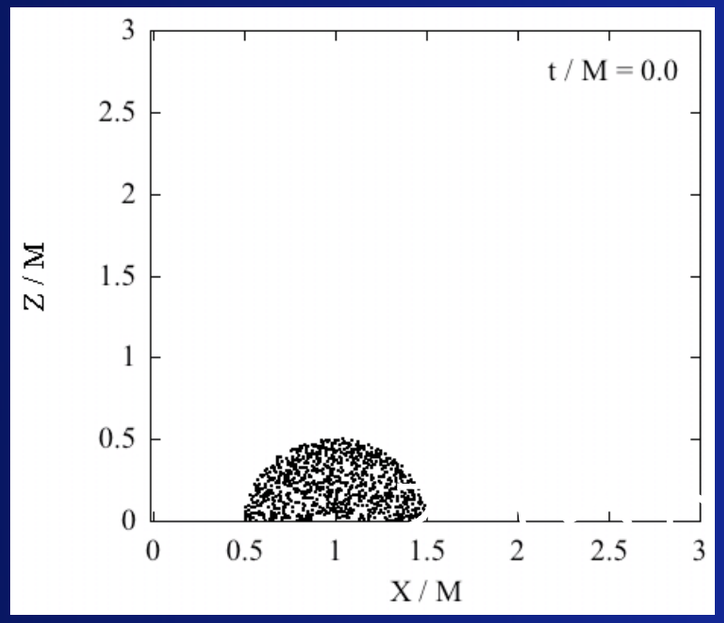

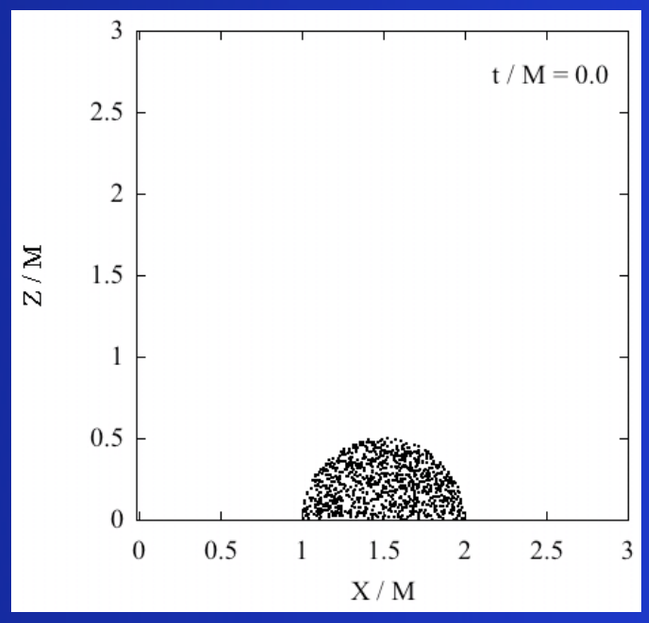

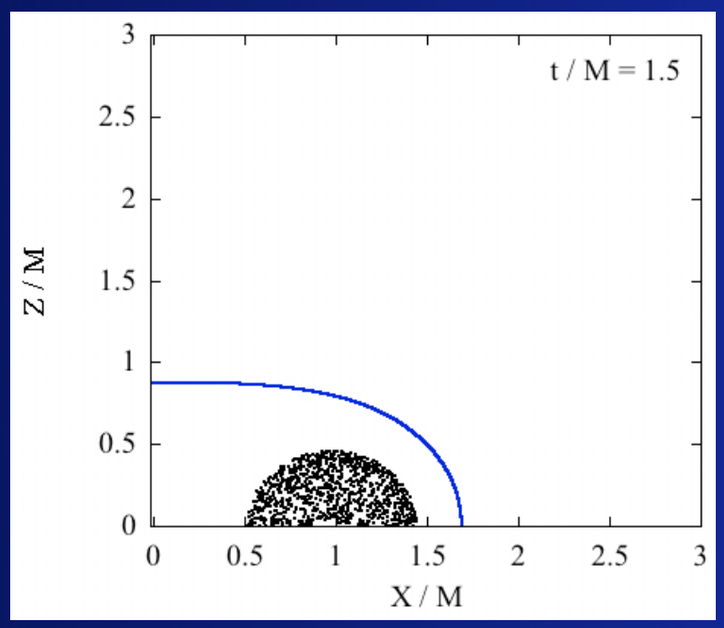

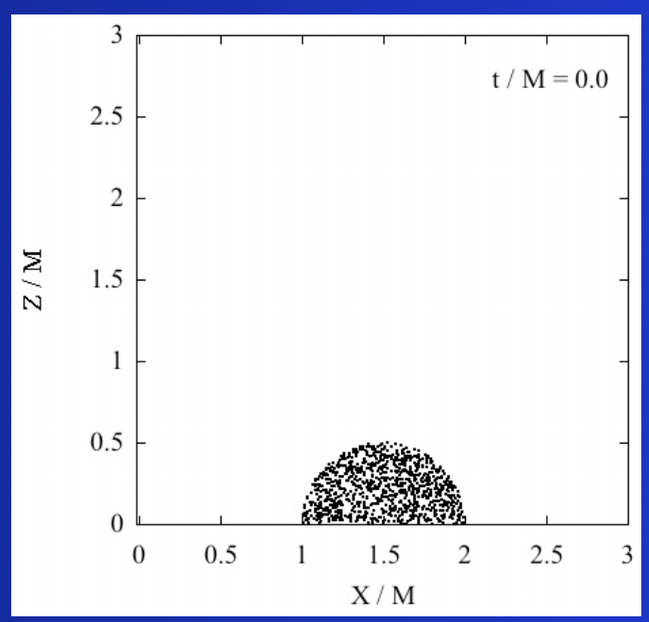

t=1.5 Common Horizon

3. Ring matter collapse
D. Evolution examples

t=0 No Horizon

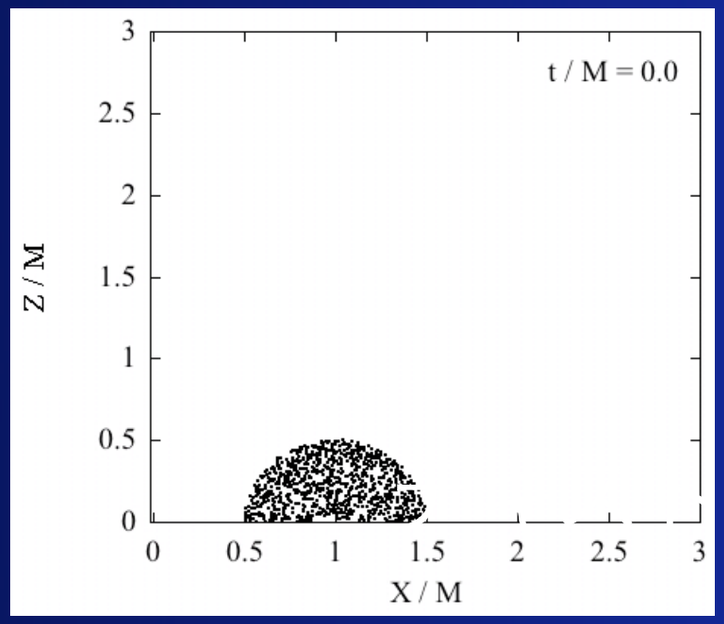

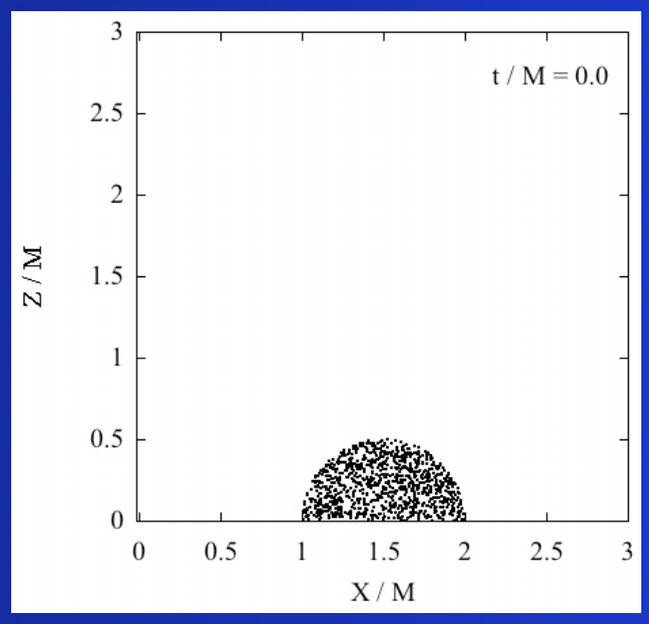

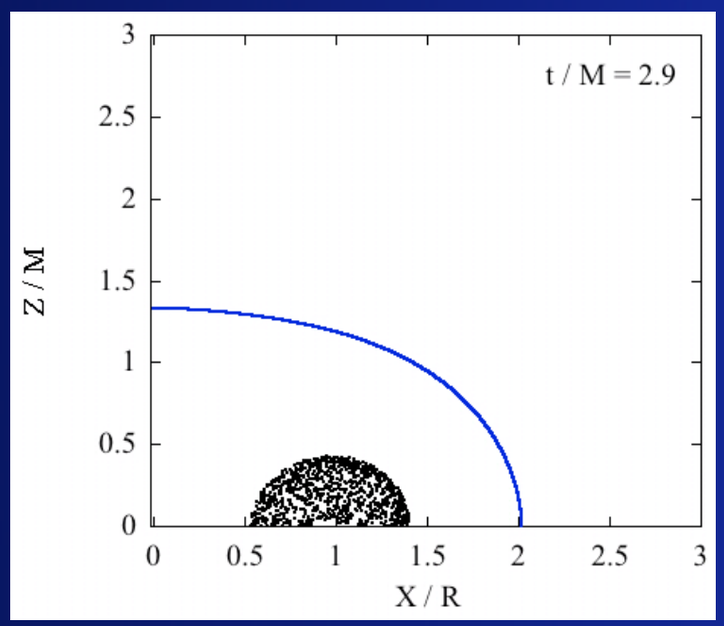

t=1.5 Common Horizon

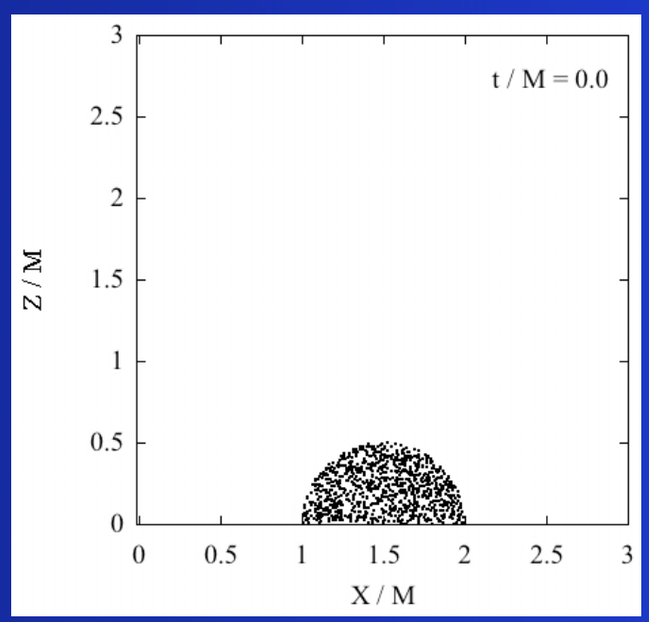

3. Ring matter collapse
D. Evolution examples

t=0 No Horizon

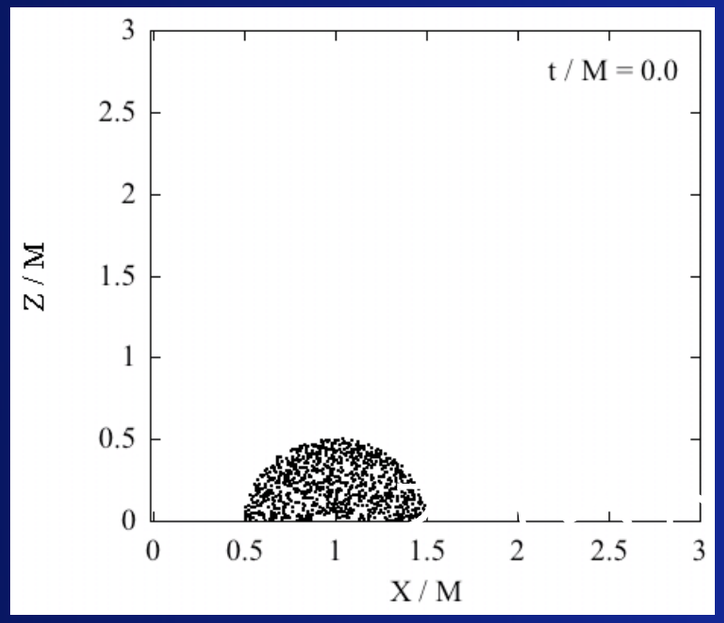

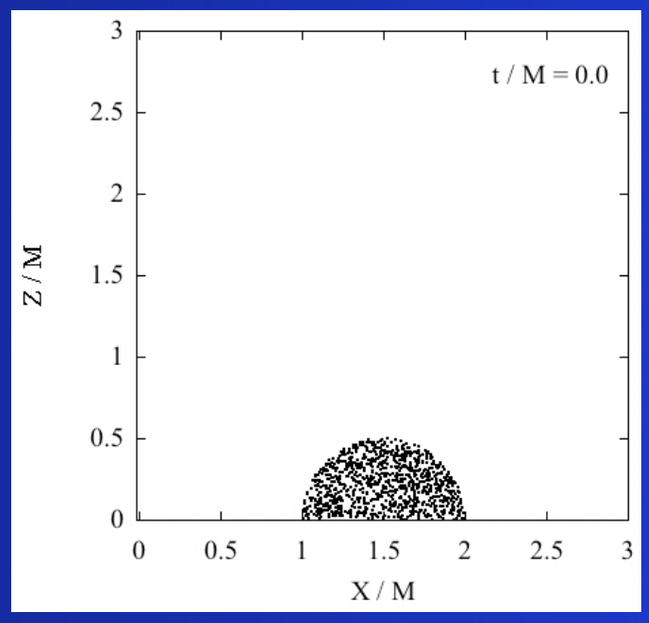

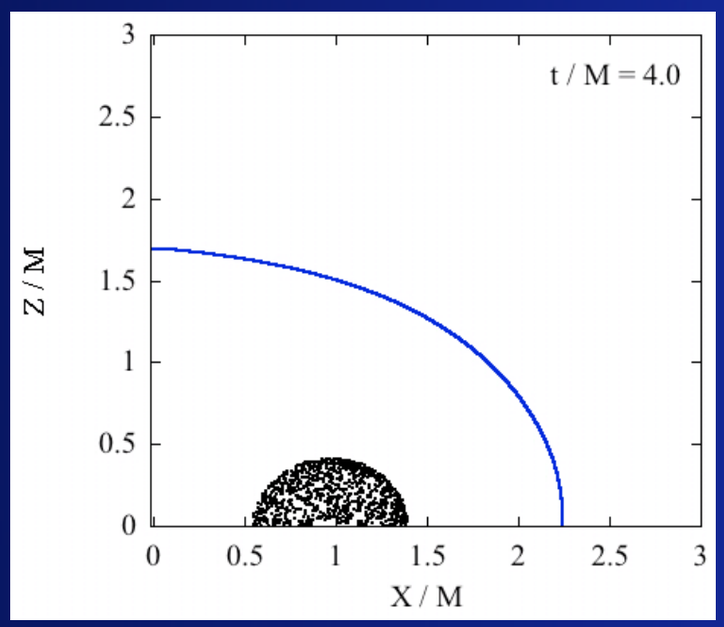

t=1.5 Common Horizon

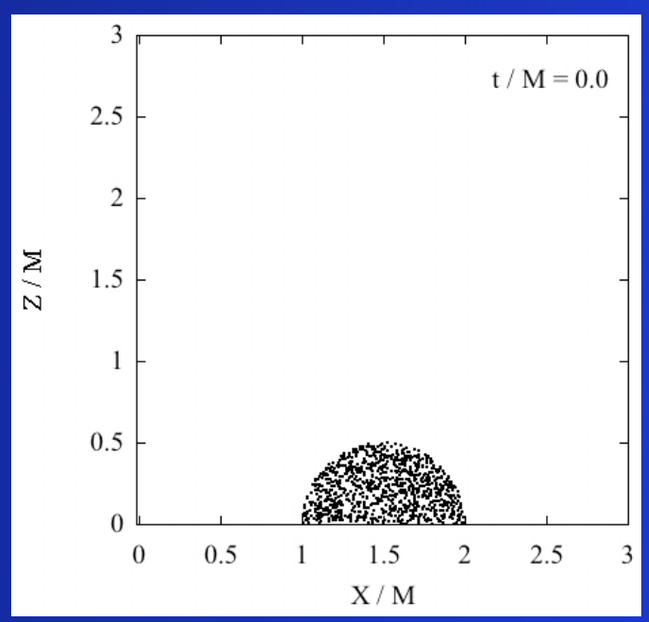

3. Ring matter collapse
D. Evolution examples

t=0 No Horizon

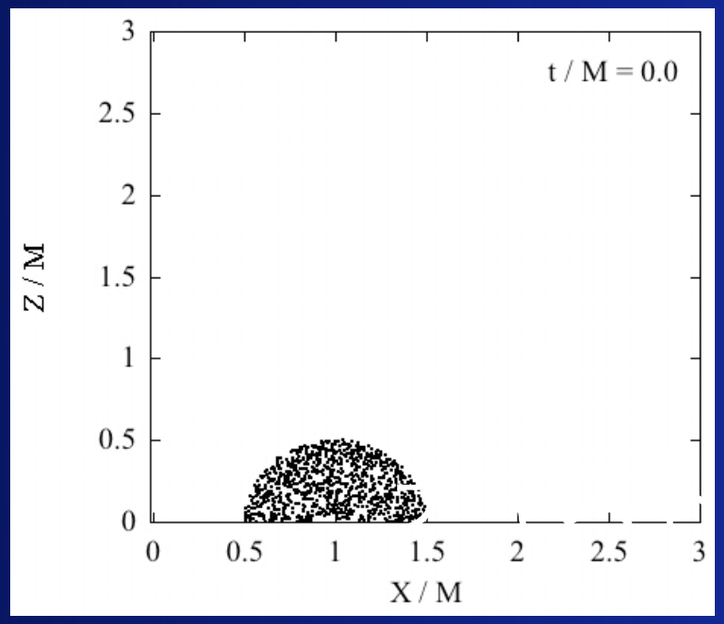

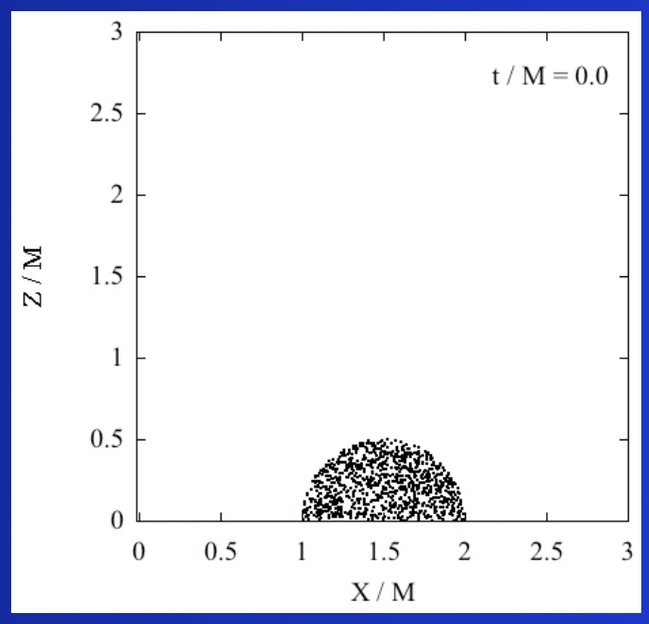

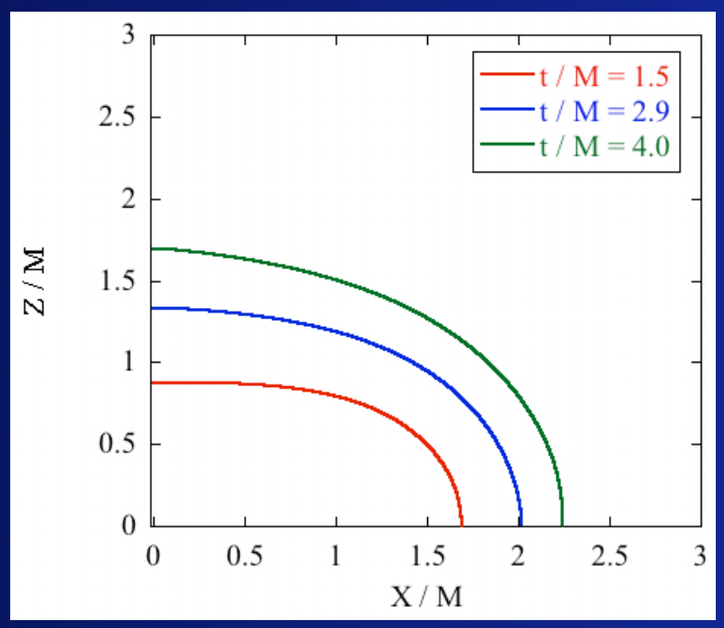

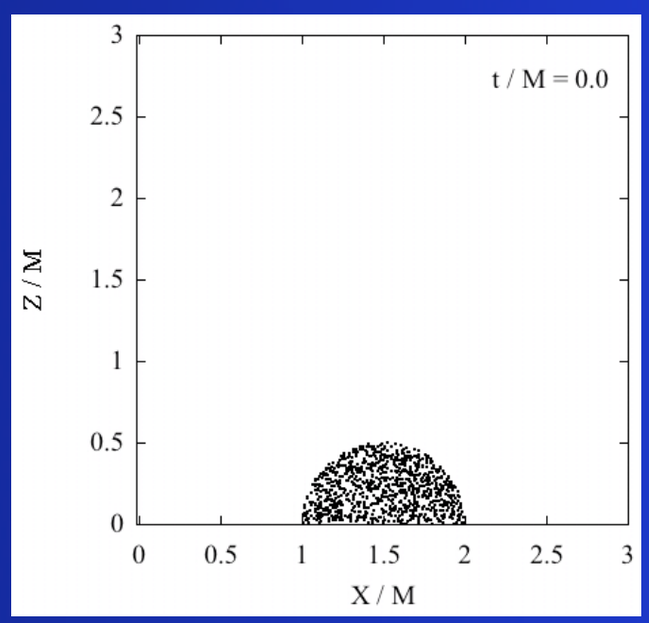

t=1.5 Common Horizon

3. Ring matter collapse
D. Evolution examples

t=0 No Horizon

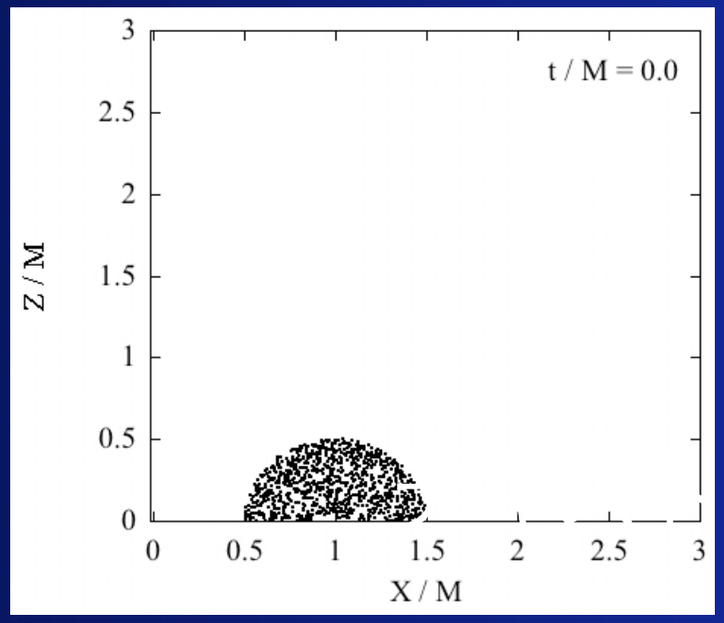

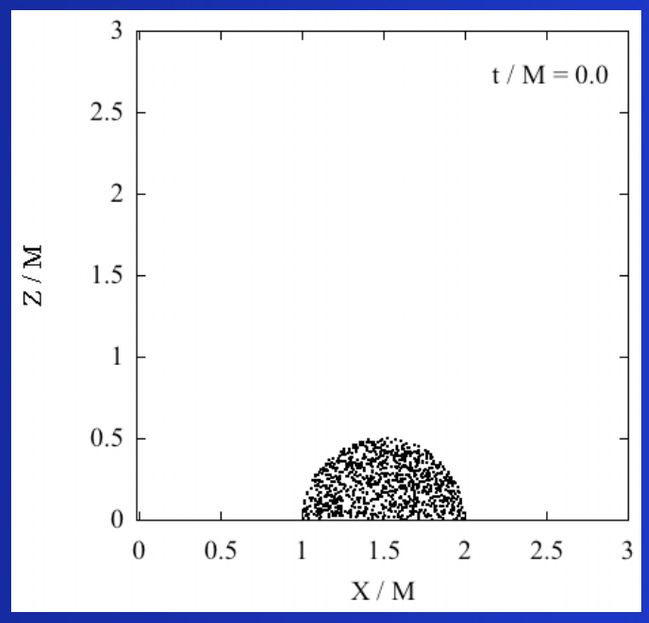

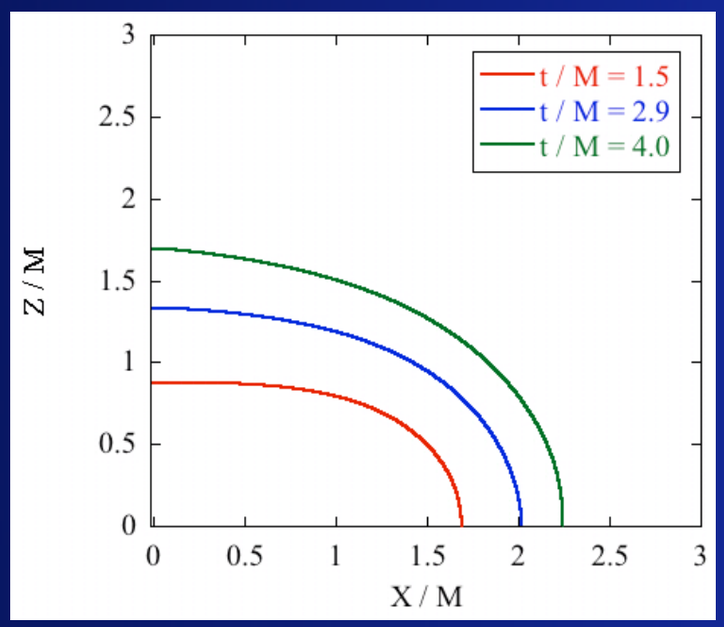

t=1.5 Common Horizon

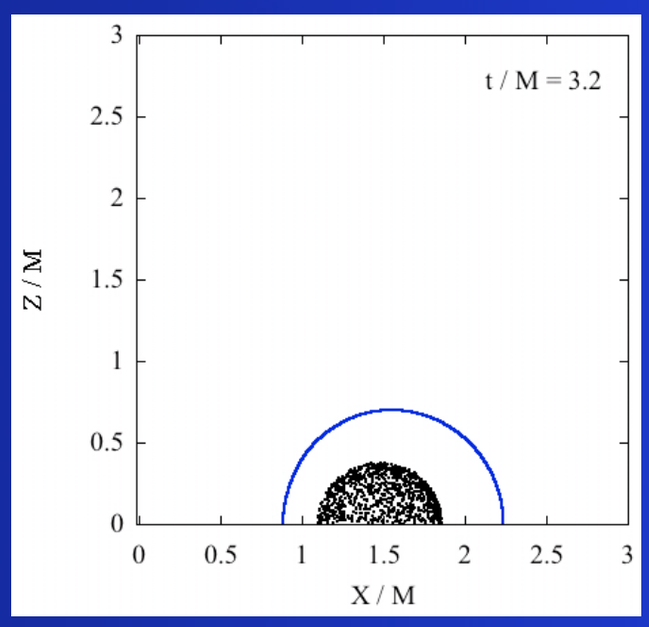

t=3.2 Ring Horizon

3. Ring matter collapse
D. Evolution examples

t=0 No Horizon

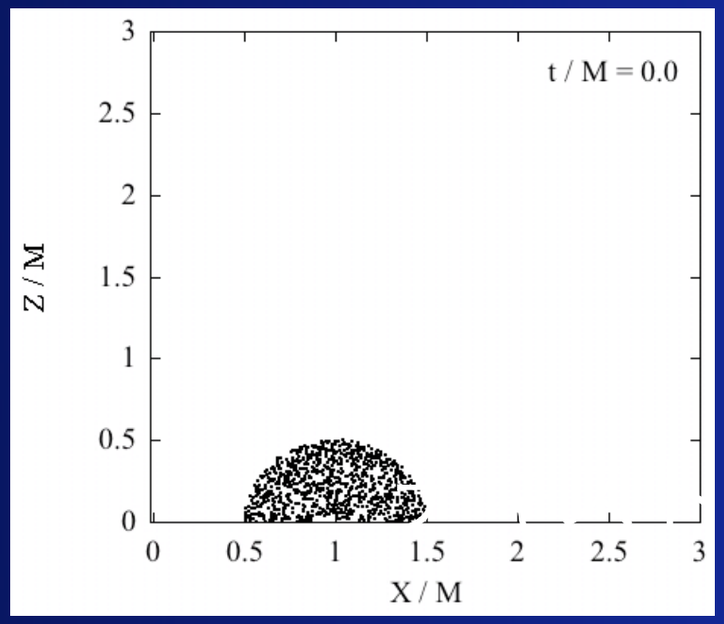

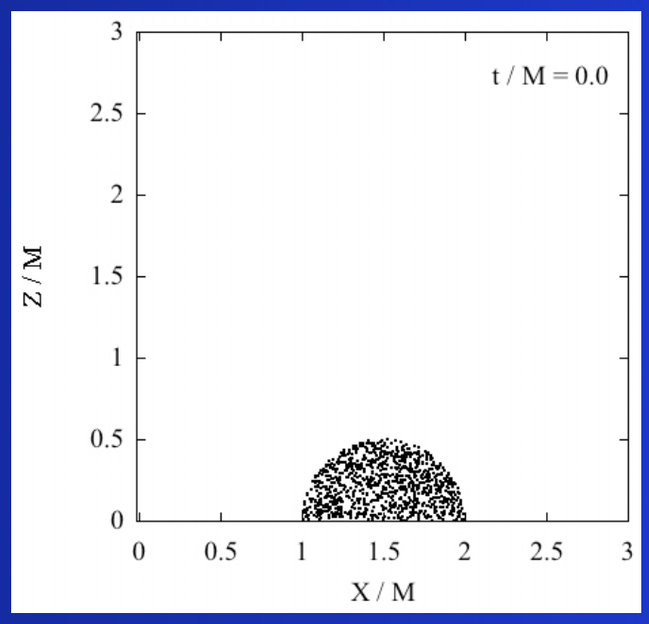

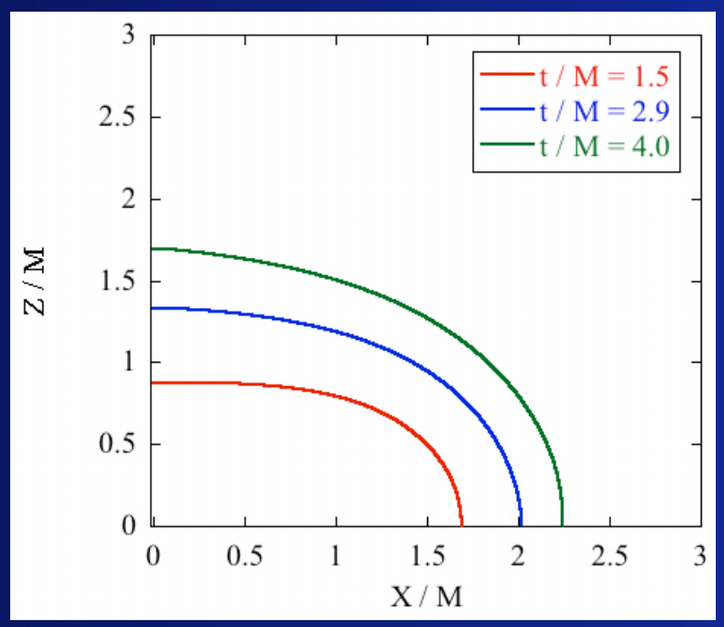

t=1.5 Common Horizon

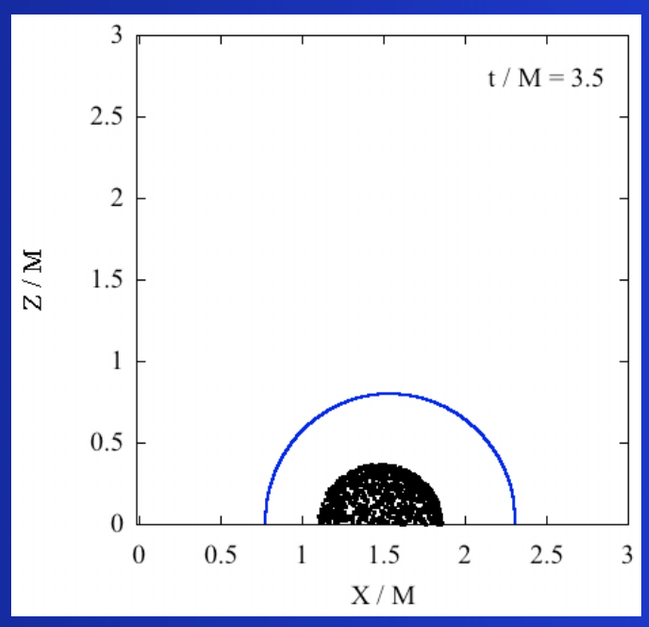

t=3.2 Ring Horizon

3. Ring matter collapse
D. Evolution examples

t=0 No Horizon

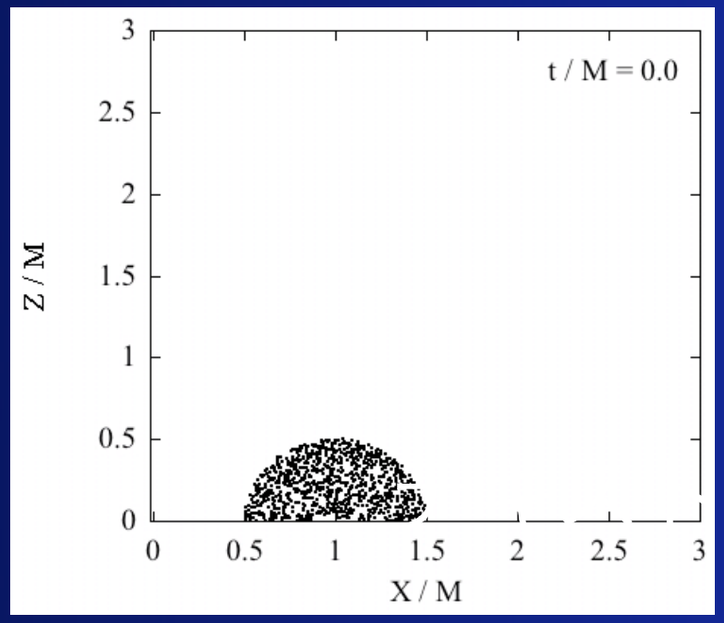

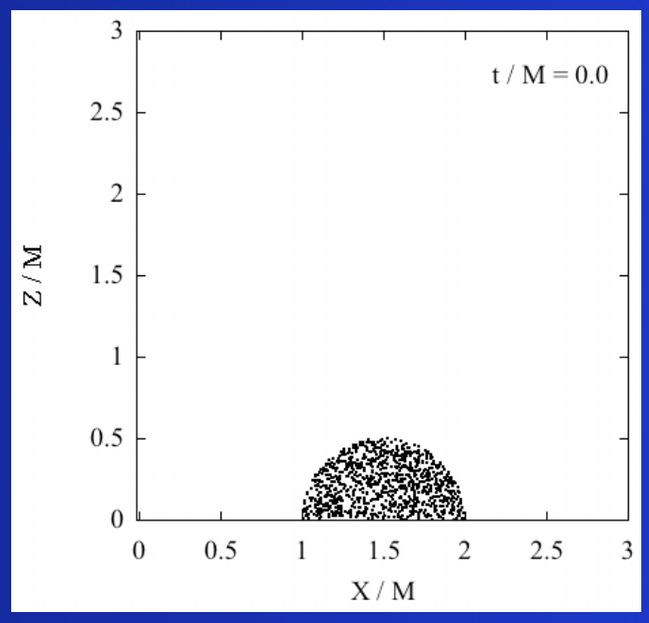

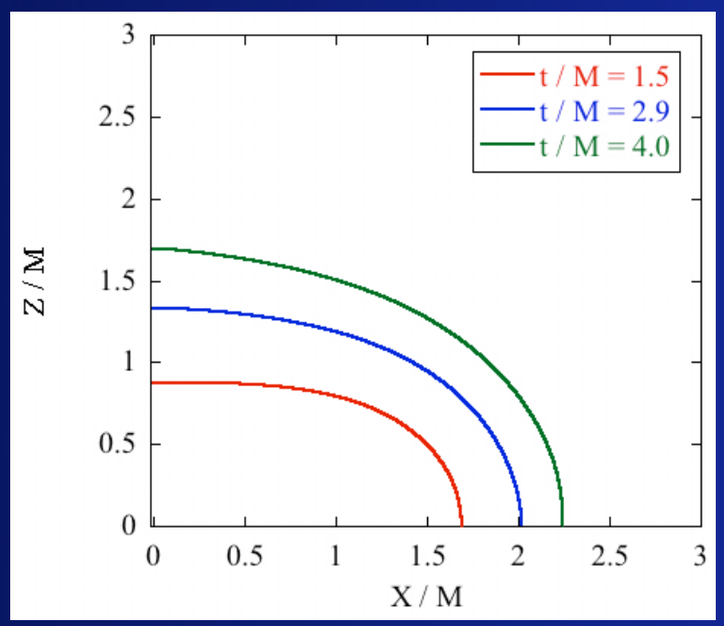

t=1.5 Common Horizon

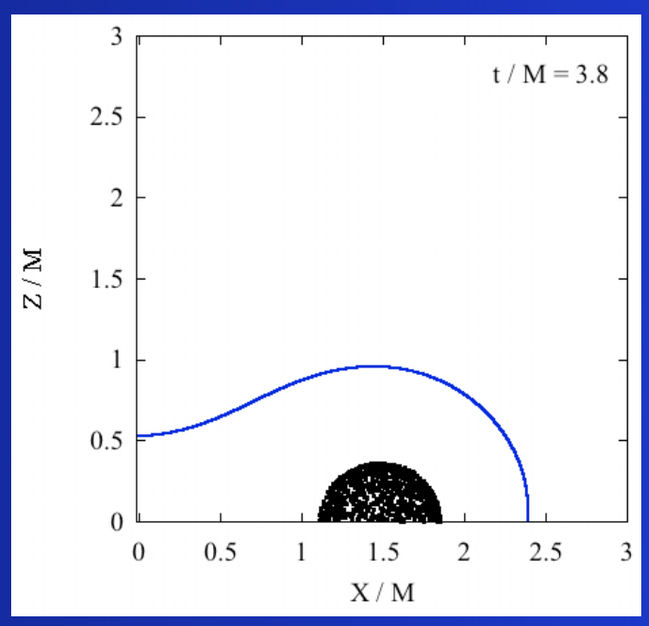

t=3.2 Ring Horizon
t=3.8 Common Horizon

3. Ring matter collapse
D. Evolution examples

t=0 No Horizon

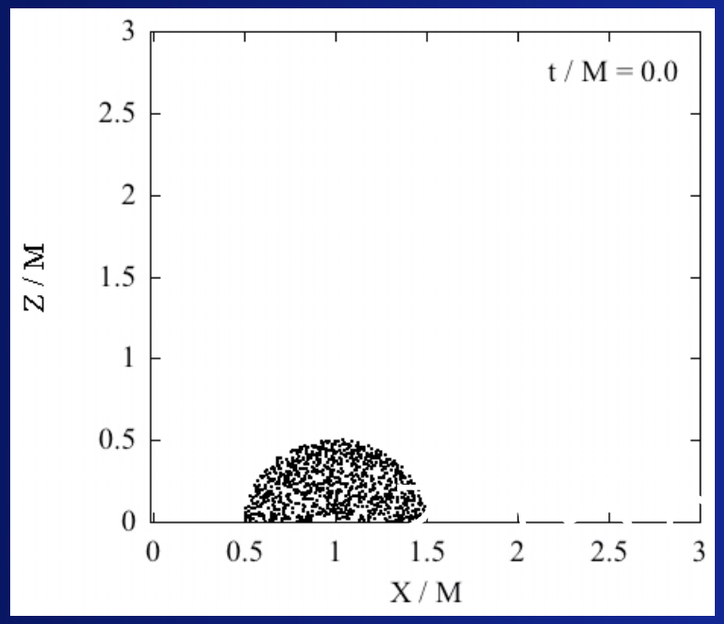

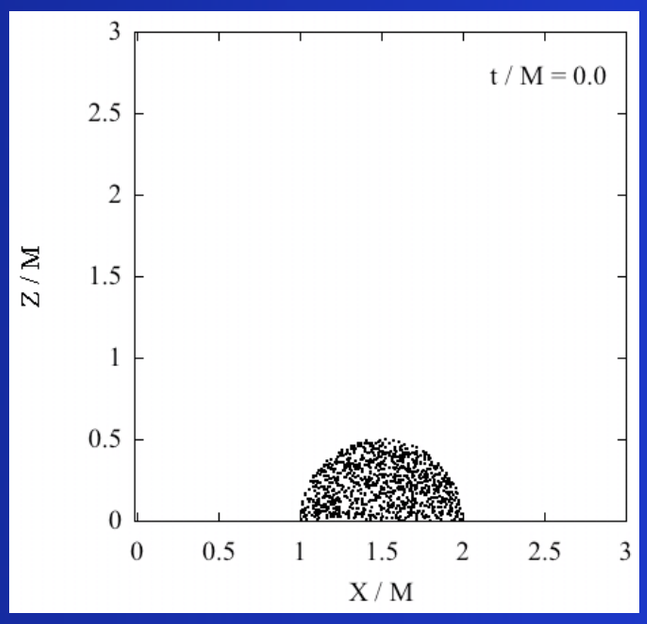

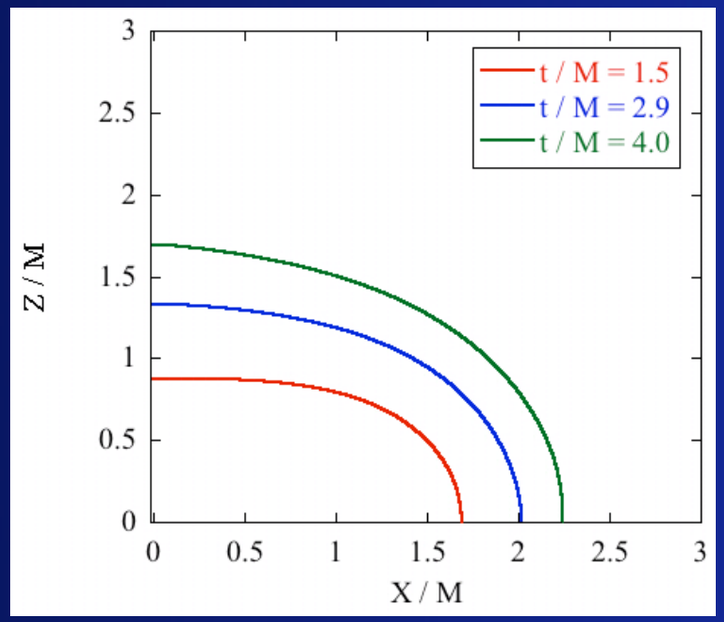

t=1.5 Common Horizon

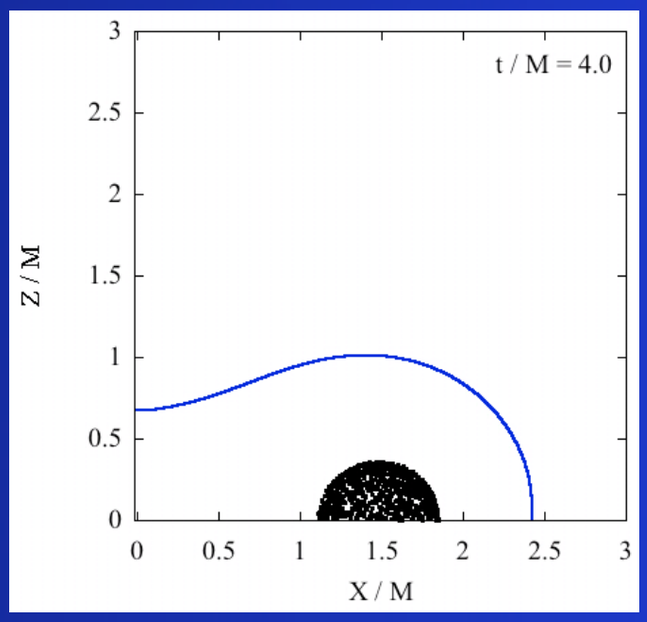

t=3.2 Ring Horizon
t=3.8 Common Horizon

3. Ring matter collapse
D. Evolution examples

t=0 No Horizon

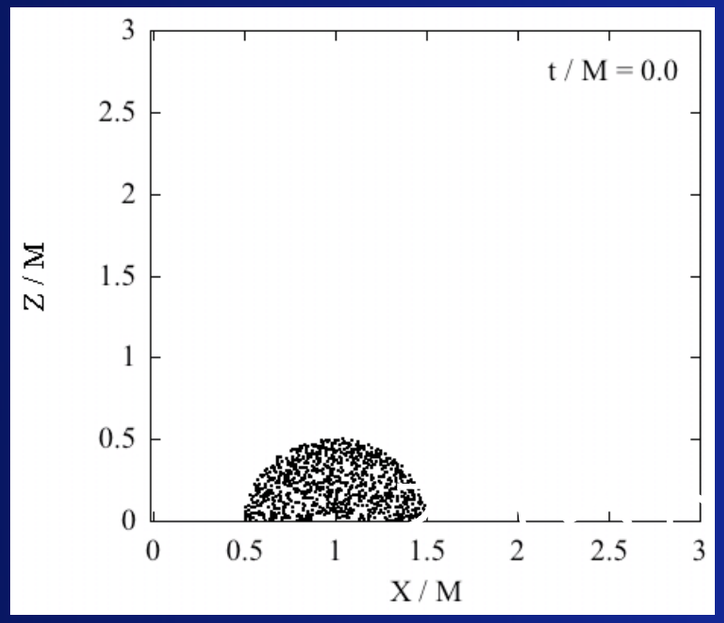

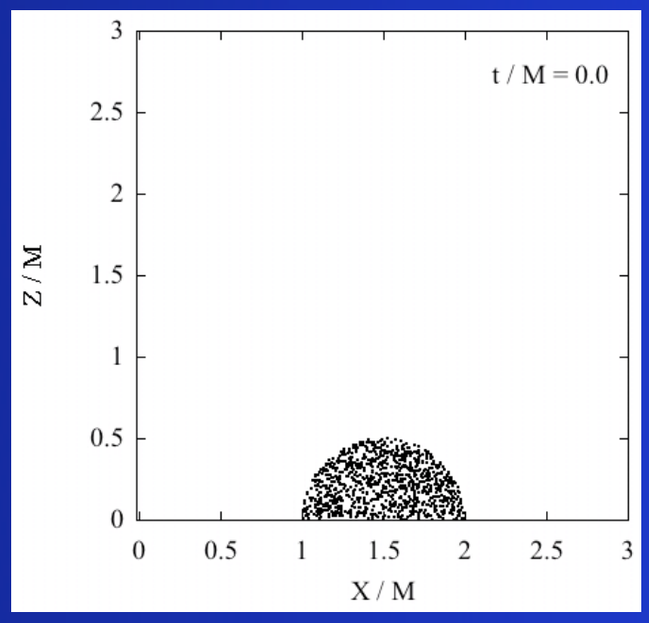

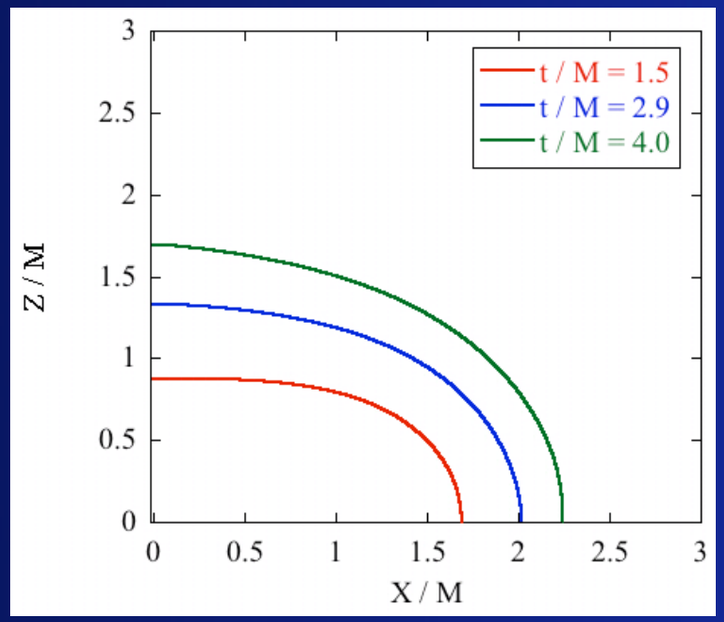

t=1.5 Common Horizon

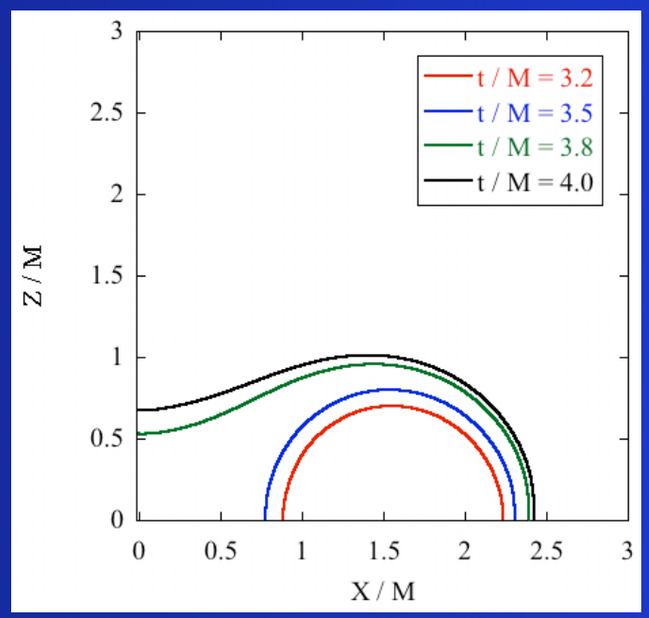

t=3.2 Ring Horizon
t=3.8 Common Horizon

4. Hoop Conjecture

A. Hyper-Hoop conjecture ?

Hoop Conjecture Thorne (1972)

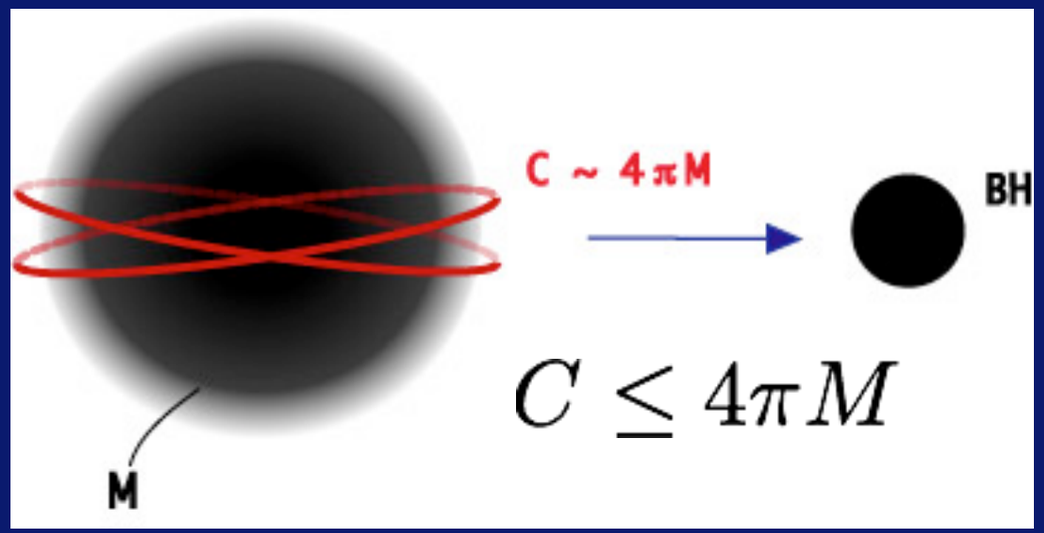

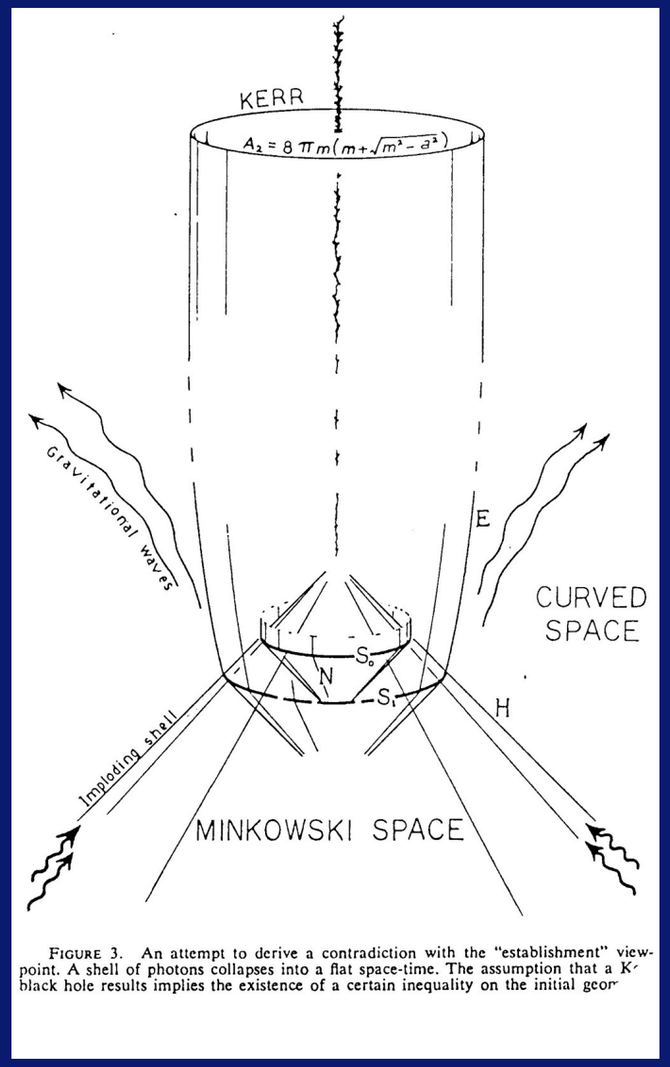

FIGURE 3. An attempt to derive a contradiction with the "establishment" viewpoint. A shell of photons collapses into a flat space-time. The assumption that a K black hole results implies the existence of a certain inequality on the initial geo

Hyper-Hoop Conjecture

Ida-Nakao (2002)

$$V_{D-3} \leq G_D M$$

Penrose (1969)

$$A \leq 16\pi M^2$$

4. Hoop Conjecture

A. Hyper-Hoop conjecture ?

Hoop Conjecture Thorne (1972)

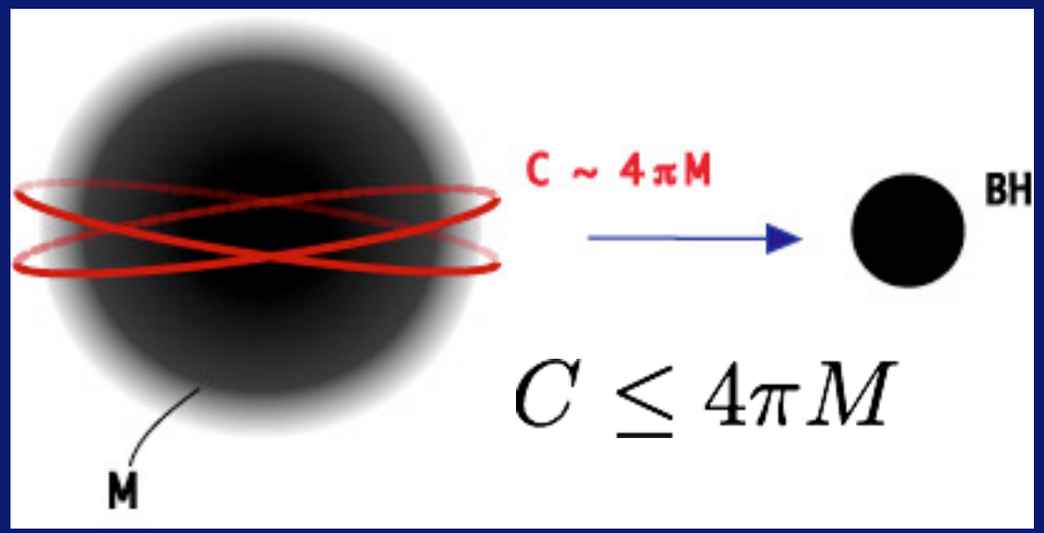

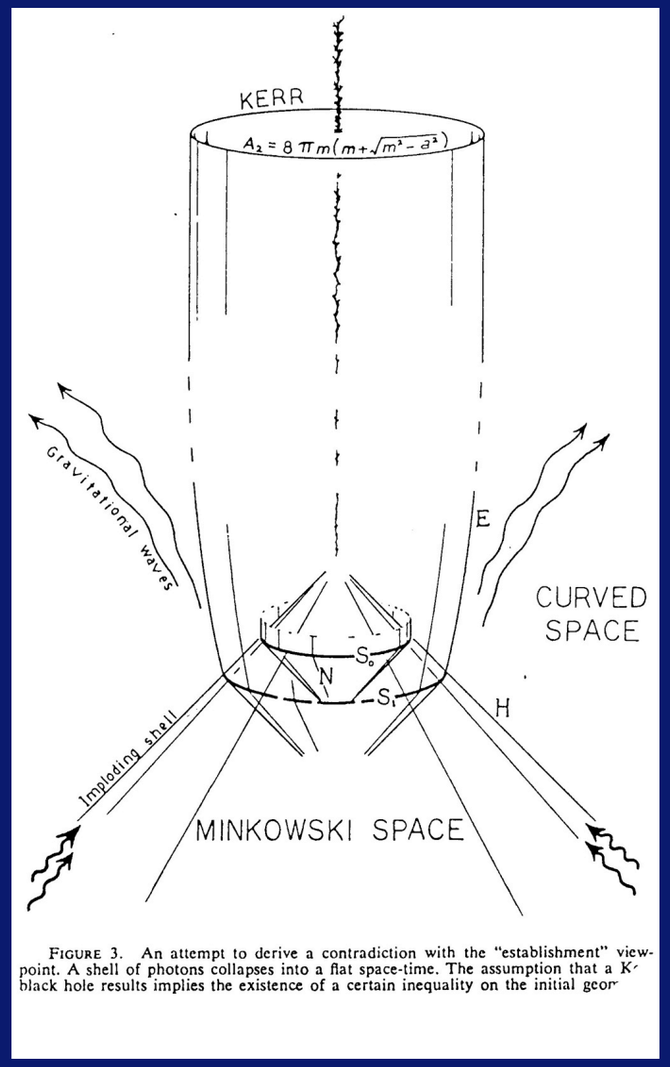

FIGURE 3. An attempt to derive a contradiction with the "establishment" viewpoint. A shell of photons collapses into a flat space-time. The assumption that a K black hole results implies the existence of a certain inequality on the initial geo

Hyper-Hoop Conjecture

Ida-Nakao (2002)

$$V_{D-3} \leq G_D M$$

In 5-D, if mass gets compacted in some area, ...

Penrose (1969)

$$A \leq 16\pi M^2$$

4. Hoop Conjecture

B. Spheroidal Cases

$$V_2 \leq \frac{\pi}{2} 16\pi G_5 M$$

Define Hyper-Hoop as the surface $\delta V_2 = 0$

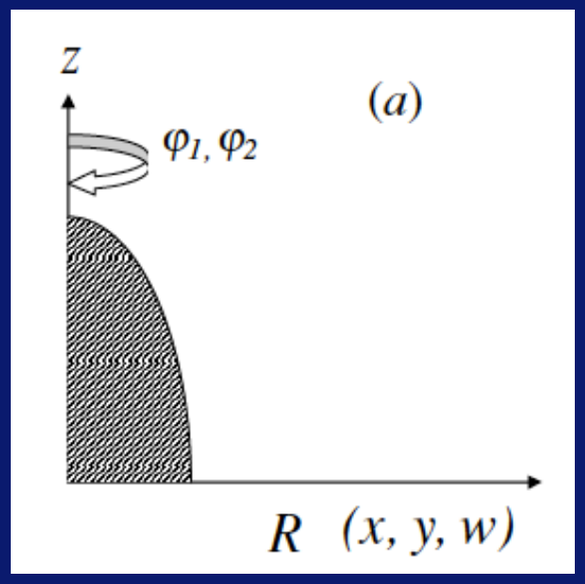

$$V_2^{(A)} = 4\pi \int_0^{\pi/2} \psi^2 \sqrt{\dot{r_h}^2 + r_h^2} r_h \sin\theta \, d\theta$$

$$\ddot{r_h} - \frac{3\dot{r_h}^2}{r_h} - 2r_h + \frac{r_h^2 + \dot{r_h}^2}{r_h} \left[\frac{\dot{r_h}}{r_h} \cot\theta - \frac{2}{\psi} (\dot{r_h} \sin\theta + r_h \cos\theta) \frac{\partial\psi}{\partial z} - \frac{2}{\psi} (r_h \sin\theta - \dot{r_h} \cos\theta) \frac{\partial\psi}{\partial R} \right] = 0$$

$$V_2^{(B)} = 4\pi \int_0^{\pi/2} \psi^2 \sqrt{\dot{r_h}^2 + r_h^2} r_h \cos\theta \, d\theta$$

$$\ddot{r_h} - \frac{3\dot{r_h}^2}{r_h} - 2r_h - \frac{r_h^2 + \dot{r_h}^2}{r_h} \left[\frac{\dot{r_h}}{r_h} \tan\theta + \frac{2}{\psi} (r_h \sin\theta - \dot{r_h} \cos\theta) \frac{\partial\psi}{\partial R} + \frac{2}{\psi} (r_h \cos\theta + \dot{r_h} \sin\theta) \frac{\partial\psi}{\partial z} \right] = 0$$

4. Hoop Conjecture

B. Spheroidal Cases

$$V_2 \leq \frac{\pi}{2} 16\pi G_5 M$$

Define Hyper-Hoop as the surface $\delta V_2 = 0$

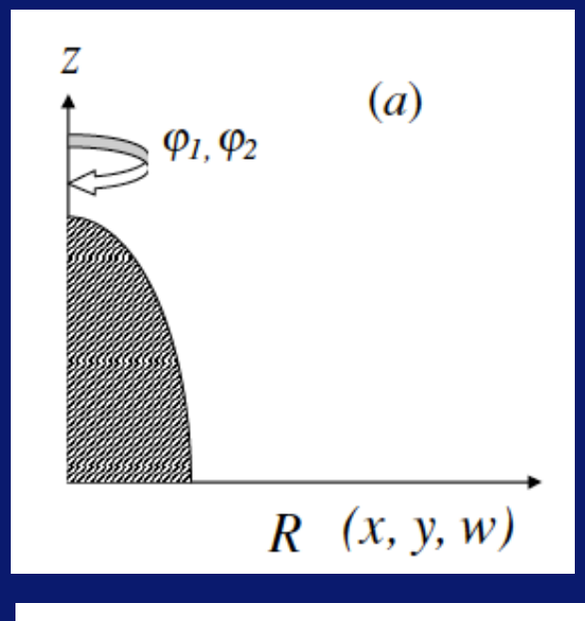

$$V_2^{(A)} = 4\pi \int_0^{\pi/2} \psi^2 \sqrt{\dot{r_h}^2 + r_h^2} r_h \sin\theta \, d\theta$$

$$V_2^{(B)} = 4\pi \int_0^{\pi/2} \psi^2 \sqrt{\dot{r_h}^2 + r_h^2} r_h \cos\theta \, d\theta$$

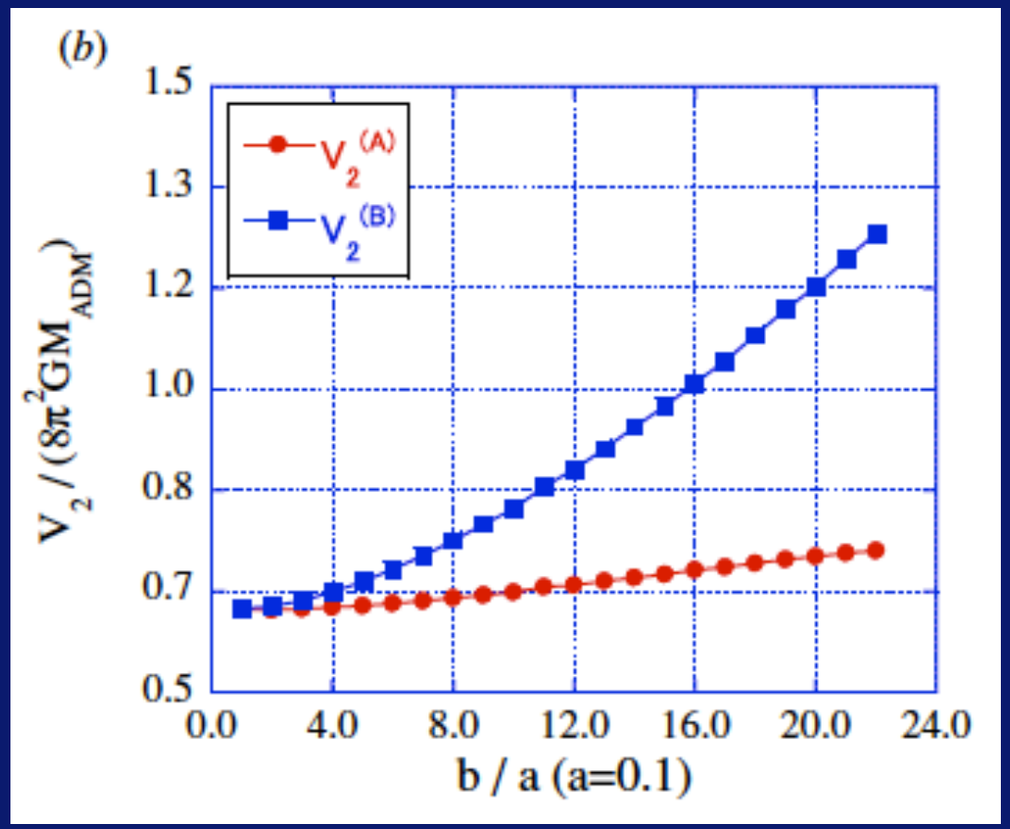

4. Hoop Conjecture

B. Spheroidal Cases

$$V_2 \leq \frac{\pi}{2} 16\pi G_5 M$$

Define Hyper-Hoop as the surface $\delta V_2 = 0$

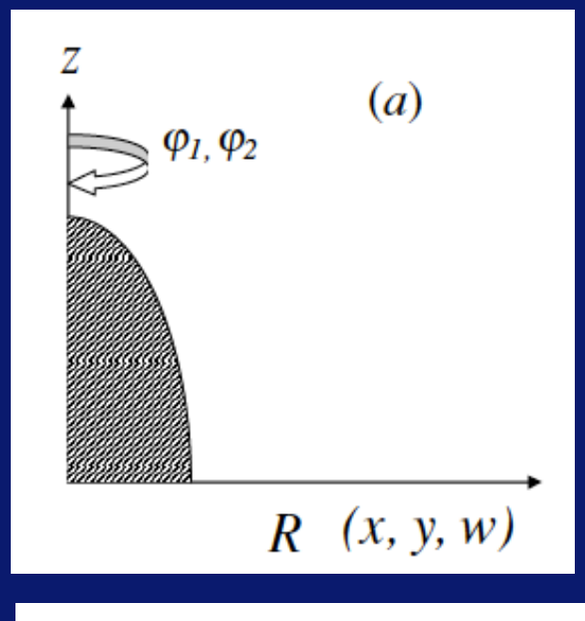

$$V_2^{(A)} = 4\pi \int_0^{\pi/2} \psi^2 \sqrt{\dot{r_h}^2 + r_h^2} r_h \sin\theta \, d\theta$$

$$V_2^{(B)} = 4\pi \int_0^{\pi/2} \psi^2 \sqrt{\dot{r_h}^2 + r_h^2} r_h \cos\theta \, d\theta$$

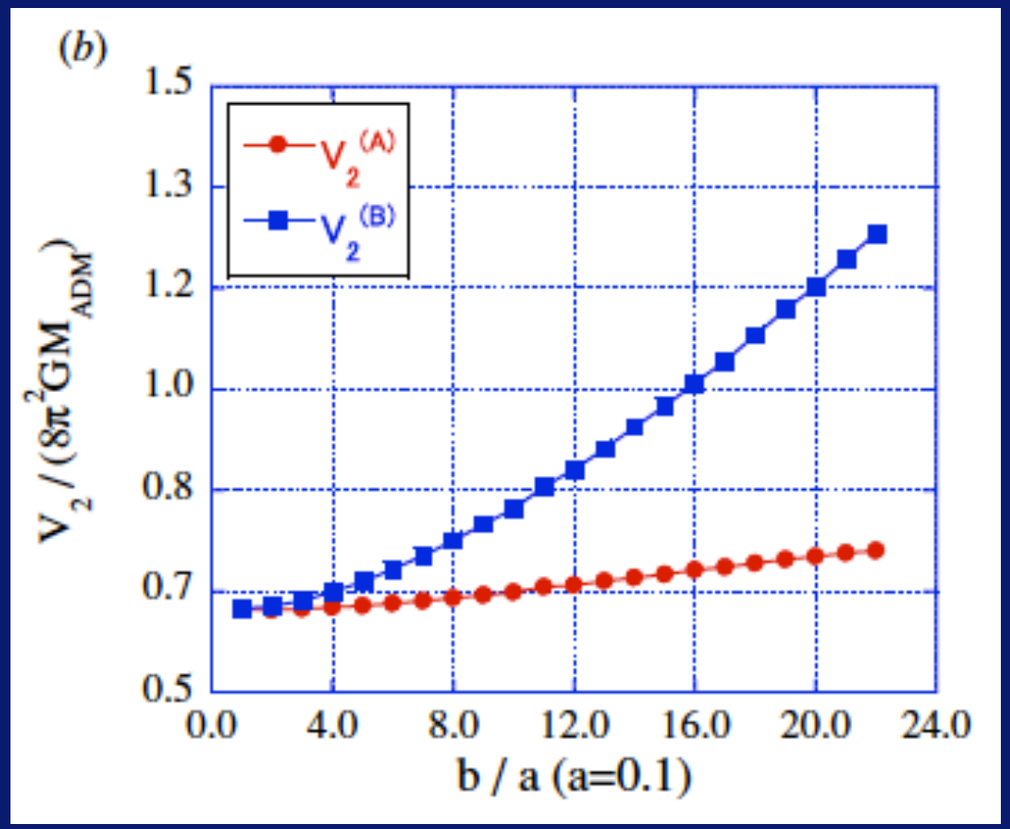

Hyper-Hoop $V_2^{(A)}$ does work for spheroidal horizons.

4. Hoop Conjecture

C. Toroidal Cases

$$V_2 \leq \frac{\pi}{2} 16\pi G_5 M$$

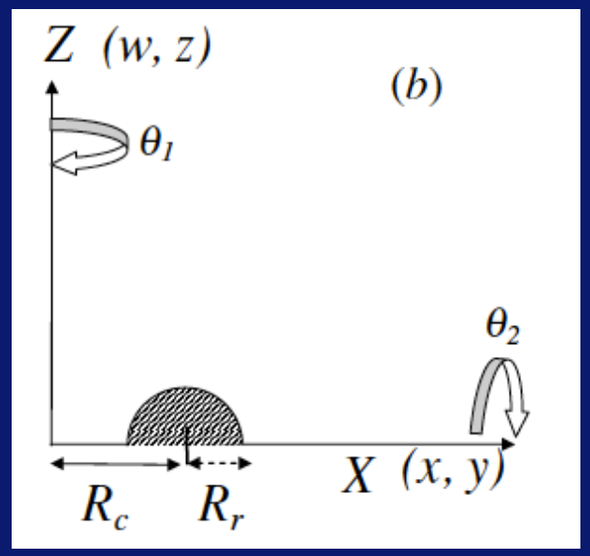

$$V_2^{(C)} = 4\pi \int_0^{\pi/2} \psi^2 \sqrt{\dot{r_h}^2 + r_h^2} r_h \cos\phi \, d\phi$$

$$\ddot{r_h} - \frac{3\dot{r_h}^2}{r_h} - 2r_h + \frac{r_h^2 + \dot{r_h}^2}{r_h} \left[\frac{\dot{r_h}}{r_h} \cot\phi - \frac{2}{\psi}(\dot{r_h} \sin\phi + r_h \cos\phi) \frac{\partial\psi}{\partial X} - \frac{2}{\psi}(r_h \sin\phi - \dot{r_h} \cos\phi) \frac{\partial\psi}{\partial Z} \right] = 0$$

$$V_2^{(D)} = 4\pi \int_0^{\pi/2} \psi^2 \sqrt{\dot{r_h}^2 + r_h^2} r_h \sin\phi \, d\phi$$

$$\ddot{r_h} - \frac{3\dot{r_h}^2}{r_h} - 2r_h - \frac{r_h^2 + \dot{r_h}^2}{r_h} \left[\frac{\dot{r_h}}{r_h} \tan\phi + \frac{2}{\psi}(r_h \sin\phi - \dot{r_h} \cos\phi) \frac{\partial\psi}{\partial X} + \frac{2}{\psi}(r_h \cos\phi + \dot{r_h} \sin\phi) \frac{\partial\psi}{\partial Z} \right] = 0$$

$$V_2^{(E)} = 2\pi \int_0^{\pi} \psi^2 \sqrt{\dot{r_h}^2 + r_h^2} (r_h \cos\xi + R_c) \, d\xi$$

$$\ddot{r_h} - \frac{3\dot{r_h}^2}{r_h} - 2r_h - \frac{r_h^2 + \dot{r_h}^2}{r_h} \left[\frac{-R_c + \dot{r_h} \sin\xi}{R_c + r_h \cos\xi} + \frac{2}{\psi}(\dot{r_h} \sin\xi + r_h \cos\xi) \frac{\partial\psi}{\partial X} + \frac{2}{\psi}(r_h \sin\xi - \dot{r_h} \cos\xi) \frac{\partial\psi}{\partial Z} \right] = 0$$

4. Hoop Conjecture

C. Toroidal Cases

$$V_2 \leq \frac{\pi}{2} 16\pi G_5 M$$

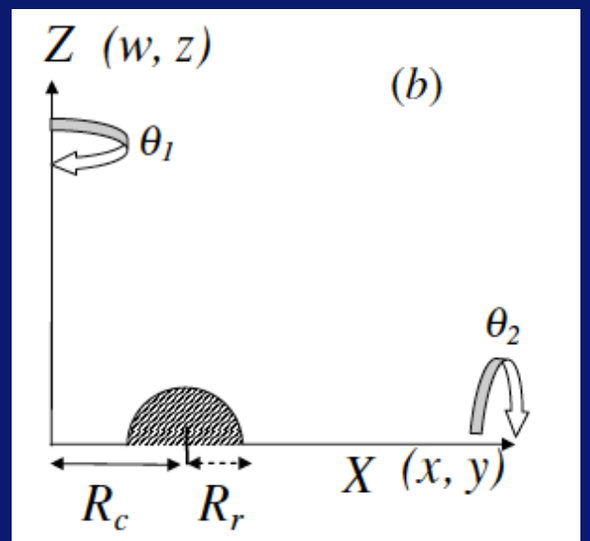

$$V_2^{(C)} = 4\pi \int_0^{\pi/2} \psi^2 \sqrt{\dot{r_h}^2 + r_h'^2} r_h \cos\phi \, d\phi$$

$$V_2^{(D)} = 4\pi \int_0^{\pi/2} \psi^2 \sqrt{\dot{r_h}^2 + r_h'^2} r_h \sin\phi \, d\phi$$

$$V_2^{(E)} = 2\pi \int_0^{\pi} \psi^2 \sqrt{\dot{r_h}^2 + r_h'^2} (r_h \cos\xi + R_c) \, d\xi$$

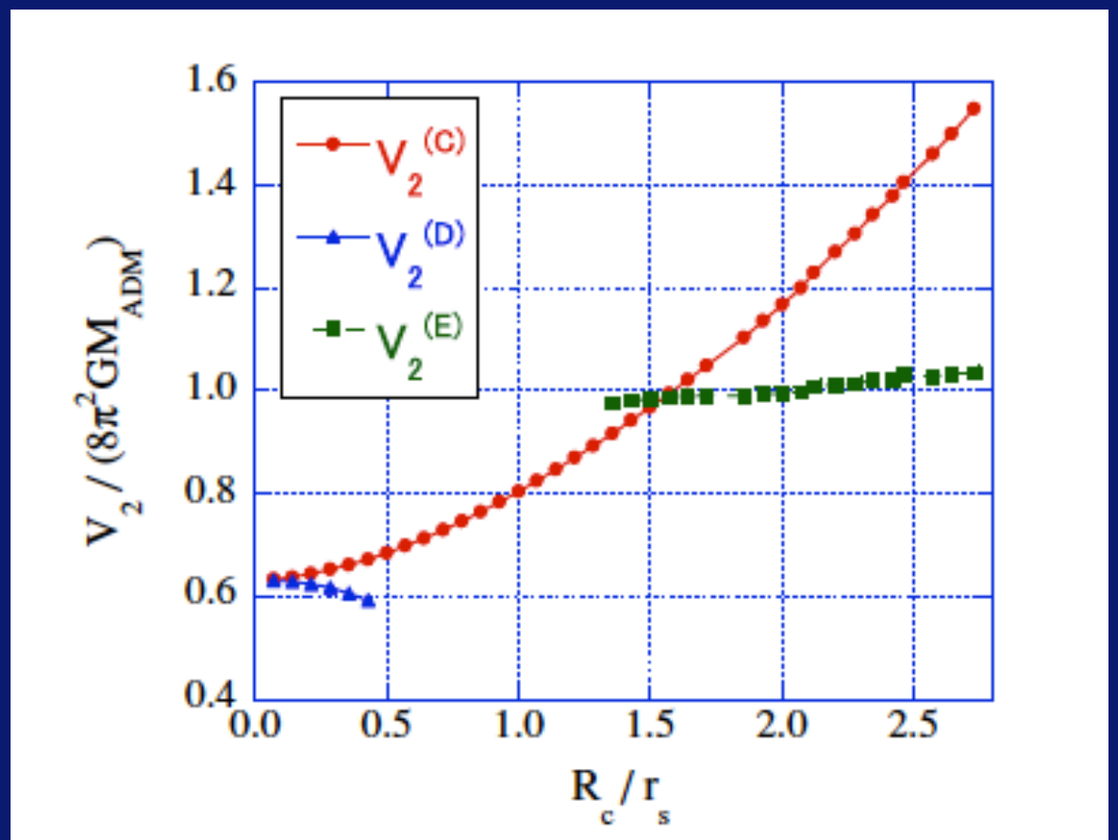

4. Hoop Conjecture

C. Toroidal Cases

$$V_2 \leq \frac{\pi}{2} 16\pi G_5 M$$

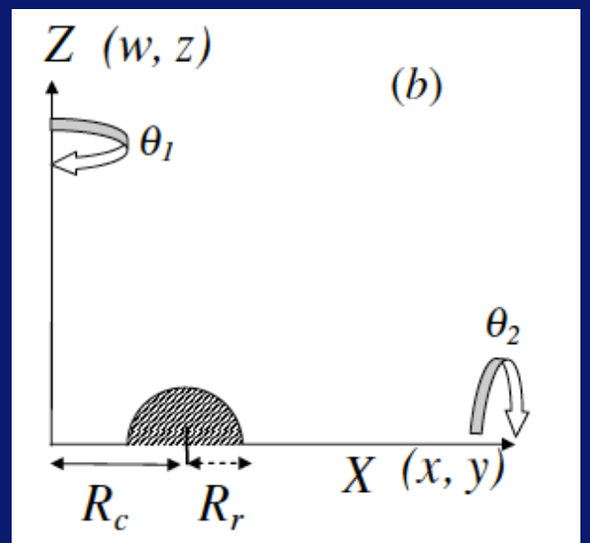

$$V_2^{(C)} = 4\pi \int_0^{\pi/2} \psi^2 \sqrt{\dot{r_h}^2 + r_h^2} r_h \cos\phi \, d\phi$$

$$V_2^{(D)} = 4\pi \int_0^{\pi/2} \psi^2 \sqrt{\dot{r_h}^2 + r_h^2} r_h \sin\phi \, d\phi$$

$$V_2^{(E)} = 2\pi \int_0^{\pi} \psi^2 \sqrt{\dot{r_h}^2 + r_h^2} (r_h \cos\xi + R_c) \, d\xi$$

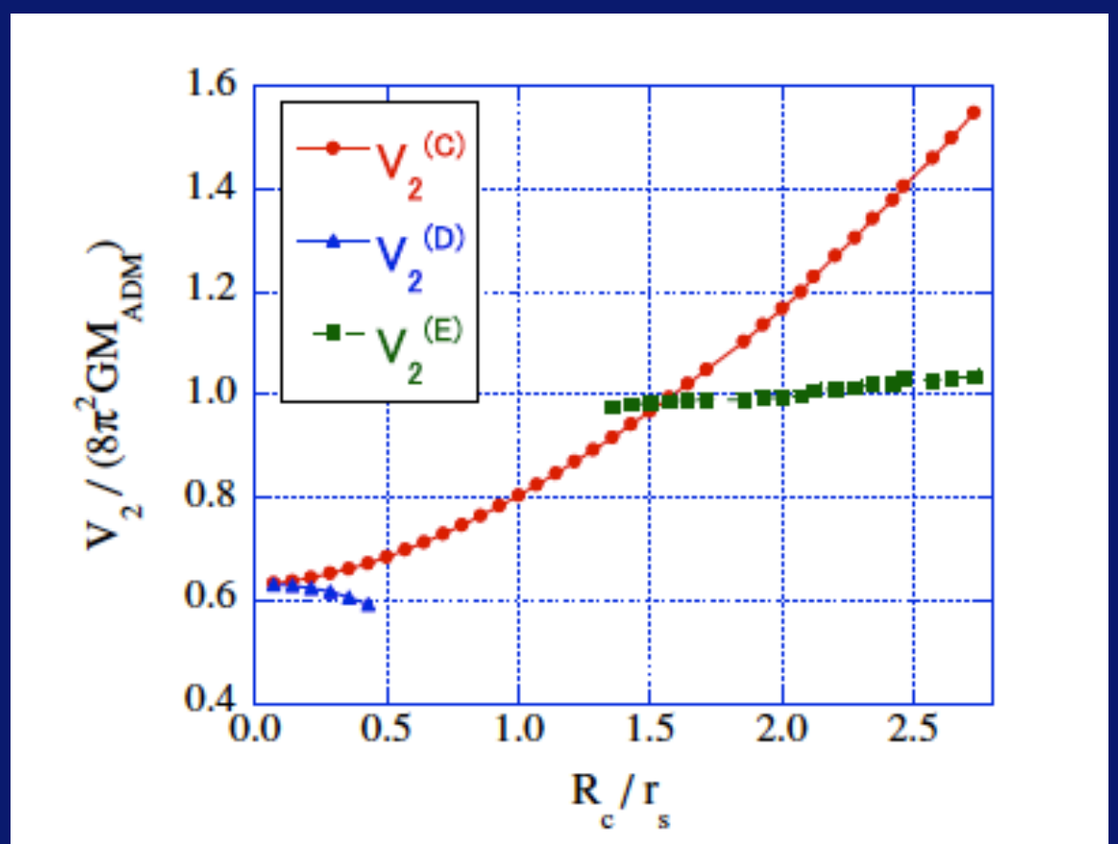

Hyper-Hoop does not work for ring horizons.

5. Summary and Future Plans

5D vs. 4D Spheroidal collapses (no rotating cases)

Collapse rapidly, towards spherical

Formation of Naked Singularity for highly prolate matter

5D Ring collapses (no rotating cases)

Hyper-Hoop prediction for BH formation

works well for formations of spheroidal black holes

but not for rings.

Future Plans:

include rotation, change slicing conditions

search various horizons,

investigate the stability, formation/decay process,....

2. Spheroidal matter collapse
C. Evolution examples

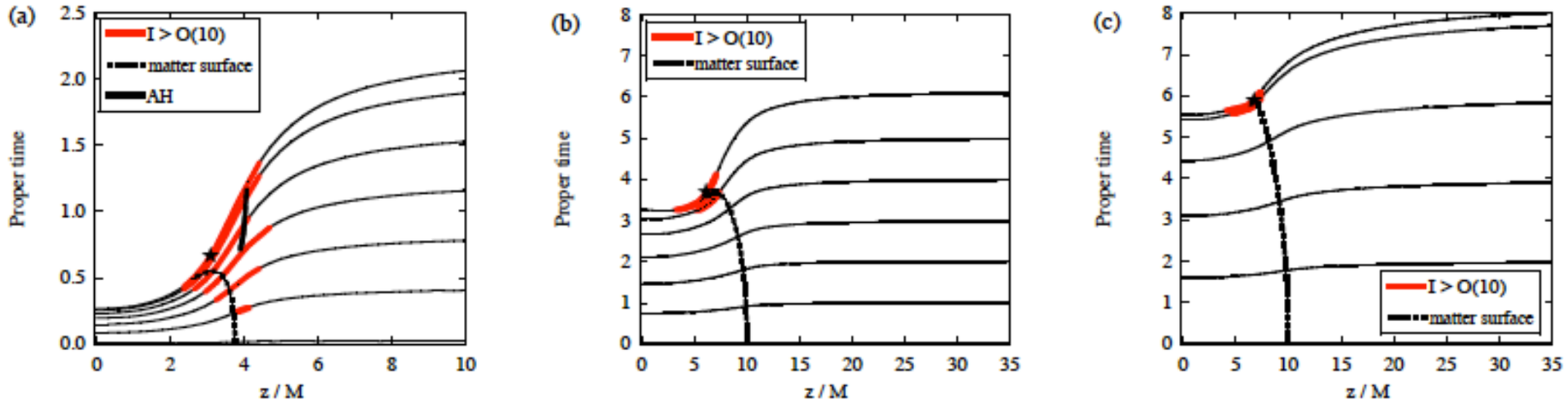

FIG. 4: The snapshots of the hypersurfaces on the z-axis in the proper-time versus coordinate diagram; (a) model 5DSβ, (b) model 5DSδ, and (c) model 4Dδ. The upper most hypersurface is the final data in numerical evolution. We also mark the matter surface and the location of AH if exist. The ranges with $\mathcal{I} \geq 10$ are marked with bold lines and peak value of $\mathcal{I}$ express by asterisks.